Water Sorption in Wood and Plant Fibres

Strømdahl, Kenneth

Publication date:
2000

Document Version
Publisher's PDF, also known as Version of record

INSTITUT FOR BÆRENDE KONSTRUKTIONER OG MATERIALER

DTU

Water Sorption in Wood and Plant Fibres

KENNETH STRØMDAHL

DEPARTMENT OF STRUCTURAL ENGINEERING AND MATERIALS
TECHNICAL UNIVERSITY OF DENMARK Series R No 78 2000

Institut for Bærende Konstruktioner og Materialer
Danmarks Tekniske Universitet

Water Sorption in Wood and Plant Fibres

Kenneth Strømdahl

Water Sorption in
Wood and Plant Fibres
Danmarks Tekniske Universitet
Kgs. Lyngby
ISBN 87-7740-293-6
ISSN 1396-2167
Electronic Publication
www.byg.dtu.dk

Preface

I am sincerely grateful for the continuous encouragement of my supervisor Associate Professor, Dr. Preben Hoffmeyer, who always inspired me and contributed with many fruitful discussions. His always loyal support has been important for the working environment and the accomplishment of my work.

Many other people have contributed to this study. In particular, I would like to express my gratitude to Associate Professor Dr. Kurt Kielsgaard Hansen for always taking the time to give me inspiring advice and encouragement. In addition, I am indebted to Dr. Kielsgaard Hansen for his large financial support of my project and discussions on the experimental design.

Especially, I also would like to give my sincere thanks to Dr. Tim Padfield for his large and fruitful contribution and guidance in the laboratory work. The cooperation and help from Signe Kamp Jensen, particularly during my time abroad, is most appreciated. Sincere thanks are also due to Ulla Gjøl Jacobsen for her uncompromising patience towards data collection in the experimental work, and Klaus Myndal for his valuable help in the construction of the climate chambers.

From my stay at the University of Maine, USA I am indebted to Professor Stephen Shaler for advice and fruitful contributions to my work there. Furthermore, I want to thank Dr. Lech Muszynski for the many inspiring discussions and his kind help during my stay.

This thesis is written and submitted in partial fulfilment of the requirements for obtaining the degree of Ph.D. The research is carried out at the department of Structural Engineering and Materials at the Technical University of Denmark. The financial support for the project received from the The Danish Technical Research Council's Programme for Biological Materials and Products, grant no. 9501157 is gratefully acknowledged.

Abstract

Water sorption properties of lignocellulosic materials may be used as a measure of material properties such as specific internal surface, porosity, pore size, pore size distribution, fibre saturation point, sorption energy, shrinkage/swelling propensity and even certain mechanical properties.

The present study contributes to the establishment of accurate experimental methods for the assessment of the sorption properties of wood and plant fibres. The study concentrates on the establishment and interpretation of sorption isotherms, i.e. the graphical representation of the relationship between the equilibrium moisture content (EMC) and the relative humidity (RH) at a given temperature (T).

In order to establish reliable sorption isotherms for wood and plant fibres climate chambers have been developed based on the mixing of two air streams containing dry and saturated air respectively. For measurements of sorption isotherms at elevated temperature an advanced and fully automated climate chamber was developed. Software to control the weighing of samples in turn has been developed together with software to monitor the temperature and RH in each chamber.

The results from sorption measurements on spruce, beech, flax, hemp and wheat straw fibres is modelled by the model of Hailwood–Horrobin providing an acceptable agreement between measured and calculated results.

It is not possible to establish reliable experimental conditions for a traditional assessment of moisture content values at relative humidities close to 100%. Therefore, attempts were made to use the pressure plate technique in the high humidity region from 93% to 99.99%. In this method, saturated fibres are put inside a pressure vessel and subject to a hydrostatic pressure of sufficient magnitude to reduce the relative humidity to values between 100% and 93% (Cloutier et al. 1995). The results show some promise but also prove that the suction technique must be further developed in order to produce accurate results for wood and plant fibres.

An attempt was made to quantify the sorption of water from a knowledge of the degree of cellulose crystallinity. The crystallinity was measured, but the limited variation between the different species makes it difficult to put unambiguous numbers on the degree of crystallinity for the investigated samples.

Results from measurements on acetylated and hygrothermally treated fibres show a significant reduction of moisture content. A hypothesis regarding the presence of micro pores in the cell wall is elucidated by acetylation. Acetylation reduces the number of available sorption sites in the cell wall, but does not influence the porosity. This suggests that micro pores where capillary condensation occurs do not exist.

Resume

Lignocellulosematerialers vandsorptionsegenskaber kan anvendes til at måle materiale-egenskaber som specifik indre overflade, porøsitet, porestørrelse, porestørrelsesfordeling, fibermætningspunkt, sorptionsenergi, tendensen til svind/svelning og endog bestemte mekaniske egenskaber.

Det foreliggende studie bidrager med tilvejebringelsen af præcise eksperimentelle metoder til fastsættelsen af sorptionsegenskaberne for træ- og plantefibre. Studiet koncentreres om tilvejebringelsen og fortolkningen af sorptionsisotermen, det vil sige den grafiske fremstilling af sammenhængen mellem ligevægtsvandindholdet (EMC) og den relative luftfugtighed (RH) ved konstant temperatur (T).

For at tilvejebringe pålidelige sorptionsisotermer for træ- og plantefibre er der blevet udviklet nogle klimakamre som er funderet på princippet om at blande to luftstrømme som indeholder henholdsvis tør og vandmættet luft. For at kunne måle sorptionsisotermer ved temperaturer højere end omgivelsernes er et avanceret og fuldautomatisk klimakammer blevet udviklet. Der er blevet udviklet software til både at styre den automatiske vejning af prøveemnerne på skift og til at overvåge og registrere temperaturen og den relative luftfugtighed i hvert klimakammer.

Resultaterne fra sorptionsmålingerne på rødgran-, bøge-, hør-, hampe- og hvedestrå fibre er blevet modelleret efter Hailwood–Horrobin modellen og har givet en acceptabel overenstemmelse mellem målte og beregnede resultater.

Det er ikke muligt at tilvejebringe pålidelige ekperimentelle forhold til en traditionel fastsættelse af vandindholdet ved relative luftfugtigheder tæt på 100%. Derfor blev det forsøgt at bruge trykmembranudstyr i det meget fugtige område fra 93% til 99.99%. Ved denne metode blev vandmættede fibre lagt ind i et trykkammer og udsat for et hydrostatisk tryk af tilstrækkelig størrelse til at reducere den relative luftfugtighed til en værdi mellem 100% og 93% (Cloutier et al. 1995). Resultaterne viste sig i nogen grad lovende, men beviste samtidigt at suction-teknikken skal udvikles yderligere for at kunne producere nøjagtige resultater for træ- og plantefibre.

Det blev forsøgt at kvantificere sorptionen af vand ud fra et kendskab til krystallinitetsgraden for cellulose. Krystalliniteten blev målt, men den begrænsede variation mellem de forskellige arter gør det vanskeligt at sætte entydige tal på krystallinitetsgraden for de undersøgte prøver.

Resultater fra målinger på acetylerede og hygrotermisk behandlede fibre viser en markant reduktion af vandindholdet. En hypotese omkring tilstedeværelsen af mikroporer i cellevæggen er blevet belyst ved acetylering. Acetylering reducerer antallet af rådige sorptionssteder i cellevæggen, men påvirker ikke porøsiteten. Dette tyder på at mikroporer hvor kapillarkondensation opstår ikke eksisterer.

Contents

CHAPTER 1
Introduction 11

1.1. Scope 12

1.2. Outline 12

CHAPTER 2
Sorption of water in wood and plant fibres 15

2.1. Introduction 15

2.2. The structure of wood and plants 15

2.3. Sorption of water in lignocellulosic materials 27

2.4. Water holding capacity 40

2.5. Thermodynamics of sorption 42

CHAPTER 3
Measurement of sorption of water 47

3.1. Introduction 47

3.2. Measurement of sorption curves 47

3.3. Measurement of moisture content 49

3.4. Measurement of relative humidity 51

3.5. Climate chamber development 54

CHAPTER 4
Design of experimental climate chamber 55

4.1. Introduction 55

4.2. Climate chamber design 55

4.3. Considerations for future improvements 65

CHAPTER 5
Materials and methods 67
5.1. Introduction 67
5.2. Materials 67
5.3. Experiments 69

CHAPTER 6
Results and discussion 73
6.1. Data processing 73
6.2. Sorption isotherms – pure fibres 78
6.3. Sorption isotherms – chemically modified fibres 90
6.4. Sorption isotherms – hygrothermally treated fibres 98
6.5. Discussion on sorption isotherms 102
6.6. Suction measurements 105
6.7. Thermodynamics of sorption 111
6.8. Crystallinity 117

Conclusion 122

Symbols and abbreviations 125

Bibliography 127

APPENDIX A
Sorption measurements 131

APPENDIX B
Suction measurements 149

APPENDIX C
X-ray diffractometry measurements 151

CHAPTER 1

Introduction

To satisfy the demands for more environmentally friendly products in the future, biological materials like wood and plant fibres are obvious choices. Today we are surrounded by many products and materials made of synthetic polymers and based on hydrocarbons as oil generated millions of years ago. The increasing consumption of energy in the world and the expected limitation on oil in the future leads to the requirement for alternative resources for the manufacturing of products.

Wood and plant fibres are inexpensive and CO_2 neutral. In addition, the energy of the fibres can be used when burning. In Denmark the amount of straw produced is about 7 million tons and the amount of wood is about 1 million tons per year. The greater part of the straw and half of the wood is not used, indicating the plentiful resources available.

Today there is a widespread use of fibres for medium density fibreboards (MDF) and masonite. The technical properties are of high quality, e.g., the ratio between strength and weight, sound and heat insulation and no sharp fracture surfaces. The disadvantage is the poor dimensional stability at varying relative humidity.

Many objects made out of polymers are subject to a possible conversion into biological materials of wood- and plant fibres, e.g., the inner shell of seats in trains and many interior parts and panels in cars. Also packaging material, boxes etc. can be substituted by fibres. Most of these products are moulded and sent through a press to create the exact shape. The perspective is to increase the amount of fibres used and to develop boards and panels without synthetic adhesives as the binding matrix. Also, the dimensional stability to humidity changes has to be improved by hygrothermal treatment or environmentally friendly chemical treatments.

The research carried out in this project is made in a cooperation with The Royal Veterinary and Agricultural University and Risø National Laboratory in a 5 years framework called BIOMAT. These partners each have knowledge about plant fibres and composite materials respectively. It is therefore natural to exploit this knowledge and their contribution to the project is valuable in the understanding of the behaviour in the final composite product. In cooperation with The Technical University and their knowledge about wood fibres, this team covers almost all aspects within the field of wood and plant fibre based products.

Much research has been carried out in an attempt to solve many of the problems regarding the use of organic fibres. One of the most important factors regarding the properties of organic fibres for industrial products is their great sensitivity to moisture content. The fact that relative humidity changes during the year and moisture content likewise therefore makes it necessary to investigate the influence of varying humidity.

The relationship between the equilibrium humidity and moisture content in the range from oven dry to the fibre saturation point is expressed by the sorption isotherm. The isotherm is determined at a constant temperature and is represented by a sigmoid curve. Accurate measurements of sorption isotherms have been attempted since the 1920's and accurate measurements are still in progress. The samples are usually very small and the equipment to measure weight changes has to be of a high standard together with an accurate climate control. These requirements are mandatory to obtain reliable results from the experiments.

The purpose of determining sorption isotherms is to quantify and understand how different materials behave under varying humidity conditions. Measurement of isotherms at different temperatures provides information about the heat of sorption and helps to understand the nature of moisture sorption. For instance, different chemical and physical treatments of the raw wood and plant fibre material to increase the performance of the final products is investigated by sorption studies. By these studies, it is possible to determine the effect of the treatments and to make comparisons with other materials. The basis for regarding the results solely obtained in the sorption studies in respect to the properties of the final product is clearly rather limited and depends on many other parameters as well, although the determination of the sorption isotherm is a crucial task.

1.1. Scope

This work serves a twofold purpose. The first purpose is the assessment of sorption of water in a selection of wood and plant fibres, necessarily some of which have been chemically or physically modified. Furthermore, the thermodynamic relation for the determination of heat of sorption has to be established by measurements of sorption isotherms at different temperatures. By combining these investigations, it may be possible to better assess the basic structure of the wood and plant fibre cell and thereby its applicability to be used in an optimal manner in composite materials.

The second purpose is to develop and design a climate chamber for high precision sorption measurements. Since almost all sorption studies in the past have been carried out on solid samples much less sensitive to short time changes in relative humidity than fibrous material another experimental set-up is needed. Wood and plant fibres are particularly sensitive to changes in relative humidity in the surroundings due to the large surface area exposed. Therefore it is attempted to characterise the sorption behaviour in a closed process where external weighings to determine the equilibrium moisture content are not needed.

1.2. Outline

This work consists of 6 chapters. The present chapter is the introduction to the project dealing with the scope. In Chapter 2 the background for sorption of water in wood and plant fibres is addressed. This chapter reviews the existing knowledge of sorption of water in wood and plant fibres and identifies the most important theories and models developed to understand and express the phenomena that takes place within the cell wall. In addition, the description of the physical character of the wood and plant fibre is presented.

Chapter 3 examines the background for measurement of sorption of water in wood and plant fibres. Focus is placed on different techniques to measure the sorption isotherm including advantages and disadvantages of each technique. In addition, equipment used in this project related to sorption measurements is mentioned and the reason for the development of the climate chamber explained.

Chapter 4 describes the design of the climate chamber since it has been such a crucial task for the assessment of the sorption curves. The most important details are explained starting at the basic principle of mixing a dry and humid air stream to achieve a specific relative humidity and ending at a description of the fully automated weighing process.

The materials and methods used in the project are addressed in Chapter 5. Treatments of the different fibres, defibration methods and specific characteristics expressed in terms of size, structure and composition are presented. Techniques used to determine different parameters are also mentioned.

The results from the experiments carried out are applied to the models described in Chapter 2 and evaluated in Chapter 6. Results from hygrothermally treated fibres together with different chemical treated fibres are also presented. Furthermore, results from suction measurements and classic calorimetry are presented.

A discussion of the results and comparisons to the models mentioned in Chapter 2 are given along with the results in Chapter 6. Finally, the main conclusion of the project is reported together with suggestions for future research in continuation of the present study.

CHAPTER 2

Sorption of water in wood and plant fibres

2.1. Introduction

This chapter reviews and discusses the existing knowledge of sorption of water in wood and plant fibres. The theories and models developed for the establishment of the relation between the equilibrium humidity and moisture content are addressed and identified. In this chapter, attention therefore is focused on the phenomena that takes place within the wood and plant fibre cell wall during the adsorption and desorption of water.

Recent theories about the relation between crystallinity and the water holding capacity are presented as is the impact of physical and chemical treatments (Salmén 1997). The concept of wood as a "swelling gel" is often used in the description of wood subjected to changing relative humidity. This concept will be discussed.

Also, the chemical and physical structure of the wood and plant fibre is described to support the understanding of where the sorption of water takes place and to give a basic demonstration of the behaviour when these materials are exposed to varying humidity conditions.

2.1.1. Background

This chapter reviews and discusses the literature that forms the background for the present work about sorption of water in wood and plant fibres. Experimental considerations are emphasized due to the large experimental effort put into this project. In terms of basic sorption studies, references are made to Stamm (1964), Skaar (1988) and Salmén (1997).

Also, the basic concepts of modelling the sorption isotherms are introduced. The modelling of the sorption isotherms has received special attention in an attempt to validate existing models and quantify the particular behaviour of the selected material. In terms of modelling of sorption isotherms, references are made to Skaar (1988) and Simpson (1979).

2.2. The structure of wood and plants

The properties of wood and plants are governed by its structure and chemical composition. Wood is divided into two main groups: gymnosperms and angiosperms. Coniferous woods or softwoods belong to the first category and have needles whereas hardwoods belong to the second category and have leaves. Usually hardwoods have a higher density and are harder than wood of softwood. In Denmark, the most common hardwoods are beech, oak, ash and elm, and the most common softwoods spruce, pine and larch.

Plants are not divided in two main groups like woods and in this context plant fibres are from non-tree sources. The major industrial uses of plant fibres are in textiles and the manufacture and preparation of pulp and paper, but significant quantities are used in applications as fibreboards and filtration products. Some plants are annual plants and others perennial plants. In this investigation, only annual plants (e.g. straw, flax, hemp) are subject to further analysis.

2.2.1. Macrostructure

Wood and plants are composed of elongated cells primarily oriented in the longitudinal direction of the stem. The individual cell has a hollow cylindrical shape and is connected to other cells by pores of different kinds. These pores are called pits. The size and thickness of the cells depend on what time of the growth season they are formed. Cells formed in the spring called earlywood are thin-walled with large cavities, and later when the rate of growth decreases the latewood is produced. The latewood cells are thick-walled and give mechanical strength to the stem. In Figure 2.1, a section from a pine stem is shown indicating the concentric growth rings or annual rings. This indication is due to the difference in the earlywood and latewood where the former is brighter and the latter is darker.

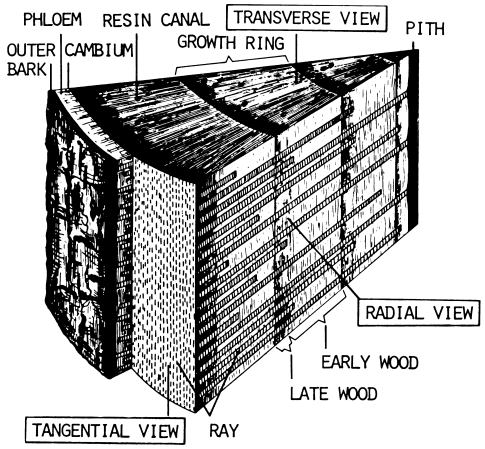

Figure 2.1. Section of a four-year-old pine stem (Sjöström 1981).

Also, cells (rays) in horizontal files are shown starting at the outer bark either to the pith or different annual rings. The pith is the centre of the stem and the inner part of the stem is called heartwood and consists of dead cells successively becoming larger and larger when the tree grows. The outer part of the stem from the heartwood to the bark is sapwood and conducts water from the roots to the foliage of the tree. At the edge of the sapwood next to the bark is the cambial zone consisting of living cells. In this thin region, new cells are formed between the inner bark (phloem) and the wood (xylem). Wood fibres are primary from the xylem due to the small phloem share of the cross section of the tree.

For plants, all the fibres are from the phloem part contrary to the woods. For flax and hemp fibres, phloem fibres are long and xylem fibres are very short. The short fibres are of limited use and therefore sorted out in the defibration process.

2.2.2. Cell types

Depending on their function the cells can be divided into three different groups. The first group is conducting cells providing the water to the tree from the roots. The second group is supporting cells also conducting water. Both types consist of dead cells containing water and air in the cavities. In hardwoods the conducting cells consist of vessels and the supporting cells consist of fibres. In softwood, tracheids perform both functions. The third category is storage cells, consisting of thin-walled parenchyma cells. The parenchyma cells serve as storage cells for transport and storage of nutrients.

2.2.3. Softwood cells

In softwood the major part of the wood substance consists of tracheids (90-95%) and ray cells (5-10%). The tracheids serve as ducts for water transport from the ground to the crown and give strength to the tree. Especially, the latewood gives strength due to its thick-walled cell structure.

Liquid moves from one tracheid to another through the pits in the cell wall, and the pits are primarily in the thin-walled earlywood. The pits are approximately 0,2µm in size (Haygreen & Bowyer 1996). Between adjacent cells are bordered pits and between tracheids and parenchyma cells are half-bordered pits, and pits without any border connect the parenchyma cells.

In Figure 2.2, cells of softwood including earlywood and latewood are shown and the difference in size between tracheids and parenchyma is indicated. The average length of Norway spruce tracheids is 2-4 mm and the width in the tangential direction is 0.02-0.04 mm. The thickness of earlywood and latewood is 2-4 µm and 4-8 µm respectively. Parenchyma cells are thin-walled living cells and in Norway spruce their length and width vary between 0.01-0.16 mm and 2-50 µm, respectively.

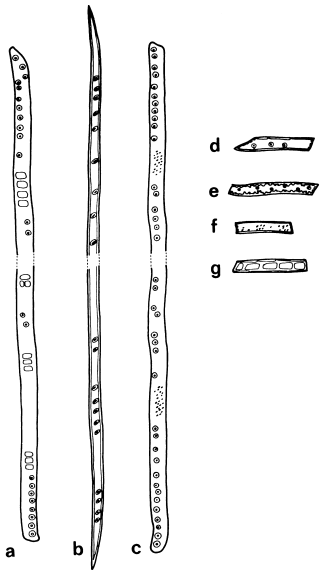

Figure 2.2. Cells of coniferous wood. An earlywood (a) and a latewood (b) pine tracheid, an earlywood spruce tracheid (c), ray tracheid of spruce (d) and a pine (e), ray parenchyma cell of spruce (f) and pine (g) (Sjöström 1981).

Finally, resin canals of softwood should be mentioned. They are tubular intercellular spaces surrounded by a sheet of small parenchyma cells. Both horizontal and vertical resin canals can exist and they may be located inside the rays (fusiform rays). The resin canals are living cells until the transformation into heartwood takes place. The diameter of resin canals is found to be from 30-160 μm depending on species.

2.2.4. Hardwood cells

In hardwood more different types of cells exist, specialized for different functions. The conducting tissue consists of vessels with large cavities compared to the supporting libriform cells. For storage purposes, parenchyma cells in rays exist. Moreover, different hybrids of cells exist, primarily supporting tissue called fibre tracheids, see Figure 2.3. The libriform fibres are thick-walled elongated cells with small cavities containing simple pits. The size of libriform beech fibres is on average 0.6-1.3 mm in length and 15-20 μm and 5 μm in width and thickness, respectively. The vessels are thin-walled and are rather short in length but they are stacked on top of each other to form a long tube in the stem. Tubes of several meters have been noticed to be capable of transporting water effectively from the roots through the stem to the leaves. Especially because of the leafing during the spring, there is a need for effective water transport. Although the vessels are very short, the ends have disappeared more or less completely thus allowing the water to flow in the tube.

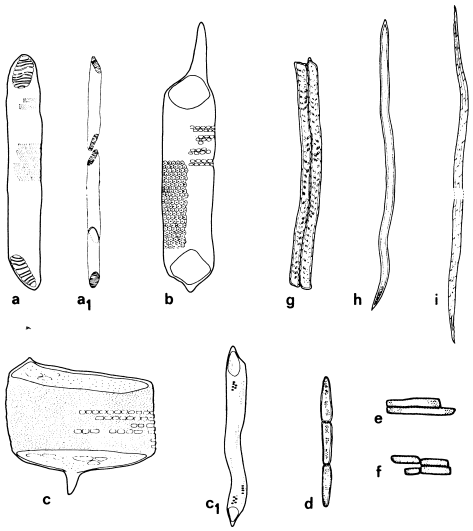

Figure 2.3. Hardwood cells. Vessel element of birch (a), of aspen (b), and of oak in earlywood (c) and in latewood (c_1), as well as a birch vessel (a_1). Longitudinal parenchyma of oak (d) and ray parenchyma of aspen (e) and of birch (f). Tracheids of oak (g) and birch (h) and a birch libriform fiber (i) (Sjöström 1981).

The size and the amount of vessels and libriform cells depend on the species. Usually the vessels amount to about 30-40% of the wood volume and the amount of fibres 40-60% of the wood volume. Rays are exclusively parenchyma cells and are about 15-20% of the wood volume with a few percent in the longitudinal direction (Fengel & Wegener 1984).

2.2.5. Plant cells

Generally, three simple tissues are recognised in plants, composed of a single basic cell type. These cell types are: parenchyma, collenchyma and sclerenchyma. In general, parenchyma cells have only a thin primary wall and the collenchyma cells have a thicker primary wall. The sclerenchyma cells have both a primary and a secondary wall (McDougall et al. 1993).

The parenchyma cells carries out a wide range of functions. Most of them are living and contribute to the mechanical strength of the plant but also transport parenchymas are present including transfer cells and cells making up the rays in wood. Last but not least, some of the parenchyma accumulate starch, proteins and oils in seeds and are known as storage cells. In Figure 2.4 different cells from flax fibres are shown at 100x magnification indicating the various shapes and sizes.

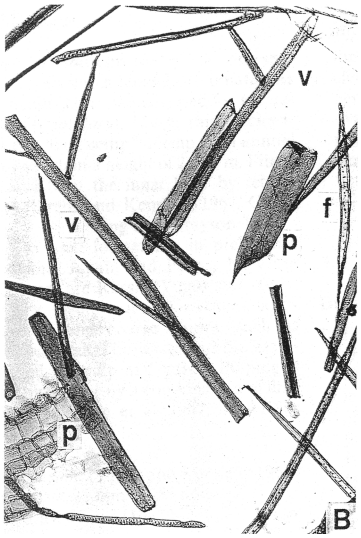

Figure 2.4. Cells from flax fibres. Short pitted fibres (f), narrow pitted vessel elements (v), and parenchyma cells (p), 100x (Sisko & Pfäffli 1994).

2.2.6. Chemical composition of the cell

Basically wood and plants are 98 to 99% organic matter and the remainder is inorganic material which forms ash on burning. The organic portion mainly consists of 70-90% carbohydrates and 20-30% of the complex polymer lignin. The carbohydrate or holocellulose portion is composed of cellulose and hemicellulose. The main component in wood and plants is cellulose and constitutes slightly less than one-half of the weight, while the variety of hemicellulose and lignin is wider.

Cellulose is formed indirectly by the photosynthesis where glucose and other simple sugars are produced with oxygen as a by-product. Cellulose is manufactured from the glucose units ($C_6H_{12}O_6$) by joining the glucose units together end to end in a complicated process where a water molecule is eliminated for each chemical linkage formed between neighboring units, Figure 2.5. Strictly speaking the repeating unit is a cellobiose unit. As a result, the long-chain cellulose polymer $(C_6H_{10}O_5)_n$ is formed, where the degree of polymerisation n is as large as 15.000 (Fengel & Wegener 1984).

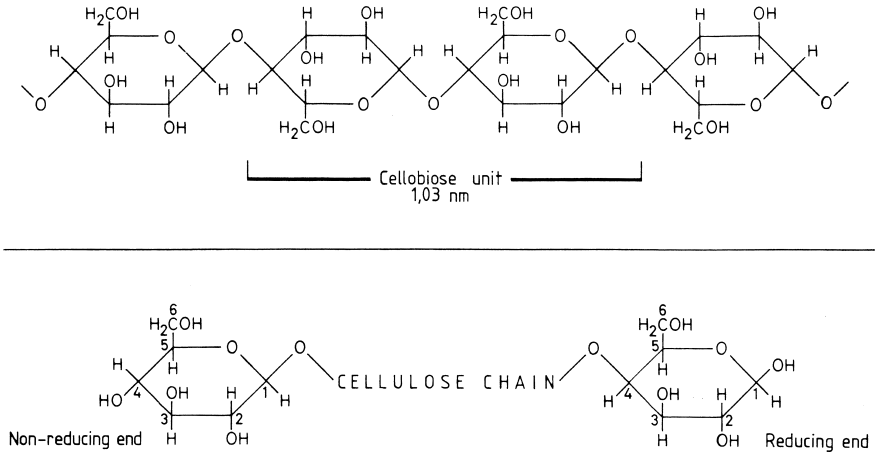

Figure 2.5. Formula of the cellulose chain (Fengel & Wegener 1984).

For many people cellulose is a familiar material, because paper and newsprint mainly contains the cellulosic fraction from wood, and because cotton is almost 100% cellulose. But still, the size of the cellulose chains is very small though the chains are made up of some 10000-30000 units. The size of the longest cellulose chain is only about 10 μm, and due to its narrow width not possible to see in an electron microscope.

In addition to the glucose units formed in the photosynthesis, several other sugars are produced to build the hemicellulose structure. The hemicellulose is characterised by a very branched structure compared to the straight-chain cellulose structure, and the degree of polymerisation is much less than cellulose, i.e. in the few hundreds rather than the thousands.

The last of the three main constituents of the wood structure is the complex polymer lignin. Lignin is not yet fully examined and therefore the chemical structure and linkages remain uncertain. Lignin is built upon one of the three percursors of phenylpropane unit shown in Figure 2.6 and serves as a binding agent in the cell wall structure. It is located between the individual fibres and within the cell wall and gives rigidity to the structure. This complex polymer and the branched structure it makes is almost impossible to extract from the wood without degrading.

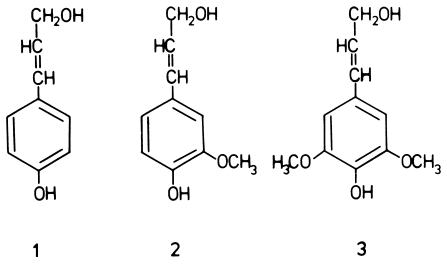

Figure 2.6. Lignin precursors. 1, p-coumaryl alcohol, 2, coniferyl alcohol, 3, sinapyl alcohol (Sjöström 1981).

Generally, there is very little pectin (close to lignin in structure) in the fibre cell walls. However, in some plants used for fibre, such as flax, there is considerable pectin in the middle lamellae between fibre and other cells (McDougall et al. 1993).

2.2.7. Cell wall

Recall the macrostructure of the wood within the cambial zone where new cells are formed to either the inside wood or the outside bark. New cells enclose themselves with a thin membranelike wall, the primary wall, consisting of cellulose, hemicellulose, pectin and protein. First, the cell lumen is filled with a fluid (cytoplasm) and then gradually the wall thickens as polymers are formed and added to the inside of the wall forming the secondary wall. The lignification starts during the formation of this secondary wall, and it is clear that the lignin is more or less arranged in tangential lamellae in the cell wall (Goring 1977). However, whether the lignin is to be considered as existing in separate layers or as a mixture with the hemicellulose, or the way in which it is incorporated in the wall represents still an area of disagreement among scientists.

The cell wall is built up of the above mentioned polymers in a very precise fashion and not as sometimes expected in a random way. The cellulose is formed in long chains and aggregated with their neighbours in a crystalline structure (Hearle 1960). It seems that none of the cellulose molecules are incorporated as individual units in the cell wall but always connected in chains. These chains show a rigid crystalline structure created by intermolecular hydrogen bonds and dipolar interactions in the arrangement. Hydrogen bonds are not nearly as strong as covalent bonds but when they are present to the extent found between cellulose molecules, they give strength to the structure.

Again, various opinions exist regarding these mechanisms. The stiff crystalline structure does not allow anything to penetrate in between the chains of molecules and therefore makes this part of the structure hydrophobic. A theory has been proposed by many researchers that the cellulose chains at regular intervals have amorphous domains allowing other substances, like e.g. water, to form hydrogen linkages (Stamm 1964, Sjöström 1981, and Fengel & Wegener 1984). According to this model, cellulose continues several crystallites throughout the fibre. It should be noted that other forms of the crystalline form of cellulose have been found. The proportion of crystalline regions in celluloses is 80% for cotton, 60-70% for woods and 40% for regenerated cellulose (McDougall et al. 1993). Later in this chapter, a description of the recent theories considering the formation of cellulose chains without amorphous domains will be presented.

The network of cellulose is known as microfibrils and because of the difficulty in isolating the cellulose without degradation, the exact size and structure is uncertain. The smallest building elements of the cellulose skeleton are considered by some to be the elementary fibrils consisting of a bundle of 36 cellulose molecules. These elementary fibrils are again arranged in crystalline and amorphous regions. The length of the crystalline region is on average 100-250 nm and the width of the cross section about 10-30 nm (Stamm 1964, Sjöström 1981). Elementary fibrils containing a parallel array of 50-80 cellulose molecules with a cross section of the order 3.5×3.5 nm is also mentioned (Bodig & Jayne 1993).

These elementary fibrils, in turn, are aggregated in microfibrillar bundles with some assistance from hydrogen bonding. The width of the virtually square microfibril is

approximately 2.5-3.0 nm (Fujita & Harada 1991) for wood and plants, but probably 5 times wider in Valonia. However, the number of cellulose chains in each microfibril can vary and then the width will change depending on whether mircrofibrils aggregate into larger units after the synthesising (Giddings et al. 1980). Later work carried out using electron microscopy, indicates no substructure in the microfibrils corresponding to elementary fibrils (Fujita & Harada 1991). But, speculation exist about different structures of the cellulose chains in the primary and the secondary cell wall. In the primary wall, triple-stranded fibrils are indicated whereas a more straight cellulose structure of a highly crystalline region is formed in the secondary wall (Ruben et al. 1989).

Hemicellulose and lignin are located in the space between the microfibrils. Different approaches have been proposed on how the cellulose is embedded in a structure of hemicellulose and lignin. The branched structure of the hemicellulose in between the microfibrils maintains a cohesion between the building blocks of the wood cell wall. The question is still whether the lignin is deposited between microfibrils into the cell wall or is incorporated in a two dimensional lamellar structure (Goring 1977) between the microfibrils. The latter is shown in Figure 2.7, where the cellulose are the structural units built into the cell wall with hemicellulose and lignin.

Another proposal suggests, on the basis of studying the Valonia cell, that the microfibrils and hemicellulose are arranged in a honeycomb structure. In such a formation, the hemicellulose is deposited at the same time as the microfibrils and acts as a spacer to hold the thin microfibrils separated at regular intervals (Terashima et al. 1993).

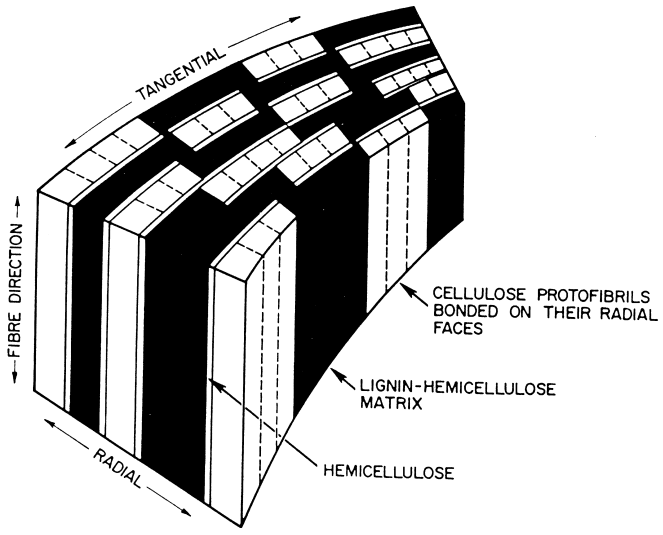

Figure 2.7. Ultrastructural arrangement of lignin and carbohydrates in the wood cell wall (Goring 1977).

2.2.8. Biosynthesis of the cell wall

How and where the formation of cellulose fibrils takes place has been one of the major questions since the early days of wood science. Different models and proposals have been suggested and new techniques like electron microscopy and freeze-fracture have improved the results remarkably in the last decades.

Previous assumptions were that the formation of the cellulose fibrils began in the ectoplasm and continued in the loose network in the young wall. When the wall gets thicker and thicker and more compact formation of fibrils in the wall is inhibited, free glucose molecules polymerise and create new microfibrils on the surface of existing microfibrils (Mühlethaler 1965). These observations were made using the negative staining method.

The biosynthetic growth of a glucose chain is, in brief, linking another glucose (diphosphate –glucose) to the C4-end of the chain and, cleaving another group, Figure 2.5 (Fengel & Wegener 1984). The reverse direction, linking to the C1-end in a glucan chain, is also possible.

The size of the fibrils is dependent on the method used for the measurement. While in the early studies, the smallest units, the microfibrils, were assumed to have a diameter ranging from 10 to 25 nm, later even smaller units, the elementary fibrils, were detected with an assumed diameter on average of 3.5 nm. However, smaller units were detected as small as 1.5 to 3.0 nm from bacteria and algae.

The microfibrils are deposited in a constrained space between the plasma membrane and the cell wall. The lamellae of the wall is one microfibril thick (3-4 nm) and the cellulose microfibril themselves are 3.6 ±1.9 nm wide (Emons & Mulder 1998). The microfibrils are deposited in helicoidal orientations with different rotation angles. The length is independent of the fibril angle and measures 250-350 μm (Emons & Mulder 1998).

An increasing number of reports are demonstrating organized particle complexes in the plasma membrane of algae and higher plants. The pattern of these complexes shows an association between the ends of the microfibrils but also a distribution and localization parallel to the pattern of these cellulose chains. Three different complexes have been described: the linear type, the rosette type and the globular type, all shown in Figure 2.8. Similar for all different types are that they are found in algae, but in recent studies an increasing number of reports indicate rosettes in higher plants as well. This leads to the notion that these structures indeed may be part of the cellulose synthesizing complexes.

The rosettes are observed in a number of higher plants and are therefore most relevant in the matter of wood and plant fibres. In Figure 2.8, B is of interest showing the two rosette types. The reports about the rosette-type structures show a hexagonal array of particles in the plasma membrane, each rosette consisting of 6 particles about 8 nm in diameter and with the rosette having an overall diameter of about 22 nm. In addition to the rosettes, terminal globules were seen on the opposite side of the membrane coincident with the hexagonal array suggested to be part of the same complex (Mueller & Brown 1980). It is in this complex that the catalytic components attached to the microfibrils are associated with the polymerisation of the glucan chains. The relationship between the globules and the rosettes is not yet clear. It has been proposed that each particle in the rosette forms 6 glucan chains and then each rosette thus produces an elementary fibril containing 36 glucan chains. However, it is still a question whether both structures are part of this process.

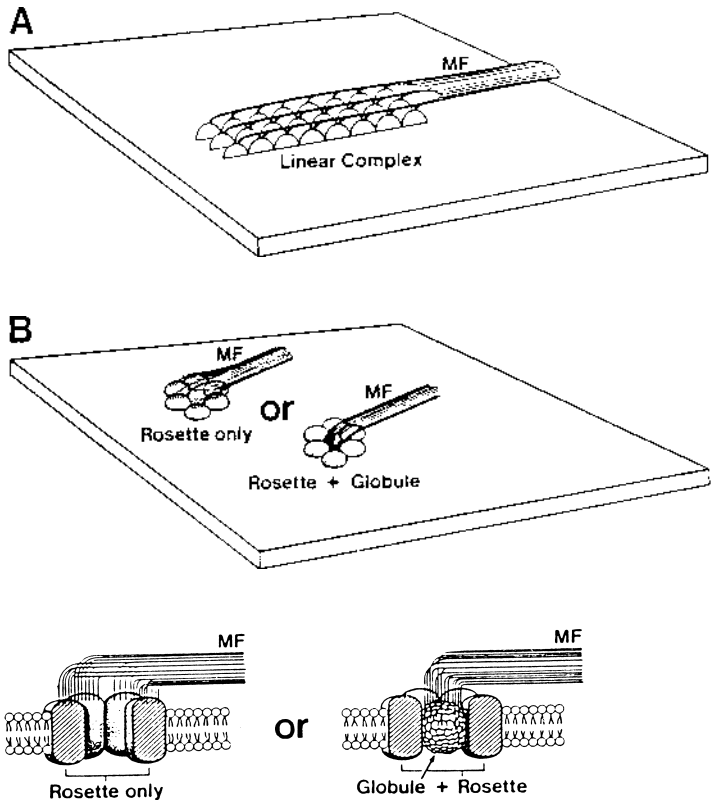

Figure 2.8. Stylised drawings of the putative cellulose synthase complexes. A, example of the linear complex seen by freeze-fracture in certain types of algae. For simplicity the number of individual subunits shown here is less than observed in the freeze-fracture images. B, Examples of two possible structures for rosette-type or rosette-globule-type complexes seen by freeze-fracture of some algae and a number of higher plants. MF, microfibril. (Delmer & Stone 1988).

What controls the orientation of the microfibrils is still unclear. Several hypotheses have been put forward in an attempt to determine what really occurs during the deposition of the microfibrils in the cell wall. The increasing number of reports of rosettes and terminal globules now seems to demonstrate where the cellulose chains are synthesised and also focuses on the relation between the pattern of the rosettes and the microfibrils. This pattern is almost exactly the same. The rosettes are supposed to control the orientation of the microfibrils. But the next question would then be what controls the rosettes? Recent advances in the ability to observe the entire microtubule network have furthered the understanding of the relationship between the microtubule network and the microfibril deposition. But still, it is proposed that the microfibril structure arises, at least in part, by a self-assembly process following deposition in the cell wall, such that interactions with the matrix polysaccharides and not the microtubules, determine the ultimate three-dimensional structure. Thus, the role of the microtubules in orienting the microfibril deposition in the cell wall still remains controversial (Delmer & Stone 1988).

Evidence of the controversial role of the microtubules is also found in another investigation (Herth 1985) showing a somewhat irregular arrangement between microtubules and microfibrils. It is there concluded that the rosettes in higher plants are oriented in tracks parallel to the microfibrils but not directly oriented by the microtubules.

Lignin is often found in the middle lamella, but can be present throughout the mature secondary wall. Lignification increases the mechanical rigidity of the wall and makes it less permeable to water.

Lignin is synthesised by a unique process. Its precursors, substituted hydroxycinnamyl alcohols, are synthesised within the cell then tranported into the wall space where they are converted to phenoxy radicals by the action of wall-associated peroxidases in a reaction requiring hydrogen peroxide. These relatively long-lived radicals then condense to form the polymer.

2.2.9. Cell wall layers

The cell wall is built up by several layers, Figure 2.9. Between the individual cells is the layer called the *middle lamella* which glues the cells or the individual fibres together. This layer is almost cellulose free and the primary constituent is lignin. The thickness, except at the cell corners, is about 0.2-1.0 μm. The middle lamella is in close contact with the primary wall, and the transition from one layer to the adjacent one is not very clear and therefore these layers sometimes are termed *compound middle lamella.*

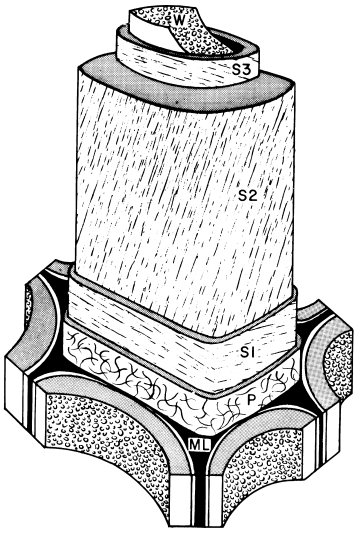

Figure 2.9. Model of the cell wall structure showing the middle lamella (ML), the primary wall (P), the outer (S1), middle (S2) and inner (S3) layer of the secondary wall, and the warty layer (W) (Sjöström 1981).

The *primary wall* is a thin layer, 0.1-0.2 μm, consisting of cellulose, hemicellulose and lignin where the microfibrils are arranged in crossing layers. Because it is the first wall in the formation of the fibre, the crossing layers allow for an expansion of the young cell. Also, the pattern of deposition of microfibrils in the primary layer is markedly different from that which occurs during secondary wall formation (Giddings et al. 1980). The latter, observed as part of the freeze-fracture investigations, is in accordance with the rosette theory.

The *secondary wall* consist of three layers, thin outer and inner layers and a thick middle layer, called S1, S2, and S3. These layers are built up by lamellae in almost parallel order but at varying slope in each layer. The outer layer (S1) is 0.2-0.3 μm thick and consists of

relatively few layers with a gently helical slope. The microfibril angle varies between 50° and 70° with respect to the stem axis. The middle layer (S2) is the thickest layer and the microfibrils run in a very steep angle to the stem axis, only a slope between 10° and 20°. The thickness is from 1 to 5 μm depending on species and this layer plays a dominant part in the strength and stiffness of the fibre and thereby the whole tree or plant. The inner layer (S3) is again a thin layer, approximately 0.1 μm in thickness with the slope varying from 50°-90° because of great variation among different wood species. This third layer in the secondary wall is sometimes mentioned as the tertiary wall.

In all types of cells, the S2 layer is dominant and it accounts usually for more than 90% of the cell wall volume. The thickness of S1 and S3 in both earlywood and latewood only changes minimally from the spring season to the autumn. However, the S2 layer is still dominant even though the latewood cells generally are thinner than earlywood cells.

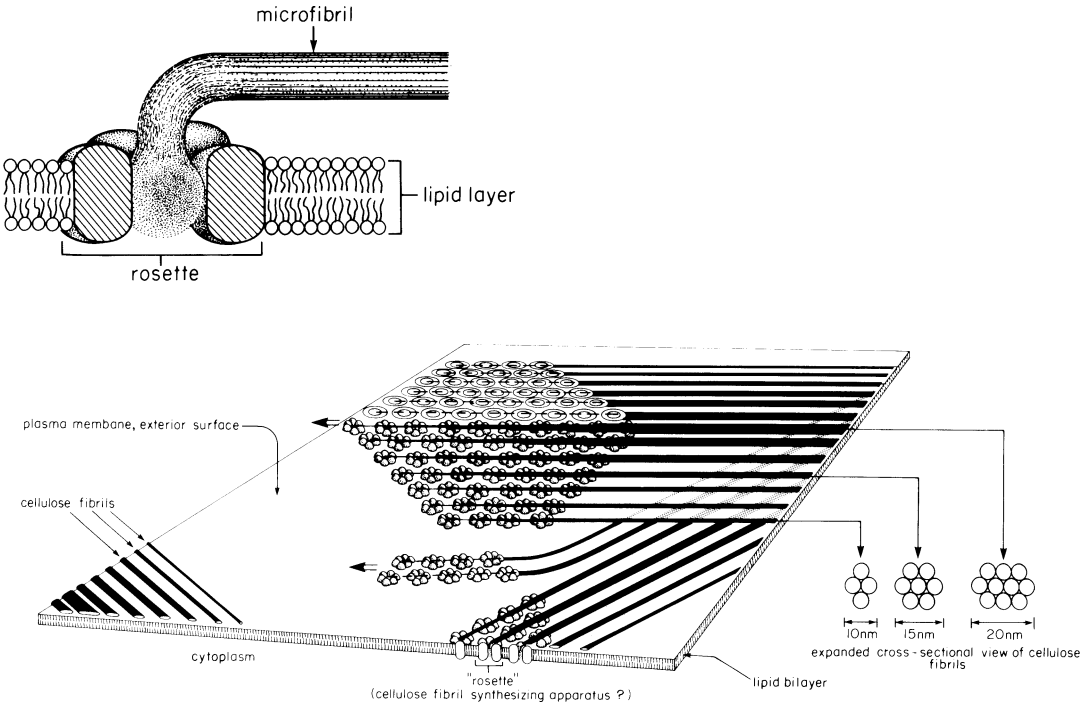

Figure 2.10. Model of the cellulose fibril deposition during secondary wall formation. Each rosette is believed to form one 5 nm microfibril. A row of rosettes forms a set of 5 nm microfibrils, which aggregates laterally to form the larger fibrils of the secondary wall. Above: side view. The stippled area in the center of a rosette represents the presumptive site of microfibril formation, although details about its structure, composition and chemical activity remain unclear. Below: surface view with expanded cross-sectional view of cellulose fibrils. (Gildings et al. 1980).

Regarding the rosette theory the model in Figure 2.10 shows the formation of the secondary wall in a surface view. The hexagonal pattern of rosettes each forms a microfibril which aggregates in a larger fibril in the wall. The larger the number of rows of rosettes, the wider becomes the aggregated cellulose fibril because the parallel rows of rosettes form a band of parallel fibrils. This is supported by observations that the distance between rows of rosettes is equal to the distance between fibrils.

2.3. Sorption of water in lignocellulosic materials

In spite of many attempts to determine the sorption phenomenon, no unambiguous theory has been proposed. The fact that the wood cell wall swells when increasing the moisture content allows more water to be sorbed into the cell wall, thus increasing the inner surface area. The wood structure acts like a swelling gel and Barkas (1949) was one of the first to compare the characteristics of wood and gels. Gels also open up pores and cracks successively when water vapour is sorbed to the surface. Swelling in gels and lignocellulosic materials may be anisotropic.

This, to some extent, continual expansion of the number of sorption sites during the adsorption process indicates that the water molecules squeeze in between the amorphous parts of the cell wall structure, i.e. the surfaces of e.g. two microfibrils, and open it like a zipper as illustrated in Figure 2.11. An analogous process takes place during the desorption where the cell wall structure closes or collapses concurrently with the evaporation of the water molecules. Whether this "zipper" hypothesis is true or false will be discussed later.

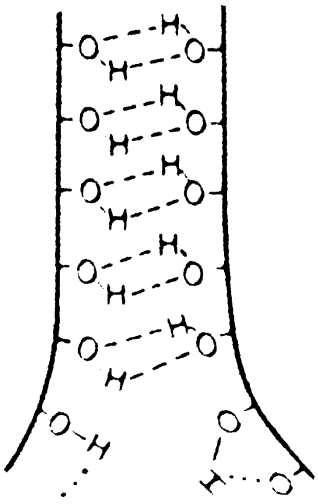

Figure 2.11. The "zipper" model for sorption of water in the amorphous parts of the cell wall. Water molecules squeeze in between the cellulose chains thus allowing new hydrogen bonds to be formed (Caulfield & Weatherwax).

However, pure adsorption or desorption only takes place very seldom and is usually an alternating process in real life. This means the sorption process often is a two-way traffic and one should imagine that the thousands and thousands of water vapour molecules fluctuate in a constant movement above the surface interrupted for periods of varying time span when more or less temporarily bound to a hydroxyl group.

2.3.1. Moisture content

Moisture content, m, is defined as the ratio of the weight of removable water at equilibrium m_1 to the dry weight m_0 of the wood. The dry weight is obtained by oven drying at 103±2°C or above a dry desiccant. The moisture content is expressed as the fractional value (kg/kg) or in percentage terms and is calculated by

$$m = \frac{m_1 - m_0}{m_0} \tag{2.1}$$

where

m_1 Weight of removable water at equilibrium (kg)

m_0 Dry weight of sample (kg)

Throughout the thesis, the moisture content is usually expressed as the fractional value and the value of m_1 is always the weight of the sample when it is in equilibrium at the specific relative humidity. Further details about the equilibrium criteria will be provided in Chapter 6.

2.3.2. The sorption isotherm

Wood and plant fibres, and lignocellulosic materials, are all porous to a greater or lesser extent. Through contact with continually changing ambient temperature and relative humidity in the surroundings, they show an apparent tendency to change the amount of water sorbed to the inner and outer surface. This tendency to adsorption and desorption when increasing and decreasing the relative humidity is a well-known phenomenon studied intensively in the past. The graphical representation of the relationship between the equilibrium moisture content (EMC) and the relative humidity (RH) at a given temperature (T) is called the sorption isotherm, Figure 2.12. The sorption isotherm is of great importance in many respects. It is used to quantify the structure and the constituents of the wood and plant species investigated. Moreover, it is used to calculate dimensional changes in solid wood and wood composites due to changing RH and used to provide input parameters in calculations of heat and mass transfer and it is used in many related fields such as wood drying technology.

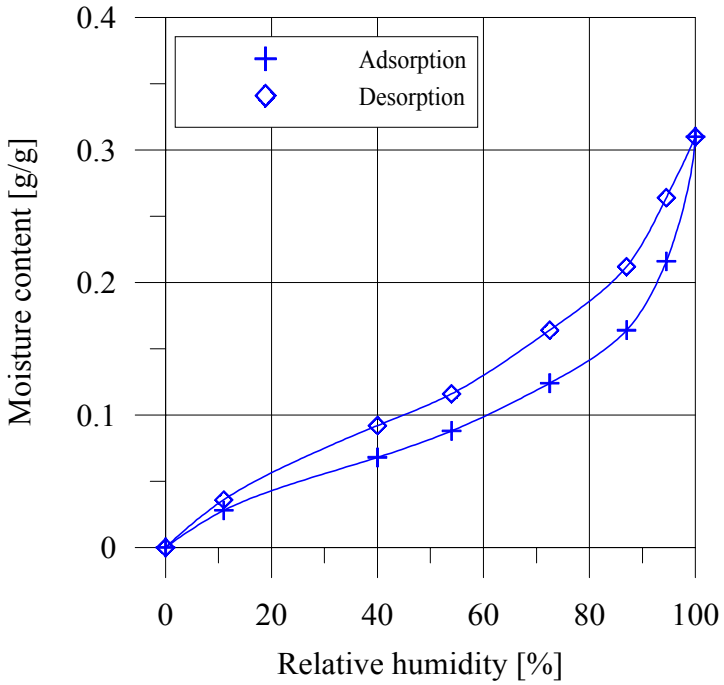

Figure 2.12. Sorption isotherm for white spruce at 25°C (Stamm 1964).

2.3.3. Fibre saturation point

The moisture content at which the cell walls are fully saturated with moisture and the cell cavities contain no liquid water is the fibre saturation point, termed M_f (Skaar 1988). The definition originally comes from the fact that the strength properties of wood depend on the moisture content. It appears that there is a moisture content below which the mechanical properties of wood increase with decreasing moisture content, but above which they are independent of the moisture content. This particular point is the fibre saturation point.

The determination of the fibre saturation point is difficult and besides mechanical tests, electrical resistance changes with moisture content have been used. Also, a shrinkage-moisture content technique as well as extrapolation of the sorption isotherm to 100% relative humidity may be used.

The estimate of M_f based on the the extrapolation of the sorption isotherm is a faulty definition and has resulted in considerable confusion. Under the assumption that capillary condensation occurs at about 99.5% RH, the fibre saturation point in reality corresponds to this relative humidity rather than 100%. In practice, values based on extrapolations to 99.5 or 100% RH are indistinguishable because the sorption curves rise so rapidly above 90% RH. Therefore, it is difficult to estimate the fibre saturation point with any certainty. Fibre saturation points are usually at moisture content between 27% and 32%, according to the literature (Stamm 1964, Skaar 1988).

2.3.4. Capillary condensation

There is still a significant amount of water uptake above 70% RH which is not pure sorbed water, but increasingly condensed water because of liquid bridges that can appear between the walls in the pores. Capillary condensation depends on the form and the radii of the pores but the fact that the wood structure swells when water is sorbed to the surface makes it difficult to determine when exactly capillary condensation may occur. The theory describing the conditions when liquid bridges may arise in the pores is given by the Kelvin equation (Stamm 1964, Skaar 1988):

$$r = \frac{2 \cdot \sigma \cdot M}{\rho \cdot R \cdot T \cdot \ln(1/RH)} \tag{2.2}$$

where

σ	Surface tension (N/m)
M_w	Molecular weight of water (g/mole)
ρ	Density of water (kg/m^3)
R	Gas constant (J/K·mole)
T	Absolute temperature (K)
RH	Relative humidity (-)

In Table 2.1, values of the size and the form of the pore, which will be filled with water at the corresponding relative humidity, are calculated for 27°C (300K). The values marked with an * are questionable because the lower pressure in the pores is not supposed to be

from the surface tension as considered in the Kelvin equation (Stamm 1964). This is due to the calculated radii are less than 5nm, the capillary diameter of the 10nm being 30 times that of a water molecule. This indicates that the contribution from capillary condensation is only valid or true above 90% relative humidity because the concept of surface tension assumes that large numbers of molecules are involved which ceases to be true.

It appears that capillary condensation only occurs to a limited degree within the cell wall. The void volume of dry cell walls is less than 2% of the cell wall volume and since these small voids are surrounded by a dense structure of cellulose chains, it slows down or even prevents the water from entering (Stamm 1964). It is likely that the major part of the capillary condensation takes place after the cell wall is almost saturated, that is when the relative humidity is above 0.90 or most likely from 0.995. However, reservations have to be taken because sorption hysteresis also has been attributed, at least in part, to capillary condensation.

The reason is that when a meniscus is receding in a capillary, as in desorption, the contact angle at the wall surface will be smaller than when it is advancing as during adsorption. Therefore, more sorbed water will be present during desorption than during adsorption and the boundary where capillary condensation occur might vary correspondingly. According to Figure 2.16 capillary condensation already begins at about 75% RH which is based on a model by Simpson. This shows the variation there exist between different models and stresses the importance of the assumptions made.

Table 2.1. Relationship of relative humidity RH, and capillary pore radius at 27°C.

Relative humidity (-)	Pore radius (μm)
1.0000	-
0.9999	10.9
0.999	1.09
0.99	0.105
0.9	0.0101
0.8	0.0048*
0.7	0.0029*
0.6	0.0021*
0.4	0.0012*

2.3.5. Suction curves

The difficulty in controlling and maintaining accurate humidity at high relative humidities has led to the use of the pressure plate and the pressure membrane technique (Cloutier et al. 1995, Tremblay et al. 1996). In this method, the fibres from a saturated condition are subjected to a hydrostatic tension of sufficient magnitude to reduce the relative humidity to values between 100% and 93%. This corresponds to hydrostatic tension values from 0 bar (100%) to 100 bar (93%) based on equation 2.4.

A thin layer of fibres is placed on a saturated porous plate and the tension is applied by a gas pressure above the plate. The pressure plate apparatus is shown schematically in Figure 2.13. The saturated layer of fibres and the plate is mounted in a pressure vessel. The vessel

is closed and nitrogen pressure is applied. Since the pores of the plate are sufficiently fine, water cannot be forced from the plate, but water is forced from the thin layer of fibres through the plate to atmospheric pressure at the outlet. This process continues until equilibrium is attained, the time where no water any longer is expelled from the plate, through the outlet. After this, the pressure is released and the thin fibre sample is removed at the moisture content determined. The procedure is repeated at other pressures until a suction curve is obtained.

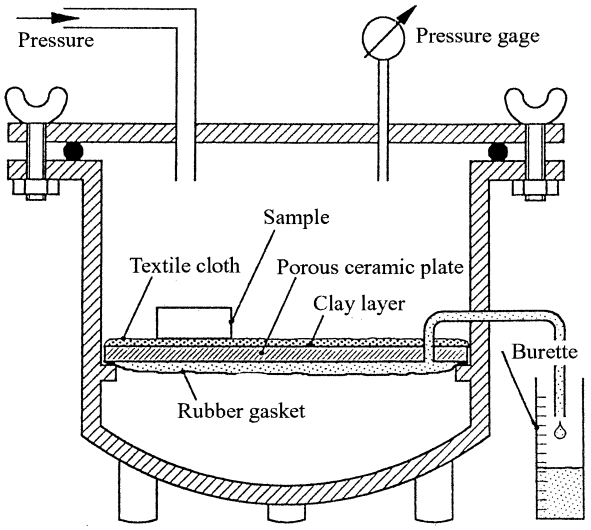

Figure 2.13. Schematic diagram of the pressure plate apparatus.

At equilibrium, the hydrostatic tension in the sample is the same everywhere. The tension is theoretically related to the curvature of the water surface, the meniscus, and the relative humidity above the curved surface. The relation between these quantities is given by the Kelvin equation 2.2 and the la Place equation 2.3 relating the hydrostatic tension P_{suc} (suction pressure) with the surface tension and the radius of curvature r.

$$P_{suc} = -\frac{2 \cdot \sigma \cdot \cos\theta}{r} \tag{2.3}$$

where
σ Surface tension (N/m)
θ Contact angle between the liquid water and solid (usually it equals 0°)
r Radius of the pore (m)

By combining equation 2.2 and equation 2.3 to 2.4 it is possible to make the calculations required to compile Table 2.2.

$$P_{suc} = -\frac{\ln(RH) \cdot R \cdot \rho \cdot T}{M} \tag{2.4}$$

Table 2.2. Relation between hydrostatic tension P_{suc} (suction pressure) and the relative humidity (temperature 20°C).

P_{suc} (bar)	Relative humidity (%)
100.0	92.86
31.6	97.69
10.0	99.26
1.3	99.91
1.0	99.93
0.4	99.97
0.1	99.99

The mechanism by which equilibrium is reached is complicated process. At low tension or pressure and high moisture contents, equilibrium is attained primarily by capillary conductivity. That is, by flow of liquid water from the thin layer of fibres to the plate. As the moisture content decreases, it is assumed that the water takes part in an evaporation and condensation process that contributes increasingly to the attainment of equilibrium.

2.3.6. Ink-bottle effect

The hysteresis phenomena have been a point of discussion for many years. In the high humidity region, where capillary condensation possibly occurs, the pore structure and size does affect the moisture content. The reason for the desorption curve to be above that of adsorption could be due to the "ink-bottle" effect. The "ink-bottle" effect is illustrated in Figure 2.14 where a part of a pore is shown

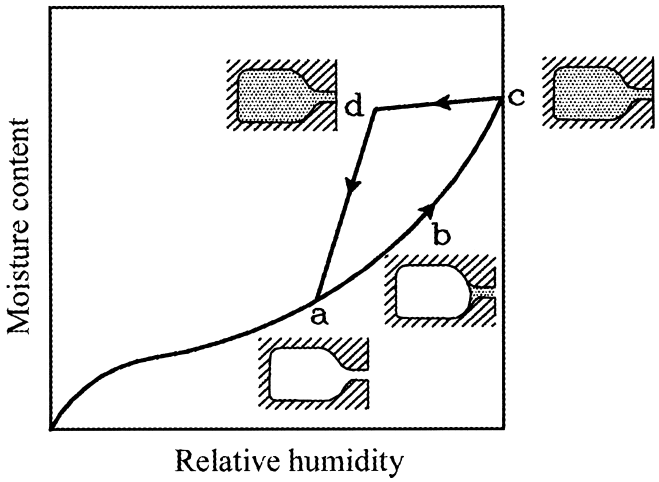

Figure 2.14. Hysteresis due to "ink-bottles".

To begin with, during the adsorption the pore is empty (a) and as the relative humidity increases the bottleneck will successively be filled with capillary water. After the bottleneck is filled, the pore will remain empty until the humidity reaches the point equivalent to the internal radius of the pore. At this state, the pore will be filled with water. Then, during the desorption process, it is the bottleneck that determines when the pore is emptied. Since the bottleneck is smaller than the internal radius of the pore, the water will be drained abruptly at the time when the humidity is equivalent to the radius of the bottleneck. Therefore, the water in the pore will be confined until a lower humidity is reached than during the adsorption process. The moisture content will likewise be higher during desorption than during the adsorption process.

2.3.7. Sorption modelling

According to sorption theories, wood and plants are considered as hygroscopic porous materials with a large internal surface. On this surface, water is sorbed as the outcome of the forces of attraction between the water molecules and the atoms composing the wood or plant matrix. The water molecules are from the beginning sorbed to the polar sorption sites available, the hydroxyl groups. From a chemical point of view, the adsorption of water molecules takes place by two main kinds of forces, either physical or chemical forces corresponding to physisorption and chemisorption.

In physisorption there is a Van der Waals interaction between the water molecules and the lignocellulosic medium. Van der Waals interactions have a long range but are weak. The energy released when a molecule is physisorbed is of the same order of magnitude as the enthalpy of condensation. Typical values are in the region of 20kJ/mol (Atkins 1994). In chemisorption the water molecules stick to the surface by forming a chemical (usually covalent) bond and the enthalpy of chemisorption is very much greater than that for physisorption. Typical values are in the region of 200kJ/mol (Atkins 1994), but in this context no covalent bonds are formed between the water and the lignocellulosic medium. Only secondary bonds as hydrogen bonds and Van der Waals forces are present.

The adsorption of water vapour is primarily due to hydrogen bonding and Van der Waals forces between the water molecules and the hydroxyl groups. The hydrogen bonding is very strong (20-30kJ/per mole of water, Stamm 1964) and is formed when the primary layer of water molecules is attached directly to the hydroxyl groups in the amorphous parts of the cell wall. Although the physical structure of the cell wall is almost completely mapped today, it is still a question where the water adsorption takes place exactly, especially when the relative humidity is above 40%.

2.3.8. Langmuir and Brunauer, Emmet and Teller (BET)

The adsorption of water has been studied from a molecular point of view by Stamm (1964) and Skaar (1988). Different theories of adsorption on surfaces have been proposed over the years for explaining the sorption isotherm. The simplest isotherm is described by Langmuir (1918) and assumes that the adsorption cannot proceed beyond monolayer coverage, and that the ability of a molecule to absorb to a given site is independent of the occupation of the neighbouring sites. The Langmuir isotherm corresponds to the BET monolayer curve on Figure 2.15.

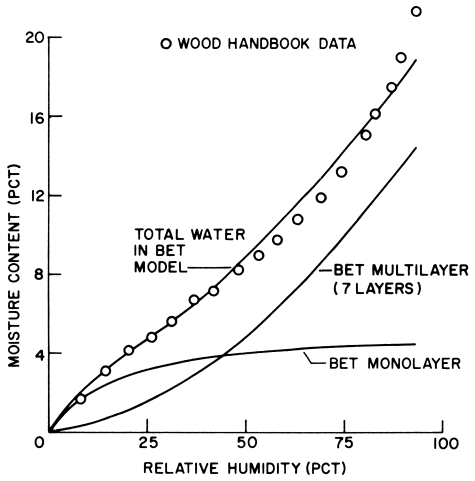

Figure 2.15. BET sorption theory fitted to sorption data at 40°C from Wood Handbook (1974).

The most widely used theory dealing with multilayer adsorption is derived by Brunauer, Emmet and Teller (1938). This particular isotherm is called the BET isotherm and is an extension of the earlier theory of Langmuir. The BET theory assumes the initial coverage to act as a substrate for further adsorption and instead of levelling off at high water activities as the Langmuir isotherm, it rises indefinitely. It rises when the relative humidity increases because there is no limit to the amount of water that may condense on the surface of the material, but the theory is limited to relative humidities below approximately 40%. However, at high relative humidities, the model does not fit satisfactorily because the number of layers is unrestricted. The BET equation was improved (Brunauer et al. 1938) to fit the sorption when the relative humidity is beyond 40% by restricting the number of layers to n. The general form of the BET model is given as

$$m = \frac{m_m \cdot C \cdot RH}{1 - RH} \cdot \frac{1 - (n-1)RH^n + n \cdot RH^{n+1}}{1 + (C-1)RH - C \cdot RH^{n+1}} \tag{2.5}$$

where

m Fractional moisture content (kg/kg)
C Constant for the heat properties of the system
RH Relative humidity (-)
m_m The moisture content when the monolayer has just been formed (kg/kg)
n Number of molecular layers (-)

When n=1, this equation reduces to the Langmuir monomolecular adsorption form

$$m = \frac{m_m \cdot C \cdot RH}{1 + C \cdot RH} \tag{2.6}$$

It is important to remember that the BET theory's greatest use is probably in estimating surface area from adsorption of gases on solids where the gas does not swell the solid.

Since adsorption of water does swell lignocellulosic materials, the application of this theory is of limited use.

2.3.9. Simpson

In continuation of the BET theory described above, Simpson (1973) modified this theory by adding the capillary contribution. He assumed cylindrical pores of length L and radius r whereas the volume of capillary water is

$$V_c = \pi \cdot r^2 \cdot L \tag{2.7}$$

where
r Radius of cylindrical pore (m)
L Length of pore (m)

and the moisture content due to capillary condensation is then

$$m_c = \frac{\rho \cdot V_c}{m_0} \tag{2.8}$$

where
m_0 Dry weight of the sample (kg)
ρ Density of water (kg/m^3)

Combining equations 2.2, 2.7, and 2.8 gives

$$m_c = \frac{\pi \cdot L}{m_0} \cdot \left(\frac{2 \cdot \sigma \cdot M}{R \cdot T \cdot \ln(1/RH)} \right)^2 \tag{2.9}$$

If the assumption is made that capillary condensation is a separate sorption mechanism operating in addition to mono- and polymolecular sorption, this contribution may then be added to that of the BET model, equation 2.5 as proposed by Simpson (1973). The result of this is shown in Figure 2.16, where the capillary contribution becomes very important at high humidities. By adding the contributions from BET monolayer and multilayer together with the capillary water, the total sorption isotherm appears.

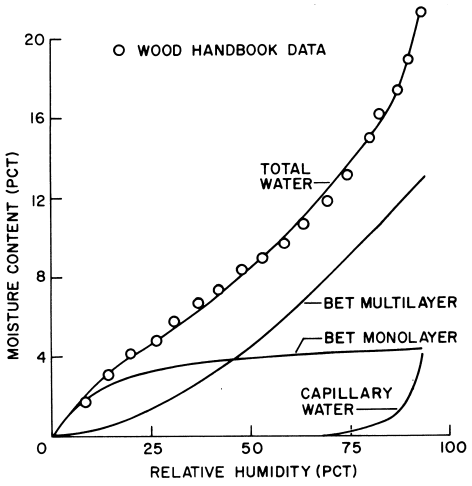

Figure 2.16. Sorption model consisting of BET model and the contribution from capillary condensation. Fitted with sorption data at 40°C from Wood Handbook (1974).

2.3.10. Dent and Hailwood–Horrobin

Dent (1977) proposed a more satisfactory description than the BET theory by small modifications of the same model. In both the Dent and the BET theories, water is presumed to be sorbed as either primary water or secondary water respectively. That is, water molecules sorbed to the primary sites are those with high binding energies, e.g. sorbed to hydroxyl groups while secondary sorption sites are those exhibiting lower binding energies, e.g. molecules sorbed on top of the primary layer. The difference between these models is that the secondary layer in the BET theory is supposed to have equal thermodynamic properties as liquid water, whereas the Dent model assumes that they are different. The Dent model is written as

$$m = \frac{m_m \cdot b_1 \cdot RH}{(1 - b_2 \cdot RH) \cdot (1 - b_2 \cdot RH + b_1 \cdot RH)} \tag{2.10}$$

where

m_m The moisture content when the monolayer has just been formed (kg/kg)
RH Relative humidity (-)
b_1 Constant equal to $A_1/(A_0 \cdot RH)$
b_2 Constant equal to $A_i/(A_{i-1} \cdot RH)$ where $i \neq 1$
A_0 Total area available for sorption (m^2)
A_1 Area covered with 1 layer of water molecules (monolayer) (m^2)
A_i Area covered with i layers of water molecules (m^2)

In the BET theory, b_2 is taken as unity since the energy of the secondary sorbed water is considered equal to liquid water. This is exactly the difference between the Dent and BET theories. Dent considers the secondary sorbed water to be different from primary sorbed water and liquid water, but the third, fourth and so on layers to be the same as the secondary sorbed water.

Hailwood–Horrobin (Skaar 1988) developed a model quite similar to the BET theory. The water and polymer (lignocellulosic material) is considered to be in solution. The water absorbed is assumed to be in two different states: Either it forms a hydrate with the polymer, that is combined to a unit in the polymer or it is in solution with the polymer like dissolved water. It is presumed that the model is based on two or more equilibria. One is between the dissolved water and the water vapour in the surroundings, along with any number of equilibria between the hydrated water and the dissolved water. The general form of the model in the case of one hydrate as used in this analysis can be written

$$m = m_h + m_d = \frac{18}{W} \cdot \left(\frac{K_h \cdot K_d \cdot RH}{1 + K_h \cdot K_d \cdot RH} + \frac{K_d \cdot RH}{1 - K_d \cdot RH} \right) \tag{2.11}$$

where

m_h Fractional moisture content corresponding to the hydrated water (kg/kg)
m_d Fractional moisture content corresponding the dissolved water (kg/kg)
W Molecular weight of the wood per mole of sorption sites (g/mole)
RH Relative humidity (-)
K_h Equilibrium constant similar to b_1 in the Dent model
K_d Equilibrium constant similar to b_2 in the Dent model

The ratio between 18 and W is the moisture content corresponding to complete hydration of each sorption site in the polymer, which is analogous to m_m, the moisture content at complete monolayer coverage in the Dent model. The 3 parameters fitted in the Hailwood–Horrobin model are m_m, K_h and K_d.

A more general model than the one based on a single hydrate is also proposed by Hailwood–Horrobin. This model is more advanced and hydrates of several kinds are proposed, each with different equilibrium constants, K. For further details, refer to Skaar (1988) and Simpson (1973, 1979).

2.3.11. SORP–model

Another variation of the BET model is the SORP model proposed by Nielsen (1993). This model extends the BET model by a finite number of layers of water molecules to be adsorbed onto the surface. Beyond 40-45% RH, the model estimates three parameters by mathematical fitting of the experimental data, the solid density of the sample and the porosity. The parameters are further used to estimate the sorption isotherm from 40-45% RH until close to 100% RH. The model then relates the adsorption of gases at low relative humidities with that of capillary condensation in the high humidity region. The BET model is based on two parameters (C, m_m) whereas the SORP model is based on five parameters (C, m_m, Q, P, M). C is a parameter that depends on the adsorption heat of the first layer and of the next layers, and since adsorption heat depends on the temperature both the BET and SORP model are temperature dependent. The result of the modified BET equation is summarized in 2.12 and 2.13.

$$m\{RH\} = \frac{C \cdot m_m \cdot RH \cdot n\{RH\}}{1 + (C-1)RH}; \quad m\{1\} = m_m \cdot n\{1\} \tag{2.12}$$

$$n = n\{RH\} = \frac{1 - RH^Q}{1 - RH} + \frac{RH^{Q \cdot P}}{1 - RH^P} \cdot (1 - RH^{P \cdot M}); \quad n\{1\} = Q + M \tag{2.13}$$

where

m	Fractional moisture content (kg/kg)
C	Constant for the heat properties of the system
RH	Relative humidity (-)
m_m	The moisture content when the monolayer has just been formed (g/g)
n	Number of molecular layers (-)
Q	Fitting parameter
P	Fitting parameter
M	Fitting parameter

Q, P and M are determined by linearization of experimental data. Best parameters are obtained optimising the quality of linear regression (r^2) with respect to Q, P and M keeping the heat properties constant $C > 0$ (Nielsen 1993).

The three parameters Q, P and M are, according to Nielsen (1993), a physical constant of the solid/gas system (Q) and, pore specific quantities (P, M) "controlling" the influence of pore geometry, i.e. shape and size distribution. Exactly the pore geometry is questionable in respect of the shrinkage/swelling properties of wood- and plant fibres. The model is also used for stiff porous materials and is likely more reliable here when it comes to pore geometry. For the modelling of the sorption isotherm with Q, P and M considered as fitting parameters current results are very reliable.

However, the SORP model is developed to estimate the pore size distribution under certain assumptions. Based on the sorption isotherm, the assumed number of layers of adsorbed water molecules and the assumed contact angle of the water, the accumulated pore size distribution is calculated. In the calculation of the pore size distribution, the Kelvin equation is used whereby the capillary condensed water is included, according to the assumptions about the surface tension as mentioned in paragraph 2.3.4. In addition to the pore size distribution, an estimation of the surface area is calculated (Nielsen 1993).

2.3.12. Cluster theory

Besides the classic mono- and multilayer theories there is a relatively less used cluster theory. This cluster theory has recently been proven by Hartley & Avramidis (1993,1994), by applying the theory of Zimm & Lundberg (1956). The water molecules are randomly attached to sorption sites until the moisture content is about 20% whereafter additional molecules show a tendency to attach to existing bridges of water molecules forming a cluster. Beyond 20% moisture content, the clusters then become larger and larger until the maximum physical size or when the radii of the pores or void spaces are too small to avoid condensation, Figure 2.17. The average size of the cluster is found to be greater than 10, but estimates of 98 are found. For bulk water the maximum number of water molecules

attached together forming a cluster is determined to about 57 (Hartley & Avramidis 1993). According to a maximum of 57 for bulk water the estimate of 98 is likely too high and the estimation method needs to be further improved in order to reach values below 57.

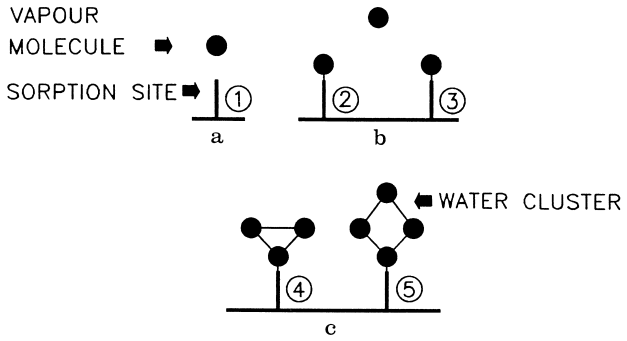

Figure 2.17. Water cluster formation during sorption of water in lignocellulosic materials (Hartley & Avramidis 1993).

With regard to the sorption isotherm and the description above, this can be divided into three regions. The first region is where the slope of the curve decreases as the relative humidity increases. In this region, the water molecules are randomly attached to free hydroxyl groups and the forces are characterised by hydrogen bonding. In the second region, only small changes take place primarily due to a balancing process where the molecules re-organise to the same energy level. In the third region, the moisture content increases substantially because the cluster formation begins and of course also due to capillary condensation in the larger pores and voids in the lignocellulosic structure. In this region, the swelling also accounts for the increased moisture content when some of the crystalline parts begin to break, thus creating more voids. It is assumed that water can squeeze in between small parts of the crystalline structure like illustrated by the zipper model and thereby create additional sorption sites.

2.3.13. Supplementary sorption theories

In addition to the theories already listed in this chapter just a few others are going to be mentioned. King (1960) derived a sorption model whose final equation is almost similar to that of Hailwood–Horrobin, but more based on the BET theory. It again distinguishes between two major portions of sorbed water, water in direct association with the lignocellulosic material and water that is somewhat removed from the direct association. Pierce (1929) developed a sorption theory which is almost like the BET, Hailwood–Horrobin and Kings model. There is water intimately bound to the polymer and water less tightly bound to the polymer by forces similar to those in liquid water.

The sorption theory of Bradley (1936) is based on the reduction in dipole attraction between the several layers of water sorbed onto the surface of the polymer. Also, Malmquist (1958, 1995) proposed a sorption theory in terms of space-dimensional factors within the cell wall. The model considers the space each molecule can occupy and whether it takes place in one, two or three dimensions. Kadita (1960) derived another equation for the sorption isotherm but still based on monomolecular and multilayer sorption.

Many other theories have been proposed and derived for biological materials, some of them exclusively for lignocellulosic materials like wood and plants. The models mentioned here are the most relevant with respect to wood and plant fibre research but for further details refer to Van den Berg and Bruin (1981) or Wadsö (1997).

2.4. Water holding capacity

All the theories listed above describe and characterise the sorption isotherm. Different theories with different theoretical basis tend to approach the experimental result by a best fit, but based on theories rather than empirical considerations. The basic question is the understanding of how the water is sorbed into the structure and what influences the moisture sorption behaviour of the material.

Basically water has been identified in three different states. It is either non-freezing water, freezing, or free water even though the non-freezing water sometimes is called freezing-bound water due to the freezing point depression. Water molecules sorbed directly to the polar groups, the hydroxyl groups, are called non-freezing water because it never freezes due to the strong binding forces. Water more loosely bound e.g. water held by acid groups are considered as freezing-bound water, i.e. water having a freezing point depression. The third category is the free water held in the lumen of the fibre.

Almost all the sorption theories are based on the assumption that water is sorbed in an amount which depends on the chemical composition of the polymer. Generally speaking wood fibres contain 40-50% cellulose, 25-30% hemicellulose and 25-30% lignin but with varying crystallinity in the cellulose. The degree of crystallinity has proven to be of importance with respect to the water uptake, and in spite of many attempts of characterising the number of water molecules sorbed onto each hydroxyl group, the degree of crystallinity gives substantial information about the sorption behaviour.

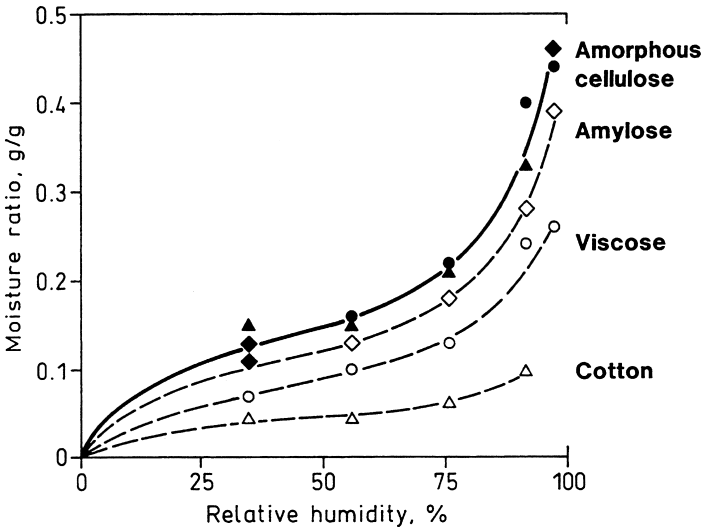

Figure 2.18. Sorption isotherms for some polymers of different crystallinity. Cotton 70%, Viscose 40% and Amylose 15%. The curve for Amorphous cellulose is estimated based on the degree of crystallinity of each of the other three polymers studied (Berthold et al. 1994).

As indicated in Figure 2.18, there is an obvious dependency on the crystallinity regarding the moisture content for materials with varying chemical composition. There is amylose which is a polymer almost like cellulose but instead of the β-1-4 bonds it is changed to an α-1-4 glucosidic bond resulting in a much lower crystallinity. After that comes viscose with 40% and cotton with the highest degree of crystallinity at about 70% and then the least amount of water sorbed. It is clear that the higher the degree of crystallinity, the less water bound to the polymer.

One can compare these results and try to figure out what would be the amount of water sorbed in the material in the case of pure amorphous cellulose. On the assumption that the crystalline parts have been removed, the "theoretical" curve for the amorphous cellulose has been estimated and shown to lie above the others curves as is expected. This is an interesting point and enables one to predict the sorption behaviour of a polymer if the chemical composition is known. These considerations are important in the view of future sorption studies.

Besides the chemical composition of the polymer, different chemical treatments can increase or decrease the sorption capacity. The water molecules are attached to the hydroxyl groups and if these groups are replaced with carboxylic acid groups, the sorption can be greatly increased, especially in the high humidity area. The carboxylic acids can be in either sodium or calcium form, which also have great influence on the sorption capacity as illustrated in Figure 2.19. On the other hand, if a decrease in the sorption capacity is desired, the polymer can be acetylated. By acetylation, the hydroxyl groups are blocked by acetyl. The acetyl is attached to the amorphous hydroxyl sites, hindering water molecules to be sorbed, and thus makes the polymer highly hydrophobic.

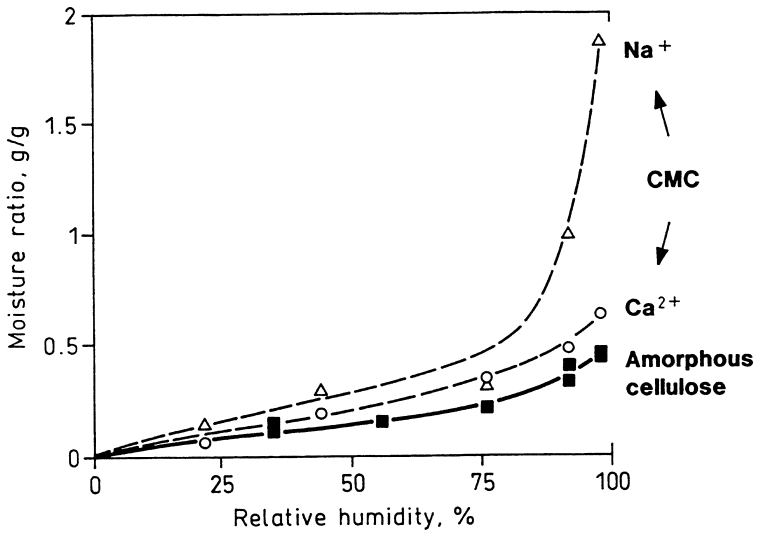

Figure 2.19. Comparison between two chemically modified celluloses, carboxymethylated in the sodium and calcium forms, and the isotherms calculated for amorphous cellulose (Berthold et al. 1994).

As emphasized above, chemical treatments can both increase and decrease the sorption capacity of the polymer. Mechanical treatments also affect the sorption behaviour. First of

all, mechanical treatments such as beating of the fibres increases the total surface area of the fibre and creates new voids and cracks within the fibre.

Evidently, one would expect an increased sorption capacity due to such a treatment. It is a fact that the total water holding capacity increases because the total pore volume is increased if for instance the polymer is immersed into water. It is argued that in a humid environment, the sorption capacity is the same because the chemical composition and the sorption capacity of the individual polymers are the same and therefore an increased number of voids would not influence the sorption behaviour.

In Figure 2.20, the isotherm for mechanically treated and untreated wood is shown indicating no difference in the sorption behaviour. Supported by these facts, the mechanical treatment does not increase the number of sorption sites or hydroxyl groups, and thus does not increase the moisture content.

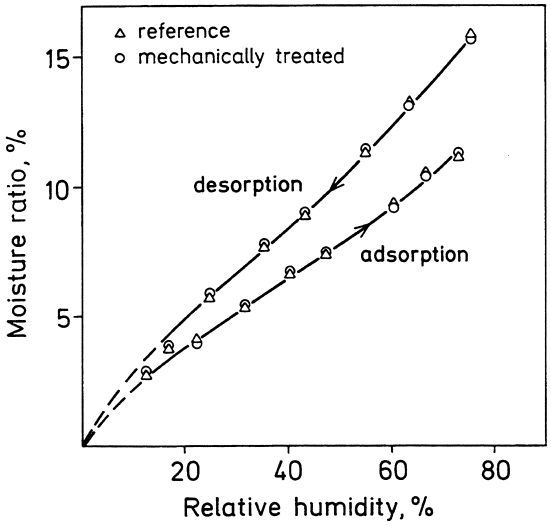

Figure 2.20. Comparison between isotherms for mechanically treated wood and reference samples (Östberg & Salmén 1991).

2.5. Thermodynamics of sorption

To characterise the wood-water system, thermodynamics has been used in an attempt to quantify several parameters related to the energy of the water, whichever of the three basic forms, solid, liquid or vapour is present. Calculations are based on theoretical considerations as well as experimental measurements.

To quantify the amount of each of the three main constituents, cellulose, hemicellulose and lignin in cellulosic materials, the enthalpy changes during moisture sorption provide useful information. Enthalpy changes like differential heat of sorption ΔH_S can be calculated by use of the Clausius-Clapeyron equation or by the calorimetric method. The first method requires sorption isotherms at two or more temperatures and the latter a calorimeter with the opportunity to measure heat changes.

2.5.1. Differential heat of sorption

Water sorbed into the cell wall is analogous to frozen water or water in the solid state in that it has a lower enthalpy than free water or liquid water. However, if the moisture content increases, the enthalpy increases until the fibre saturation point above which the enthalpy is essentially the same as liquid water. The magnitude of heat of vaporization of sorbed water ΔH_V, is always greater than the heat of vaporization of liquid water ΔH_0, and the difference, ΔH_S, is the differential molar heat of sorption.

This means that ΔH_S is the additional heat needed to evaporate sorbed water instead of liquid water. This is in agreement with the fact that enthalpy of frozen water is lower than the enthalpy of free water H_W as stated above, that is

$$\Delta H_s = \Delta H_V - \Delta H_0 = H_V - H_S - (H_V - H_W) \tag{2.14}$$

$$H_S = H_W - \Delta H_S \tag{2.15}$$

Based on Clausius-Clapeyron equation (Skaar 1988), the molar heat of vaporization ΔH_0 of liquid water at Kelvin temperature T is written

$$\Delta H_0 \approx -R[d\ln(p_0)/d(1/T)] \tag{2.16}$$

where R is the gas constant, p_0 is the saturation vapour pressure of water at temperature T. The heat of vaporization of sorbed water is given by

$$\Delta H_V \approx -R[d\ln(p)/d(1/T)]_m \tag{2.17}$$

p is the partial vapour pressure of water. Combining equations 2.14, 2.16 and 2.17 an analogous equation for the calculation of the heat of melting ΔH_m of ice is given

$$\Delta H_S \cong +R[d\ln(p_0/p)/d(1/T)]_m \tag{2.18}$$

If ΔH_S is constant between the Kelvin temperatures T_1 and T_2 and the corresponding relative humidities of the wood are RH_1 and RH_2, respectively at constant moisture content, the Clausius-Clapeyron equation can be written

$$\Delta H_S \approx R \cdot T_1 \cdot T_2[\ln(RH_2/RH_1)/(T_2 - T_1)]_m \tag{2.19}$$

If the sorption isotherms at two different temperatures are known, equation 2.19 can calculate ΔH_S at any wood moisture content on the curves as shown in Figure 2.21.

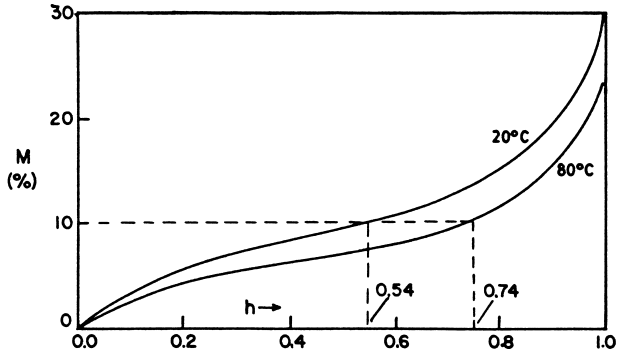

Figure 2.21. Sorption isotherms for wood at 20°C and 80°C, showing increase in activity h (relative humidity) with increase in temperature for wood at constant moisture content M (Skaar 1988).

From the differential molar heat of sorption, ΔH_S, the differential heat of sorption Q_S is achieved from the definition $Q_S = \Delta H_S/M_w$, where M_w is the molar mass of water (18 g/mol). To obtain the full relationship between Q_S and the wood moisture content, calculations of Q_S are made for all the values of ΔH_S at each particular moisture content. Curves similar to Figure 2.22 will then appear.

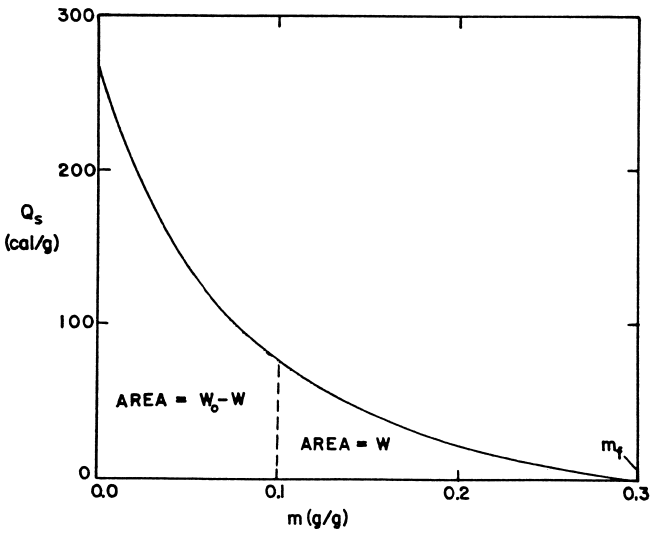

Figure 2.22. Typical curve for the differential heat of sorption Q_S in relation to moisture content. The area to the left of m=0.1 is the integral heat sorption (W_0-W). The area to the right of m=0.1 is equal to the heat of wetting W, and the total area is equal to the total heat of wetting W_0 (Skaar 1988).

2.5.2. Heat of wetting

As mentioned in the beginning of this section, enthalpy changes are possible to measure experimentally by calorimetry. In practice, it is a difficult task, since it requires accurate equipment for the measurements and one needs to be careful when the experiments are carried out. Prior to the experiment, a small amount of particles are equilibrated at a

constant relative humidity within the calorimeter and to the initial calorimeter temperature. Water is then added until the particles are immersed in an excess of water to make sure the particles are fully saturated.

Along with this process, the heat generated from the particles is measured by the calorimeter due to the temperature rise as part of the reaction. The heat generated, divided by the dry mass of the sample, is defined as the heat of wetting W for the sample. For wood at initially zero moisture content, the heat of wetting is the total heat of wetting symbolized by W_0. The difference W_0-W is the integral heat of sorption for particles at some higher initial moisture content m. W_0 and W are related to Q_S as follows

$$W = \int_{m}^{m_s} Q_S dm \tag{2.20}$$

$$W_0 = \int_{0}^{m_s} Q_S dm \tag{2.21}$$

$$W_0 - W = \int_{0}^{m} Q_S dm \tag{2.22}$$

In Figure 2.22 the relationships of these equations are shown graphically where W_0 is equal to the total area under the curve, and W is the area under the curve to the right from the initial moisture content m corresponding to W. The area W_0-W under the curve is from zero to the initial moisture content m corresponding to W.

If the heat of wetting is known as a function of the moisture content, it is possible to determine Q_S at any particular moisture content, because

$$Q_S = d(W_0 - W)/dm = dW/dm \tag{2.23}$$

since W_0 is a constant.

CHAPTER 3

Measurement of sorption of water

3.1. Introduction

In Chapter 2, it was shown that the determination of the sorption isotherm is a crucial task in the validation of the sorption behaviour of wood and plant fibres. To quantify the complete character of the material, measurements of sorption curves at elevated temperatures as well as accurate measurements and control of the relative humidity are important.

This chapter reviews and discusses existing knowledge of measurement of water in wood and plant fibres. The most ordinary methods used to determine sorption curves are evaluated and advantages and disadvantages are described. As a result, the reason why the climate chambers have been developed as part of this investigation is explained.

In addition to the interpretation of the different techniques, the measurement of the relative humidity is explained. Different humidity sensors and principles of measuring dew point are discussed and special attention is focused on the equipment used in the climate chambers.

3.2. Measurement of sorption curves

3.2.1. Desiccator method

The desiccator method is one of the ordinary methods used within sorption studies on wood and plant fibres, solid wood and porous materials in general. Saturated salt solutions of inorganic salts are placed in a desiccator to obtain a specific and constant relative humidity, Figure 3.1. The samples are located above the aqueous solution and vacuum is often applied to decrease the time to equilibrium of the samples.

The samples are cut into small pieces to increase the surface area thus again decreasing the time to reach equilibrium, and placed in small containers. Every time the mass is determined, the samples are in turns moved to a balance and afterwards returned to the desiccator. This procedure is repeated until the equilibrium mass is obtained.

The advantage of this technique is that it is robust and relatively simple. However, time to equilibrium is quite long. To decrease the time to equilibrium, vacuum is sometimes applied but is unfortunately released every time the desiccator is opened. Because the samples cannot be weighed inside the vessel, it is necessary at regular intervals to open the desiccator. Moreover, temperature fluctuation may also influence the results. To keep the temperature constant the desiccators are often placed in a temperature controlled water bath.

Figure 3.1. Desiccator containing a saturated salt solution and small samples in glass containers.

3.2.2. Water activity measurements

Another method, less used than the desiccator method, is measurements of the relative humidity (water activity) inside the samples. Equipment for water activity measurements is primarily designed for food science but can be used for porous materials as well. The apparatus is shown in Figure 3.2. Samples conditioned to equilibrium at different moisture contents are enclosed in the apparatus and a humidity sensor is located inside the small probe above the sample. After relatively short time, a few hours, equilibrium humidity is established inside the probe and the relative humidity is measured.

Figure 3.2. Probe for accurate measurements of the equilibrium humidity inside small samples.

The weight of the sample is not measured by this method and thereby not the moisture content in the sample. To obtain values of moisture content and relative humidity one need to measure the moisture content separately. If the weight of the sample is determined just before it is placed into the water activity apparatus it has to be handled with caution. Even a small amount of water can evaporate when the sample is moved from one apparatus to another disturbing the result. A disadvantage is the limited size of sample possible to place into the small apparatus compared to e.g. the desiccators. On the other

hand, the apparatus is very easy to use and the time it takes to obtain results is very short in comparison to other methods. To keep the temperature constant the apparatus is prepared for water cooling or heating. Otherwise, it has to be placed in a thermostatically controlled room.

3.2.3. Vacuum balance apparatus

In this method, the equipment is build up of several glass tubes connected to each other with applied vacuum inside. The measuring principle is as follows: First, the vacuum is applied and then a small amount of water vapour is let into the tubes giving a certain relative humidity. Because of the air free system the vapour pressure can be measured directly inside the tube system as the total pressure. The sample is suspended from a helical spring balance made of special spring wire or quartz fibres. The change in weight is due to the humidity variation and is determined directly from the change in the length of the spring. Since the spring constant is known the weight can be calculated.

To control the temperature during the experiment all the glass tubes, and thereby actually all the equipment, are immersed in a water bath with constant temperature. Operating the equipment immersed in a water bath makes it slightly more difficult. Together with difficulties in general, the use of the very sensitive spring balance often limits the use of this method. However, if the equipment set up is complete an advantage is the fact that very accurate measurements can be obtained. Another advantage is the sorption process proceeds faster than in an air filled system.

3.2.4. Sorption balance

To automate the process of measuring sorption isotherms several companies have developed small highly sophisticated sorption instruments to manage the relative humidity as well as the weighing process. A microbalance is usually the main component in the apparatus along with a precise humidity generator. The equipment is controlled by a computer and the software provided allows one to program points and intervals for the measurement. Unfortunately this type of equipment is very expensive and almost exclusively made for pharmaceutical research thus limiting the weight of samples to mg rather than g, which is less convenient for research in porous materials as wood and plant fibres.

3.3. Measurement of moisture content

The moisture content, m, is already defined in Chapter 2. It is defined as the ratio of the weight of removable water at equilibrium m_1 to the dry weight m_0 of the wood. The moisture content is expressed as the fractional value (kg/kg) or in percentage terms and is calculated by

$$m = \frac{m_1 - m_0}{m_0} \tag{3.1}$$

where
m_1 Weight of removable water at equilibrium (kg)
m_0 Dry weight of sample (kg)

When wood and plant fibres are saturated, liquid water is present in the cell lumen and the cavities. This is sometimes called free water to distinguish from water sorbed to the cell wall then called bound water. When the material is dried the free water in the cavities is lost first since it is held by weaker forces than the bound water in the cell wall. The moisture content at which all the free water in the cavities is lost and only contains water vapour and bound water in the cell wall is designated the fibre saturation point FSP. As mentioned in Chapter 2 this generally ranges from 27% to 32% of the dry weight of wood (Stamm 1964, Skaar 1988). Many different methods have been used to measure the moisture content of wood and some of the most conventional methods are briefly described here.

3.3.1. Measuring methods

The gravimetric method is based on the weight of the moist sample and subsequent drying of the sample until the dry weight is attained. The weight is measured using a balance sufficiently accurate to obtain the desired precision. Depending on the required precision the dry weight is obtained in an oven, vacuum oven or above a strong desiccant. The drying is discussed later in this chapter.

In the distillation method the wood sample is heated up in a water immiscible liquid which is a solvent for the volatile wood extractives. The water is condensed and separated from the solvent and finally the amount of water is measured volumetrically.

An improvement of the distillation method is the Karl Fisher Titration method giving a more precise result. The method is particularly useful for materials containing volatile components. The technique is today more or less fully automated but only usable for small samples.

Other methods are the use of nuclear magnetic resonance (NMR) techniques, again for very small samples. In addition, different electrical moisture meters measuring the electrical resistance, the dielectric constant or electrical permittivity of the wood are in use. Nuclear radiation techniques using gamma rays or neutrons and subsequent measurements of the intensity of radiation reflected or transmitted through the material are among the more sophisticated techniques.

3.3.2. Drying procedure

The complex of drying is discussed in terms of drying the samples before and after sorption experiments are carried out. As mentioned earlier different ways of drying material samples is used in relation to wood and plant fibre science. At many laboratories abroad, tradition rather than sound considerations dictates which procedure is used. The most conventional methods are oven drying at 103±2°C. However, this method is less precise than vacuum drying or the use of a strong desiccant. Objections to the use of oven drying follows from the fact that there is a risk of evaporation of volatile constituents other than water and the dependence of temperature in the oven and the ambient temperature

and vapour pressure. In addition, the ventilation in the oven may affect the result. The relative humidity in the oven can be calculated using the equation given by Skaar (1988)

$$\left(\frac{p}{P_0'}\right)=\left(\frac{p}{P_0''}\right)\cdot\left(\frac{p_0''}{P_0'}\right) \tag{3.2}$$

where

p	Vapour pressure (Pa)
p_0'	Saturated vapour pressure in the oven (Pa)
p_0''	Saturated vapour pressure (Pa)
(p/p_0')	Relative vapour pressure in the oven (-)
(p/p_0'')	Ambient relative vapour pressure (-)

To illustrate the influence: Say the room temperature is 30°C and the humidity 60%, the relative humidity in the oven at 103°C can be calculated from equation 3.2. Expressing p_0 in Pa $(p/p_0)'=(0.6)(4242/101320)=0.025$. In the case where the ambient temperature is 20°C and the humidity 35% $(p/p_0)'=(0.35)(2338/101320)=0.0081$, less than 33% of the value obtained in the first case. This variation in the ambient conditions might affect the moisture content in the samples after oven drying.

Alternatively, vacuum drying could be used at a lower temperature too because of the low ambient relative humidity. The lower temperature is less harmful to the sample but the time to reach the equilibrium weight takes longer time than at elevated temperatures.

3.4. Measurement of relative humidity

A very important aspect in the measuring of sorption curves is the relative humidity in the environment surrounding the samples. When a sample is in equilibrium, the equilibrium moisture content is measured as well as the corresponding relative humidity. The relative humidity or vapour pressure can be measured by a variety of techniques. The most ordinary techniques are hygrometers including different humidity probes based on resistive or capacitive sensors, psychrometers and dew-point instruments. Depending on the measuring interval different sensors are preferred in different intervals. Especially at high relative humidity, beyond 0.90, it is difficult to measure the accurate value of the relative humidity. Therefore, the determination of the sorption isotherm in this region is a difficult task.

3.4.1. Hygrometers

Today hygrometers are often used because they are easy to use and because of their low price. Electrical hygrometers are based on changes in resistance or capacitance caused by either a decrease or increase in the humidity. Resistance hygrometers generally consist of hygroscopic salts or activated films that are sensitive to humidity changes. The most widely used element is made from a low concentration of lithium chloride in a plastic binder. To protect it from contamination the sensor can be enclosed in a cellulose acetate film. The humidity range is from 15% to 99% relative humidity with an accuracy of ±2% RH in

typical use or ±1% RH in narrow range. The temperature range is from –10°C to 80°C (Wiederhold 1997).

Capacitive sensors use either a polyamide or cellulose acetate thin film deposits between conductive electrodes. The film acts as a capacitor dielectric and changes its dielectric constant as moisture is adsorbed or desorbed by the thin film. As the water molecule is highly polar, even small amounts of water can change the sensor capacity to a measurable extent. The relative permittivity is 80 for water compared to 2 to 6 for the polymer material. This property of the water molecule makes capacitive measurement an obvious choice for humidity measurement (Wiederhold 1997).

The capacitive sensors have the following advantages: Can be used down to 2% RH, that is a humidity range of 2% to 99% RH. The sensor can be used at higher ambient temperatures, to 185°C in some cases, that is a temperature range of –10°C to 185°C.

There is a large price span on these sensors depending on the quality, response time, hysteresis and long term reproducibility. The intervals where the sensors are fully usable depend on whether the sensors are applied to temperature correction or not, and in case they are, they are often usable in a wide humidity range e.g. 10-90% relative humidity. Calibration at appropriate intervals is needed to make sure the sensor is valid, which is greatly affected by the humidity range and temperature in which the sensor is used. At high humidity and temperature the conditions are harsh and much more regular calibrations have to be performed.

3.4.2. Psychrometer

The wet- and dry-bulb psychrometer is based on the principle of evaporative cooling. The sling psychrometer consists of a wet- and dry-bulb thermometer attached to a hand-operated sling. The wet-bulb thermometer is enclosed in a saturated wick and when rotating the psychrometer air is passed over the wick at a velocity sufficiently high to assure maximum evaporation rate from the wick. Based on these two temperatures, the wet- and dry-bulb, the relative humidity can be determined. The relative humidity can be determined with an accuracy of about ±3% and usually it becomes difficult to use psychrometers below 15% RH due to the problem of cooling the wet-bulb to its full depression. Also measurements below 0°C are difficult to obtain due to freeze-up.

Instead of the sling psychrometer, the air passed over the wick could be generated from a fan. To obtain accurate measurements, if the moistened wick is enclosed and air is passed through, several factors are important (Skaar 1988). For adequate air ventilation over the wick, a minimum 5 m/s is needed. The water reservoir must be replenished at frequent intervals. Unless clean, distilled water has to be used to avoid contamination, or else error will result. Also important are identical calibration of the wet- and dry-bulb temperature sensors and the shielding of the sensors from extraneous sources of energy.

For continual measurements of the relative humidity psychrometers are not yet available. Reliable psychrometers are still not developed ready for connection to a data acquisition unit. One of the problems is to maintain the wick saturated all the time and thereby assure the right wet-bulb temperature to be measured. Apart from that the psychrometer is based

on a simple principle and the results are very precise and are a nice alternative to the electrical hygrometers.

3.4.3. Dew-point sensor

The dew-point sensor or chilled mirror hygrometer is the most accurate, reliable, and fundamental hygrometer commercially available and is therefore widely used as a calibration standard. A drawback of the equipment is that it is very expensive and therefore not used for general measurements. The equipment also requires maintenance by skilled personnel as does monitoring and care of the installation. Most instruments offer an accuracy of ±0.2°C but instruments with accuracies as high as ±0.1°C are available.

The measuring principle for the dew-point instrument is the detection of the dew-point by cooling a reflective condensation surface until water begins to condense. The condensation surface is a mirror and the cooling of the mirror is in modern instruments obtained by thermoelectric cooling. The detection of the condensation is by way of an electro-optic detection system. As condensate forms on the mirror, light scattering occurs, which is detected and amplified by suitable instrumentation. The great sensitivity to contamination of the mirror surface is solved by a unique cycling mirror control technique. However, this is at the expense of some of its measurement properties and the accuracy of the instrument.

Operation of the basic optical dew-point hygrometer is shown in Figure 3.3. The surface temperature of a small gold or rhodium-plated copper mirror is controlled by a thermoelectric cooler (heat pump). A high intensity light-emitting diode (LED) illuminates the mirror. The quantity of reflected light from the mirror surface is detected by a photo-transistor or optical detector.

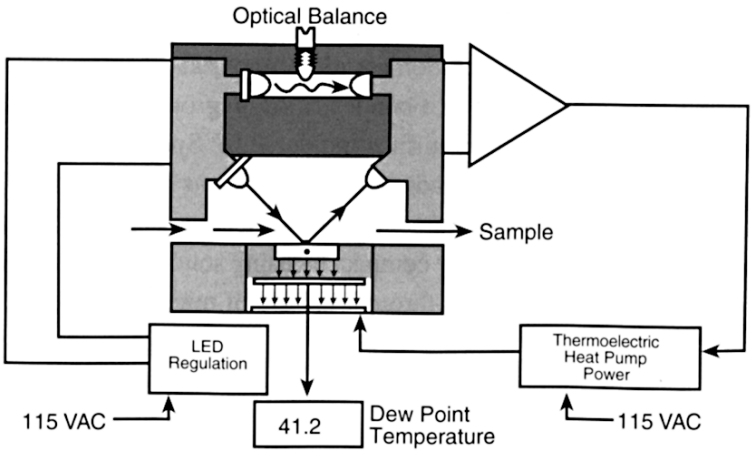

Figure 3.3. Schematic of conventional dew-point hygrometer.

Reflectance is high when the surface temperature of the mirror is above that of the dew-point (dry mirror) and maximum light is received by the optical detector. However, when the thermoelectric cooler reduces the mirror temperature below the dew- or frost-point (if below 0°C), moisture condenses on the surface causing light scattering, thereby reducing the light received by the detector.

The dew-point temperature is displayed on the front panel of the instrument. In addition, some instruments are equipped with a separate temperature sensor to measure the ambient temperature whereby the instrument can calculate and display the relative humidity directly.

3.5. Climate chamber development

Long experience with the employment of the traditional desiccator method in the determination of sorption isotherms, initiated the process of developing a new climate chamber. Considering the disadvantages of the desiccator method, particularly in the field of wood and plant fibre research, many obvious reasons for this appear.

Among the disadvantages are e.g. the following: It is difficult to control the relative humidity inside the desiccators especially when vacuum is applied. One needs to believe in a defined value for the relative humidity instead of real measurements. Furthermore, every time the samples are weighed the equilibrium process is thrown into disorder by lifting the samples from the desiccator to the balance placed in the laboratory surroundings. In addition, all the inconvenience managing the desiccators, opening and closing the lid and applying vacuum is tedious. Moreover, the physical size of samples is very restrained in the desiccators.

Developing a climate chamber increases the size of the conditioned room and thereby allows samples of much larger size to be investigated. Moreover, the relative humidity can be adjusted to exact the preferred value instead of the predefined values from the saturated salt solution. Thereby the most interesting regions in the sorption isotherm can be investigated more intensely and the number of measuring points is almost infinite.

Improvement of the weighing procedure is possible since the samples can be weighed inside the chamber instead of in the surroundings, as is the case with the desiccator method. This will provide a more realistic picture of the sorption process as it assumes to decrease the time to reach equilibrium.

Finally, the relative humidity and temperature can be monitored automatically within each chamber by data acquisition. These data proves the accuracy of the measurements and displays the humidity and temperature history for the experiment.

CHAPTER 4

Design of experimental climate chamber

4.1. Introduction

In this chapter principles and applications of a newly developed climate chamber are presented. The climate chamber was developed during this investigation of the sorption isotherm for wood and plant fibres. The basic principle is based on the mixing of two air streams containing dry and saturated air respectively. Mixing air from these streams makes it possible to generate air with relative humidities between 3% and 96 %.

For measurements of sorption isotherms at elevated temperature an advanced climate chamber has been developed. This chamber is constructed as a double chamber due to condensation problems thus making it impossible to weigh the samples manually within the chamber through a glove in the front. Hence, an automatic carrousel has been developed to weigh the samples in turn.

The process control of the humidity in the chambers is managed by PID-controllers. They open and close the dry and saturated air stream alternately to keep the humidity at the determined set point. The PID-control is connected to at humidity and temperature sensor within the chamber.

In this chapter, description of the important details in the construction of the climate chambers is brought into focus, details that were crucial to overcome for the development of a high precision climate chamber.

4.2. Climate chamber design

4.2.1. Practical approach

As already argued in the previous chapter's last section there are several reasons for developing the climate chamber. Humidity is a crucial parameter in the evaluation of the use of wood and plant fibres for potential industrial purpose.

The outcome of the development process has been five climate chambers where four are for measurements at ambient temperature and one is for elevated temperatures as well. Only the climate chamber for elevated temperature measurements is equipped with an automatic weighing carrousel. Figure 4.1 shows a picture of some of climate chambers developed.

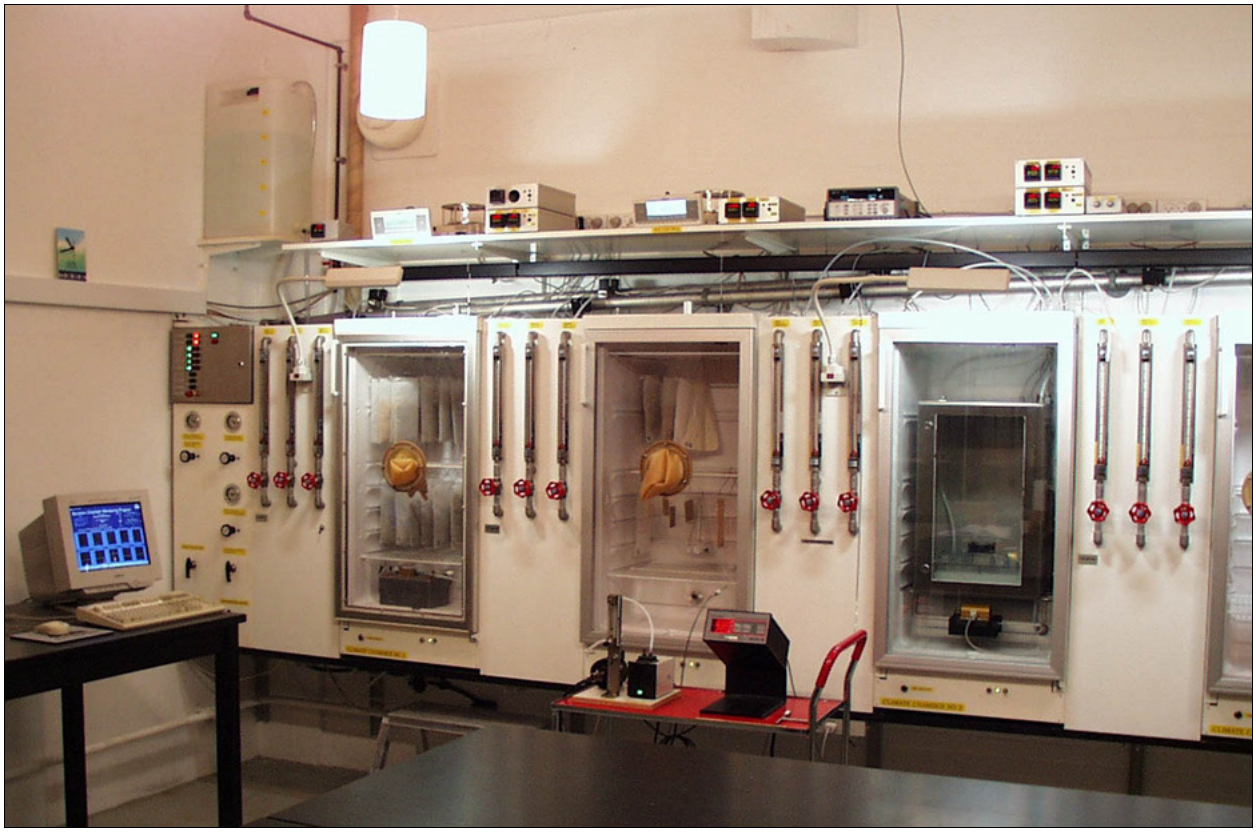

Figure 4.1. Climate chambers specifically developed for sorption studies.

4.2.2. Humidity generation

In the climate chamber the humidity is based on mixing two streams of dry and saturated air respectively. All the air used, both the dry and the saturated stream, is from the same source: The main compressor in the laboratory with approximately 7 bar pressure. First, all the air is sent through a reducing valve to decrease the pressure to 5 bar after which it is sent through an aerosol filter to clean the air for impurities. At this point, the air stream splits into two parallel streams. A dry and a saturated stream.

The dry air stream is obtained in a two-step process beginning in a cool dryer where the air is dehumidified from a relative humidity of 5% to about 1% to 2%. In the second step the air stream is sent through an absorption dryer to reach a dew point at –60°C corresponding 0.002% RH. The principle in the absorption dryer is based on drying at elevated pressure. The air which is already compressed to 5 bar pressure, is dried above silica gel and then expanded to 1 bar pressure (atmospheric pressure in the laboratory). During that process, the relative humidity in the air decreases drastically and the air becomes dry and ready for use.

The saturated air stream is prepared by bobbling air through a vertical cylinder shaped water tank (main saturator). Above the surface of the water, there is a honeycombed stainless steel mesh to separate water aerosols or drops into water molecules before entering the saturated stream. Although it sounds easy to prepare the saturated air, this is

in fact a complicated discipline. Obstacles appear if the temperature fluctuates in the surroundings of the main saturator.

The sensitivity to the ambient temperature is significant. If the relative humidity is adjusted to 96% a change of temperature from 20°C to 21°C causes a change in RH from 96% to 93%. This is of course unacceptable if the measurements are expected to be held at 96 % RH. Even though efforts in insulating the tubes with the saturated air stream and the water tank are attempted, it is almost impossible to avoid such small changes in the inlet air temperature. In an attempt to avoid these effects from the surroundings the climate chamber was installed in a thermostatic controlled room.

In each climate chamber there is a ventilator to stir the dry and saturated streams of injected air. This is to make sure there is a homogeneous distribution of the conditioned air in the entire chamber.

During evaporation of water in the main saturator, the heat of energy required decreases the water temperature below ambient temperature and then the relative humidity in the chambers decreases too. To keep the water temperature constant a heating element is placed in the water inside the water tank. The heating element is controlled by a PID-controller connected to a thermocouple inside the water tank. To ensure a constant water level in the water tank the height of the water surface is controlled by two optical sensors. The sensors are placed in the side of the water tank and connected to a solenoid for opening and closing the water inlet. In Figure 4.2 it is illustrated how the tubes containing the dry and saturated air stream are connected.

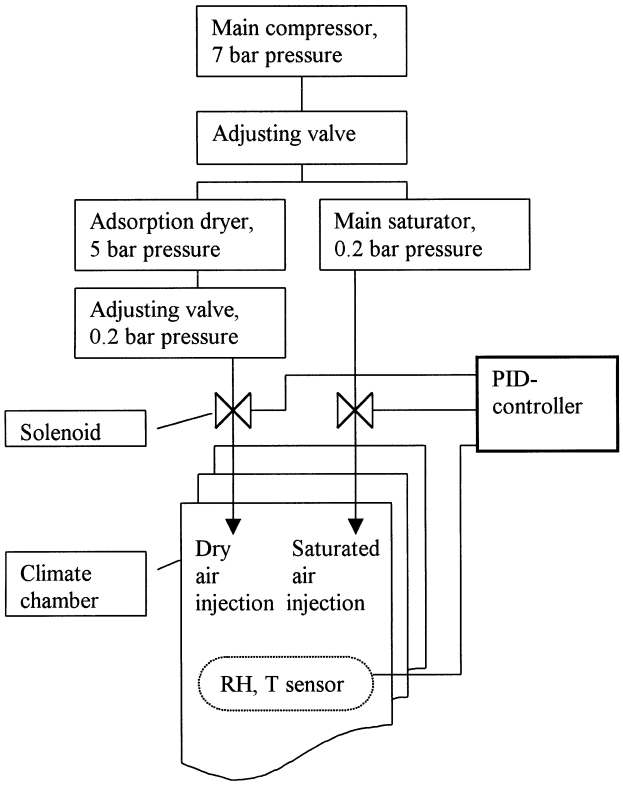

Figure 4.2. Diagram showing the principle of the dry and saturated air streams.

4.2.3. Extra saturator

Since the sorption installation is constructed of five climate chambers in one line, the control of a continuous high relative humidity in each chamber becomes more difficult because of risk of condensation and pressure drop in each individual chamber. An additional saturator as well as the main saturator is therefore developed and installed in each climate chamber. The purpose of this extra saturator is to keep the relative humidity in the saturated air stream as high as possible when it is injected into the chamber. This additional saturation of the saturated air stream is only necessary at relative humidities in the region above 70% when the moisture content in the air becomes high.

In each extra saturator a small heating element is installed due to the energy used for evaporation of water. The heating element consists of a teflon insulated constantan wire coiled around a small cylinder submerged in the water. The temperature of the water in the extra saturator is also controlled by a PID-controller connected to a thermocouple in the water.

4.2.4. Rate of adsorption and desorption

To obtain moisture equilibrium is faster in the climate chamber than in desiccators. This is due to the constant injection and circulation of air in the chamber.

The sample containers also contribute to improve the rate of adsorption and desorption. In the beginning, it was planned to use standard glassware from the shelves as containers for the samples. To increase the rate of sorption a non-adsorbent fine perforated polyester bag was chosen for sample containers. The samples were filled in the polyester bags allowing the air to pass through. The size of the holes in the bags are smaller than the fibres thus keeping them from falling through. The shape of the bags is wide and flat to increase the surface area and the exposed area of the sample, increasing the rate of sorption. Figure 6.2 in Chapter 6 shows an example of a curve depicting the rate of sorption. This curve shows the mass increase versus time when the relative humidity is changed from 15% to 25%.

4.2.5. Relative humidity measurements

The relative humidity in the individual climate chamber is measured by a small humidity and temperature probe installed permanently in each chamber. The probe is a Hygroclip from Rotronic with a temperature range from –40°C to +85°C and a humidity range from 0% to 100% relative humidity. The accuracy is ±0.3°C and ±1.5% relative humidity. The temperature probe is PT100 and the humidity sensor is of the capacitive type. Each sensor is routinely calibrated above certified salt solutions and thereafter adjusted according to the instructions from the producer. In addition, every time a sensor has been exposed to humidities above 90% relative humidity it is calibrated and adjusted to make sure there is no subsequent offset.

As a reference and to calibrate the humidity measurements a chilled mirror hygrometer is used. It is used to measure the dew-point of the conditioned air in the individual climate chamber. It also measures the ambient temperature and thereby directly calculates the relative humidity within the chamber. In a daily routine, the hygrometer is connected to the chambers in turns to spot check the relative humidity measured by the probes. In the front door of each chamber is a terminal for connecting the hygrometer through a tube

and a small pump provides the right amount of air sent through the chilled mirror per minute. Since it is important to supply the hygrometer with a very precise amount of air, an adjustable meter is mounted between the pump and the hygrometer.

The chilled mirror hygrometer also requires to be calibrated on a regular basis. Due to the sophisticated construction and sensitive devices, it requires maintenance by skilled people. Hence, once every second year the chilled mirror hygrometer is sent to the National Physical Laboratory (NPL) in England for certificate calibration. The certificate proves the accuracy and traceability.

4.2.6. Process control

Generally, the process control of temperature and humidity is managed by PID-controllers (Process Integrated Derivative control). The PID process controllers operate in one of three different ways. The determined set point is controlled in on/off control, proportional control or PID-control. Depending on the purpose of the experiment, the time available and the requirement for accuracy one of the three processes has to be chosen. A short description of each of the three processes is given.

The on/off controller is the simplest form of temperature control device. The output from the device is either on or off, with no middle state. An on/off controller will switch the output only when the temperature crosses the set point. For heating control, the output is on when the temperature is below the set point, and off above set point.

Since the temperature crosses the set point to change the output state, the process temperature will be cycling continually, going from below set point to above and back again below. On/off control is usually used where a precise control is not necessary, in systems which cannot handle the energy being turned on and off frequently, where the mass of the system is so great that temperature changes extremely slowly.

The proportional controller is designed to eliminate the cycling associated with on/off control. A proportional controller decreases the average power being supplied to the heater, as the temperature approaches set point. This has the effect of slowing down the heater, so that it will not overshoot the set point, but will approach the set point and maintain a stable temperature. This proportioning action can be accomplished by turning the output on and off for short intervals. This "time proportioning" varies the ratio of "on" time to "off" time to control the temperature.

The proportioning action occurs within a "proportional band" around the set point temperature. Outside this band the controller functions as an on/off unit, with the output either fully on (below the band) or fully off (above the band). However, within the band, the output is turned on and off in the ratio of the measurements difference from the set point. At the set point (the midpoint of the proportional band), the output on:off ratio is 1:1; that is the on-time and off-time are equal. If the temperature is further from the set point, the on- and off-times vary in proportion to the temperature difference. If the temperature is below set point the output will be on longer; if the set point is too high, the output will be off longer.

The PID-controller type provides proportional, with integral and derivative, control, or PID. This controller combines proportional control with additional adjustments, which

help the unit automatically compensate for changes in the system. These adjustments, integral and derivative terms, must be individually adjusted or "tuned" to a particular system, using a "trial and error" method. It provides the most accurate and stable control of the three controller types. It is best used in systems that have a relatively small mass and those that react quickly to changes in energy added to the process. It is recommended in systems where e.g. the mass changes often and the controller is expected to compensate automatically due to frequent changes in set point. For further details refer to the literature.

In this investigation, the PID process is chosen in an attempt to reach the relative humidity set point without exceeding the set point at any time during the experiment. If the set point is exceeded hysteresis is likely to occur which is undesirable. Especially porous materials like wood and plant fibres are among materials performing this behaviour, which makes it very important to keep RH at the correct side of the set point.

4.2.7. Weighing procedure

The ordinary desiccator method requires that every weighing of a sample usually takes place outside the humidity controlled environment. Consequently, the samples are exposed to ambient air and humidity for which reason hysteresis is initiated. To avoid hysteresis it is important to weigh the samples within the chamber. However, are not able to work at 100% relative humidity and therefore must be placed outside the chamber. For this reason the balances are located above the chambers and a thin steel wire is fixed to the bottom tap of the balance and passed through a small hole in the top of the climate chamber. Inside the chamber there is a hook on the wire and the samples are in turn hanged on the hook. A computerized data acquisition system is installed.

The manual placing of each sample on the hook is done be means of a glove mounted in the front door of the chamber instead of opening the door. During the weighing process both the injection of air and the ventilator are stopped. This is due to air friction through the hole for the balance wire, which will lighten the samples. In addition, it keeps the samples calm during the weighing.

4.2.8. Temperature control

The saturated air is particularly sensitive to temperature changes. To avoid condensation on the inner chamber surface with resultant inaccurate relative humidity the chamber must be kept slightly cooler than the room. This can be achieved naturally by using heat of evaporation of water to cool the nearly saturated air stream. Though it sounds easy to keep the temperature constant naturally, that would be too much trouble.

The fact that the chambers are in at thermostatic controlled room indicates the need for a small adjustment of the temperature inside the chambers. As mentioned above the evaporation of water decreases the temperature naturally, but usually too much. Therefore, a small heater is mounted in each chamber, managed by at PID process controller to keep the chamber temperature at a set point below the room temperature. In practice, the room temperature is close to 21°C when the experiments are carried out at 20°C.

4.2.9. Sorption curves above room temperature

Part of the sorption studies is to investigate the influence of temperature. Consequently, one of the climate chambers is designed for experiments at elevated temperatures, and experiments are carried out at 40°C and 60°C. As already mentioned it is a difficult task to control the relative humidity particularly beyond 90% and increasing the temperature does not improve it.

The fundamental principle is a double chamber, as illustrated in Figure 4.3, where the outer space is at the inner temperature but with low humidity. The climate chamber has the same outer frame, a refrigerator, as the climate chambers for ambient temperature. However, inside the chamber is a build in stainless steel chamber in which the relative humidity is controlled. Because no saturated air stream is blown into the space between the outer chamber and the inner chamber the relative humidity is naturally low and no condensation on the surfaces occurs.

Figure 4.3. Climate chamber exclusively developed for measurements at elevated temperature.

When experiments are carried out at e.g. 60°C the temperature in the steel chamber is at 60°C but the outer space is usually slightly higher, about 61°C, to get rid of condensation problems. The heater in both the inner and outer chamber are PID-controlled. A fan is mounted to circulate the air in the space between the inner and outer chamber as well as in the inner chamber. Although it sounds difficult to maintain two different temperatures, it is in fact no problem because the heat of evaporation of water cools the air in the inner chamber.

In the steel chamber the dry and saturated air stream is mixed in the same way as in the other climate chambers. However, because the amount of water molecules in the air increases almost exponentially when the temperature increases from 20°C to 60°C the extra saturator is thus more important. There is again a coiled heater placed in the extra saturator controlled by a PID-controller. Since the huge amount of water required to saturate the air at 60°C the current sent through the heater is variable. The current is adjusted manually to agree with the temperature set point of the water in the extra

saturator, and usually the water temperature is at the same set point as the climate chamber temperature or slightly above. Again, the primary reason for the heating element in the extra saturator is due to the heat of evaporation of water, which cools the water temperature and then lowers the relative humidity.

Moreover, there is an additional detail concerning the heating element in the extra saturator. Because of the mixing principle of the air streams where either the dry or the saturated stream is injected, none of them at the same time, the current through the heater is only connected when the saturated stream is open. This is to avoid unnecessary evaporation of water when the dry stream is open.

4.2.10. Automation of the weighing process

Weighing the samples in the inner chamber is problematic! Weighing through a double chamber is tricky because of the temperature gradient from inside to outside, but also convective air movement through the opening to the balance is a serious problem. The glove box principle applied in the chambers for ambient temperature is impossible to use considering the condensation problem, which will take place on the outer side of the glove.

The only usable solution is a more or less automated weighing process to avoid the samples being exposed to the surrounding environment. For this purpose, a carrousel was developed to move samples successively onto the balance. The balance is placed outside and above the climate chamber, as is the case in the climate chambers for ambient temperature.

The samples hang on a circular plate rotated and lifted by two step-motors alternatively hanging the samples onto the hook to the balance. The carrousel is software controlled, and interacts with the balance to decide when the sample weight is determined, before it moves on to the next sample on the plate. The automated weighing on the balance has been a very difficult task, but crucial for the assessment of the equilibrium moisture content.

When most samples have a mass about 10g and the accuracy of the balance is 1/1000g, the balance therefore is very sensitive to small movements of the sample during the weighing process. Through experience it is decided to let the software collect three consecutive weighings of each individual samples and then keep the last weighing as the final weight. The first two weighings are too uncertain.

Because of the high temperature and at times high relative humidity, the opening to the balance must be sealed when not in use to reduce the loss of heat and humidity. This is done at the end of the weighing process by the step-motor elevating the circular plate, and at the same time elevating the device on the balance, which has a conic closing in the lead-in at the top of the chamber, see Figure 4.4.

Figure 4.4. Climate chamber with conic device to seal the gap to the balance lead-through.

4.2.11. Sorption'99 and Sorption Monitor software

The automation of the weighing process in the climate chamber for elevated temperature is controlled by a program (Sorption'99) exclusively made for this purpose (HBJ 1999). By automation one lets off doing it manually which is tedious and time consuming. In addition, the weighing can be repeated more times each day. At each weighing routine, the program switches off the fan in the climate chamber and stops injection of air at the same time the carrousel moves to the initial position. This is to avoid the samples moving during the weighing process causing unnecessary fluctuations in the data from the balance.

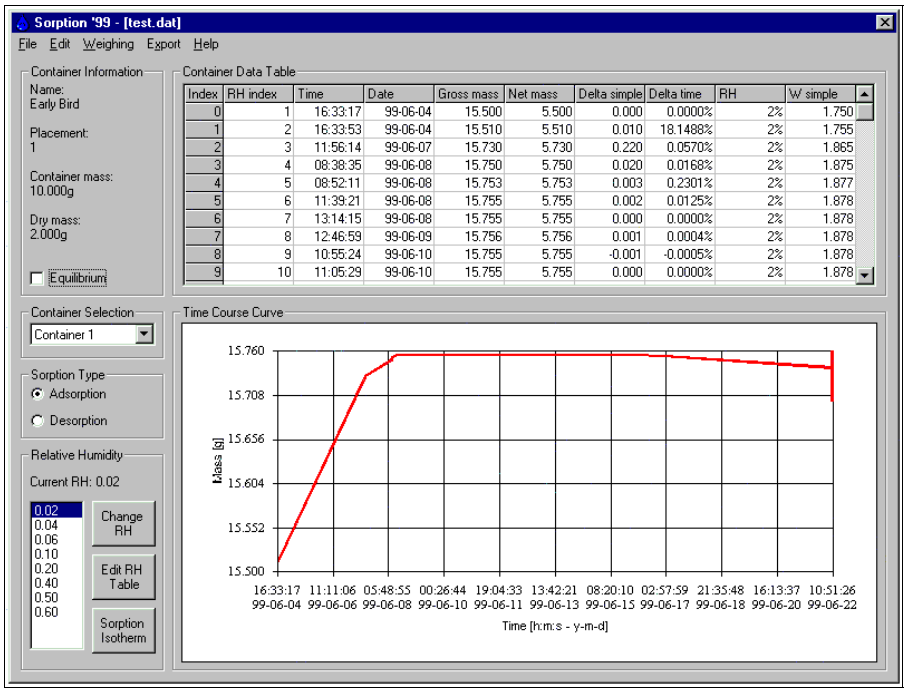

Figure 4.5. Screen layout in the Sorption'99 program.

The program collects the weighing data from each sample and calculates the moisture content and the relative change in the weight of the sample since last weighing. Furthermore, the time course curve is shown on the screen, Figure 4.5. The very important question about when equilibrium is reached is decided in the light of these informations. This decision is subjective and requires experience within sorption measurements in general and knowledge about the particular materials investigated.

The same program is used for the chambers at ambient temperature, but instead of the automated weighing procedure, a manual procedure is selected. Here the operator pushes a button every time when weighing data from the balance is required. All other characteristics of the program are exactly the same.

In addition to the automatic weighing program Sorption'99 a monitor program Sorption Monitor has been developed (HBJ 1999). This program monitors both the temperature and the relative humidity in all the climate chambers. The temperature and relative humidity sensors in the climate chambers are connected to a data acquisition unit (HP data logger) and this again connected to a computer with the monitor software. The software is to prove a constant and precise temperature and relative humidity in the climate chamber all time they are running. Online curves on the computer screen show the actual temperature and relative humidity state in each chamber, as shown in Figure 4.6.

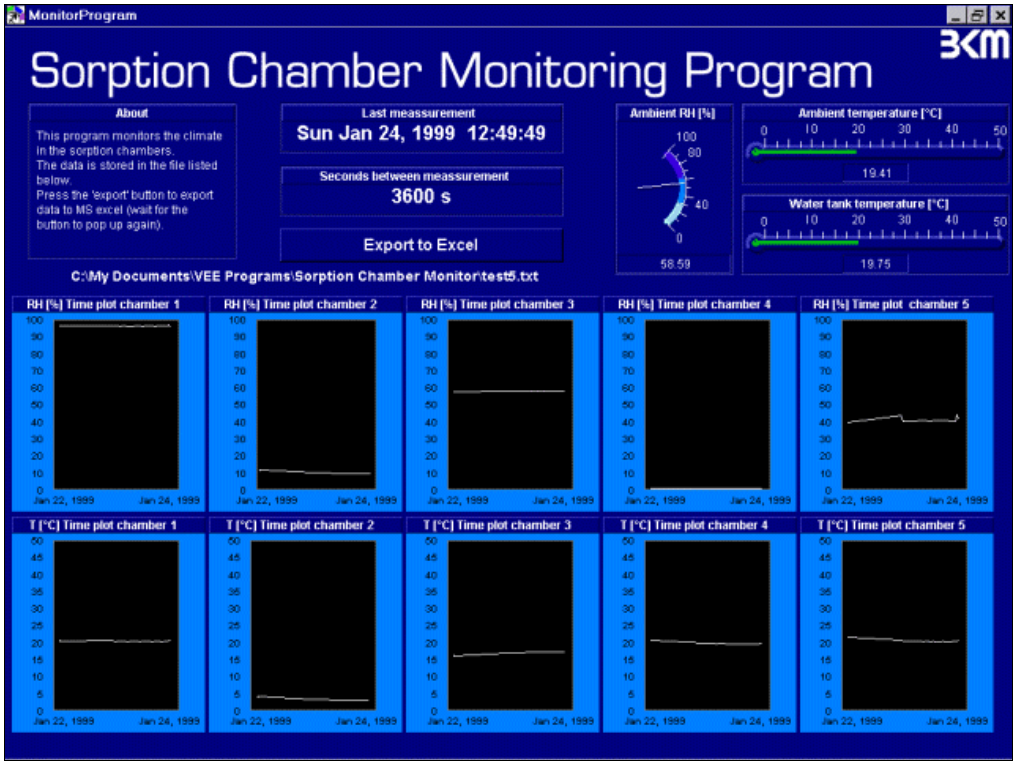

Figure 4.6. Image of the on-line screen in the Sorption Monitor program.

4.3. Considerations for future improvements

Measurements of sorption isotherms below ambient temperature are not yet possible in the newly designed climate chambers. The question is how it is possible? Currently the climate chamber frame is a refrigerator without cooling compressor and installing a cooling compressor will make it possible to decrease the temperature. Under these circumstances, the temperature range will be from 2°C until ambient temperature when a heating element is mounted within the chamber.

Fundamentally, the same principle of generating the dry and saturated air stream and controlling relative humidity can be used again. Contrary to elevated temperature measurements the amount of water molecules in the air falls when the temperature decreases thus facilitating the generation of the saturated air stream. Perhaps there will no longer be a demand for an extra saturator.

Alternatively, the basic underlying principle for controlling the relative humidity could be changed. Instead of mixing dry and saturated air streams, peltier cooling elements could be used to cool or to heat two water baths placed inside the chamber. The temperature of the water baths should then be at the dew point and the wet bulb temperature respectively, corresponding to the desired relative humidity.

Other improvements concern the existing equipment. For instance, the weighing device to the balance in the double chamber for elevated temperature measurements could be more sophisticated. This device ought to be improved to avoid any kind of noise and disturbance during the weighing process causing errors in the results. Currently, the device and the lead through in the top of the chamber are very sensitive to movements caused by the samples when these are hanged on the hook as well as small vibrations from the surroundings.

CHAPTER 5

Materials and methods

5.1. Introduction

In this chapter the materials and methods used in this investigation are described. First, the assortment of wood and plant fibres is described with special reference to the different treatments applied.

This description is followed by an explanation of all the methods used in the characterisation of the sorptive properties. These methods are among other things sorption measurements in climate chambers, suction measurements in pressure planet apparatus, calorimetry measurements, and finally crystallinity measurements by x-ray diffractometry.

5.2. Materials

The different wood and plant fibres including a few solid wood species investigated are presented in Table 5.1. As indicated, the wood fibres have been treated by different methods too. All the fibres are refined by the thermomechanical process (TMP), which is a combination of mechanical and thermal pulping. The process is the Asplund process where the wood chips or the plant fibre stems have been subjected to steam as they pass through the refiners, generally in two passes. The first stage of the thermomechanical pulping is normally done under pressure, with the material subjected to superheated steam at a temperature 110-135°C. It this case a steam pressure of 7 bar was applied and the temperature was 170°C. In some systems, steaming is done at atmospheric pressure.

The heat serves to soften the lignin, allowing fibre separation with less fibre damage then can be obtained by either the stone groundwood pulp (SGW) or the refiner mechanical pulp process (RMP). This improves the strength of the fibres.

Table 5.1. Assortment of wood and plants fibres used in this investigation.

Wood fibres	Wood, solid	Plant fibres
Spruce *(Picea abies)*	Spruce	Hemp *(Cannabis sativa)*
Spruce, acetylated	Beech	Flax *(Linum usitatissimum)*
Spruce, enzyme treated		Wheat straw *(Triticum sativum)*
Spruce, hygrothermally treated		
Beech *(Fagus sylvatica)*		
Beech, acetylated		
Beech, enzyme treated		

5.2.1. Acetylation

The spruce and beech fibres have been acetylated in an attempt to prove a hypothesis about the presence of micro pores in the fibre cell wall, but also to see how strongly this treatment will influence the hygroscopicity. The fibres were acetylated by Forest Products Laboraty (FPL), Madison, USA and the procedure is the following.

First, the fibres were dried at 105°C for 24 hours before acetylation. Fifteen grammes of dried fibre was dipped in acetic anhydride (Eastmann Chemical Company) for 1 minute. Thereafter the excessive solution was drained for 5 minutes. The fibres were then placed in a one litre glass reactor which was then heated in an oil bath at 120-125°C for 20, 60, and 240 minutes. (Oil: Glycerin USP, Sargent-Welch Scientific Co.). Cheese cloth was used to hold the fibre together in the dipping and treating steps. The treated fibres were then oven dried at 105°C for 24 hours and weighed. The weight gain or mass acetyl content was then calculated.

5.2.2. Enzyme treatment

Spruce and beech fibres have been enzyme treated, in brief to investigate an expected improvement of the bonding of fibres in a composite material. Since the enzyme treatment is expected to decay as the humidity and moisture content increases sorption experiments were carried out to determine this influence.

Deionized water previously heated to 40°C was added to the fibres such that a consistency (water up-take) of 4% (by dry fibre mass) was obtained. The suspension was then left for ½ hour. The temperature was kept at 40°C during all steps in the treatment procedure. The pH was then adjusted (NaOH) to pH=4.5 and the suspension left for 1/2 hour and readjusted if necessary. Enzyme was then added to the suspension at a dosage D LACU/g fibre dry mass and the suspension stirred for a few minutes. Residence time for the enzyme treatment was 1 hour whereupon the water was drained from the fibres, which were then rinsed with 2 litre deionized water and dried in an oven for 24 hour at 40°C.

Treatment with no addition of enzyme serves as comparison (control). It has been established (results not shown) that the treatment induced modifications are not due to *passive* effects of the enzyme, ie. there were no detectable differences between a treatment where no enzyme was added and a treatment where heat inactivated enzyme was added.

Of each fibre type two different treatments were made: One control and one with enzyme dose D: 300 LACU/g.

5.2.3. Hygrothermally treatment

In this investigation, only spruce fibres were hygrothermally treated. These were treated in an autoclave at four different temperatures and two different time spans. The temperatures were 160, 170, 180 and 190°C and the treatment times were 20 and 40 minutes.

The fibres were placed in a perforated stainless steel basket in amounts from 1 to 5 litres at a time. Prior to reaction, steam was generated to the desired temperature. The basket was placed in the autoclave and the treatment started by injecting steam into the autoclave under pressure for the desired treatment time. The steam pressure was maintained at the

determined temperature and condensed water was drained in the bottom of the autoclave. After the treatment the steam pressure was released and excess steam ventilated. The fibres were removed from the basket and conditioned at ambient temperature until use.

5.3. Experiments

5.3.1. Sorption isotherms

The sorption isotherms obtained in this investigation are all measured in the newly designed climate chambers. The principle of controlling the relative humidity and temperature in the climate chambers are described in details in Chapter 4. Moreover, an explanation of the weighing procedure for measurements of sorption curves at both ambient and elevated temperature is also mentioned in Chapter 4. A satisfactory description of the measurements of the sorption isotherms is therefore obtained by comparison of this particular section and Chapter 4.

The wood and plant fibres are placed in fine perforated non-absorbent polyester bags. The size of the bags is 150mm × 250mm shaped like an envelope to expose as large surface area as possible of the fibres. An amount of 10g – 15g of fibres is used on average in each bag depending on the individual species. The very light polyester bag increases the ratio of the sample mass and the mass of the empty container in comparison to the desiccator method thus improving the accuracy of the measurements.

First, the experiment starts by drying the samples in the climate chambers at 3% relative humidity and 20°C until equilibrium is established. The starting point of 3% was chosen because it is the lowest relative humidity possible to obtain in the chambers. Samples at measurements at 40°C and 60°C are of course dried at 40°C and 60°C respectively.

The samples, hanging on a bar in the climate chamber, are usually weighed once a day. Every time the data is computerised and used for on-line demonstration of the time course curve and calculation of the moisture content. These informations are used to determine when equilibrium is obtained. The criteria for equilibrium is according to prEN ISO 12751:1999 expressed as “Constant mass is reached of the change of mass between three consecutive weighings, each made at least 24h apart, is less than 0.1% of the total mass.”

When equilibrium is reached the relative humidity set point in the climate chamber is changed in accordance to the schedule of planned humidities for this particular experiment. Either it is the relative humidity which is increased or it is decreased. The procedure of daily weighings of the samples is thus continued until equilibrium again is obtained and so forth.

All the experiments carried out begin with adsorption. When the highest relative humidity is reached, usually at 96%, the process is turned around and the measurements of desorption begin and continues until 3% relative humidity is reached. This procedure involves the samples to be maintained within the climate chamber in the whole experiment. The standard set of values of relative humidity used in this investigation for the determination of the sorption isotherm were: 3%, 9%, 15%, 25%, 55%, 70%, 85%, 90%, 94%, 96% and vice versa.

For the experiments at 40°C and 60°C, the weighings are done automatically by the carrousel. Hence, these samples were usually weighed four times a day and the equilibrium criteria therefore followed more closely. For this reason and due to the general decrease in time to obtain equilibrium at elevated temperature these experiments were running faster.

After the experiment in the climate chamber, the samples were dried to obtain the dry weight of the sample for the exact calculation of the moisture content. First, the samples were dried above the strong desiccant magnesium perchlorate $Mg(ClO_4)_2$. The samples are dried above the desiccant in an evacuated desiccator for two weeks at room temperature until equilibrium is reached whereupon the samples are weighed on a balance. Just before the drying is initiated, the magnesium perchlorate is regenerated. This takes place by drying it for 24 hours at 150°C with vacuum applied. The advantage of this method is the careful treatment of the samples compared to the oven drying.

5.3.2. Suction curves

To extend the sorption curve in the high humidity region, where the humidity in the climate chambers is difficult to control or even to establish, suction measurements have been carried out. In order to measure the moisture content versus relative humidity the pressure plate and pressure membrane apparatus is used. The samples are then subjected to a hydrostatic pressure inside the vessels of a sufficient magnitude to reduce the relative humidity to values between 100% and 93%. This corresponds to a hydrostatic pressure of 0 to 100 bars, which is the possible region for the equipment to measure.

The pressure plate technique was developed for soil moisture studies and later applied to solid wood (Cloutier et al. 1995). The experiments were conducted at 20°C for beech and flax fibres. The pressure plate apparatus was used for relative humidities from 99.26% to 99,99% and the pressure membrane apparatus was used for values of 92.86% to 99.26%. The laboratory setup of the pressure plate apparatus is shown in Figure 5.1. The setup of the pressure membrane apparatus is almost similar except that the extractor is heavier and a cellulose membrane is used within the vessel instead of a ceramic plate.

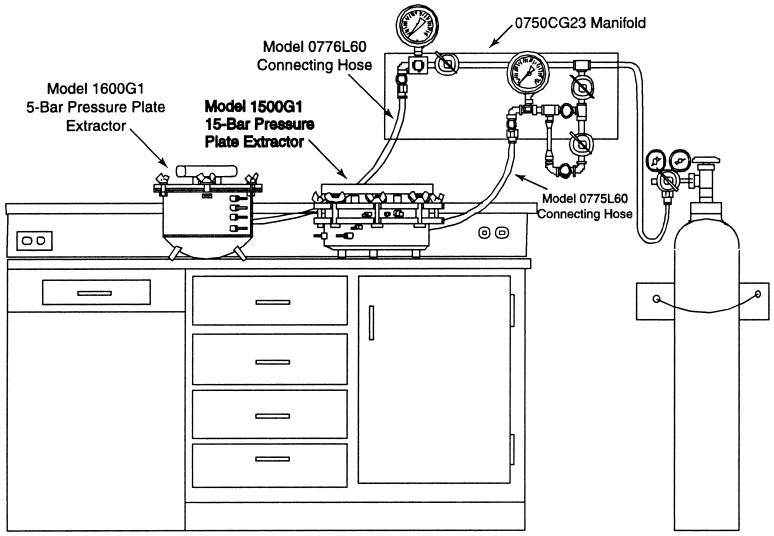

Figure 5.1. Laboratory setup of the pressure plate apparatus.

The following procedure was adopted. The samples were brought to full saturation by immersing the fibres into water for 24 hours at ambient conditions. For the experiments performed, the fibres were first placed in a small sample container illustrated in Figure 5.2. The container is made of non-adsorbent polyester cloth secured by a ring of solid acetate plastic. It was attempted to place the fibres in a single layer on the fine mesh in the sample container. The fibres, or rather bundles of fibres, were placed by a squeezer when the sample container was submerged into water in a small petri dish. Thereafter the container was removed and put into the pressure plate apparatus.

Figure 5.2. Sample container for pressure plate and pressure membrane apparatus. Exclusively for wood and plant fibres.

A saturated clay layer about 2-4mm thick was formed on the porous ceramic plate to ensure good hydraulic contact with the samples. On the cellulose membrane in the pressure membrane apparatus no clay layer was used because the soft saturated cellulose membrane was in good contact with the sample container. Once the samples were in place, the vessel was hermetically closed and the pressure applied gradually. Nitrogen from a pressure bottle is admitted to the required pressure. Water is then progressively expelled from the sample and drained in a burette. The burette readings were started and continued until the outflow became zero for at least 48 hours. Then the pressure was slowly released and the weight of the samples was determined by the gravimetric method. This weight corresponds to the equilibrium moisture content (Strømdahl 1997).

The procedure is repeated at other pressures until a curve of moisture content versus pressure is obtained.

5.3.3. Differential scanning calorimetry

Heat of wetting measurements were performed in a differential scanning calorimeter (DSC) of the brand Calvet from Setaram. The fibres are themselves small particles as required to minimize the time to thoroughly wet all the material in the calorimeter. The wood and plant fibres are first equilibrated to some constant moisture content in a climate chamber. A small amount of material, usually 100-200mg, was weighed in a stainless steel

container (sample holder) for the calorimeter. The fibres were packed in this container within the climate chamber and sealed to make sure the moisture content is maintained when removed to the calorimeter.

The sealed cell containing the sample is mounted in a device to admit water. This device, exclusively designed for this particular calorimeter, allows water to be admitted after the sample is equilibrated to the specific temperature of the calorimeter. The sample container is submerged into the calorimeter and after about one hour, it is equilibrated to the 30°C as is the specific temperature used in this investigation. Just before water is added to the sample, vacuum is applied for 10 seconds to the cell, whereby the saturation of the fibres is secured to be complete. The influence of the applied vacuum is measured and the 10 seconds of evacuation is found to be negligible.

The fibres are then soaked in an excess of water from the sample holder device, and the temperature increase due to the reaction is measured. The heat generated by the reaction is calculated from the measured temperature rise of the calorimeter.

5.3.4. Degree of crystallinity

Crystallinity measurements were performed on a variety of the wood and plant fibres used in this investigation. The fibres were conditioned to ambient temperature (20°C) and humidity before measurements in the x-ray diffractometer.

X-ray powder diffraction was carried out in reflection mode with Ge-monochromized Cu radiation (25 mA/40kV) on a STOE StadiP diffractometer. A linear position sensitive detector from STOE, measuring over 7 degrees, was used. Pellets of the fibres were pressed uniaxially at 1-5 tons, and gave quite robust disks, 1-2mm thickness, 13mm diameter. Samples were rotated with 100 rpm in the vertical plane during the step scan. Typical step size: 0.2 degree, count time in each step 5-15 seconds. The graphics used was from the Visual X^{POW} software from STOE.

CHAPTER 6

Results and discussion

In this chapter, all the measurements of sorption isotherms obtained from the climate chambers are presented. The results from the mathematical modelling of the sorption isotherms are included as are the measurements from the suction apparatus. The modelling of the sorption isotherm is based on the following four models: BET, Hailwood–Horrobin, and a combination of the BET and capillary condensation theory explained by Simpson (1973) and finally the SORP model.

Results obtained from calorimentry are analysed and calculations based on the Clausius-Clapeyron equation are made from sorption isotherms measured at 20°C and 60°C. Measurements and calculations are thereby compared and discussed.

In an attempt to explain the nature of the sorption isotherm on the basis of the crystalline structure of the wood and plant fibres, x-ray diffractometry was carried out to determine the degree of crystallinity. Results from a selection of wood and plant fibres are presented, along with reference materials.

6.1. Data processing

This section describes how the sorption data are processed before the modelling is carried out. This process is divided into three steps beginning with the determination of the mass at equilibrium, followed by the determination of the corrected mass due to an unexpected degradation during the experiment. Finally, the measurements of the relative humidity are adjusted after calibration of the humidity sensors.

Based on the measurements in the climate chamber, the moisture content is calculated and the corresponding values of relative humidity and moisture content at a specific temperature are plotted in a sorption isotherm. In each series of measurements, the data contains the gross mass from every weighing and the nominal value of the relative humidity. Knowing the mass of the empty container and the calibration of the temperature and humidity sensor, allows one to calculate the weight of the sample and the real humidity.

6.1.1. Mass loss during the sorption process

Contrary to expectations, the results showed a mass loss (degradation) during the sorption process. When the experiments were finished, the corresponding values of moisture content and RH showed a curious behaviour at the last part of the desorption curve. On Figure 6.1, the blue desorption curve crosses the adsorption curve beyond 25% RH which should be impossible from a theoretical point of view.

After having carefully analysed the results, it is found that the equilibrium weight of the sample at 3% RH desorption is less than the equilibrium weight at 3% adsorption. This strange behaviour only appears for the fibrous material investigated in this work and not for samples of e.g. solid wood. During the experiment, mould or rot was noticed on one of the samples indicating biodegradation. This phenomenon only took place at high relative humidity conditions where the moisture content is above 20%, identical to a very high relative humidity within the sample. Rot or mould usually only appears when samples are exposed to such hazardous conditions (Haygreen & Bowyer 1996). The reason for the weight decrease could also be due to chemical reactions or, more likely, both mechanisms.

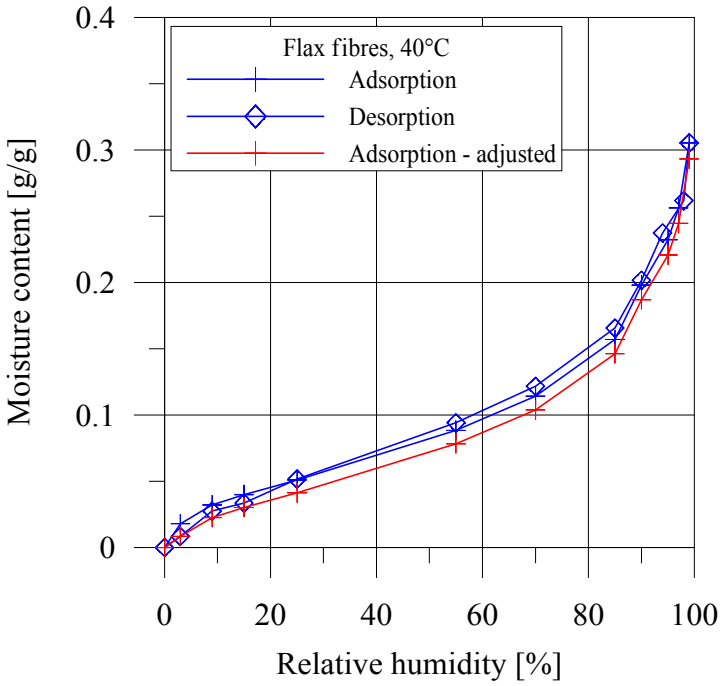

Figure 6.1. Sorption isotherm for flax fibres before and after adjustment.

The exposed surface area of the wood- and plant fibres is much larger than for a similar amount of solid wood and this seems to be a reasonable explanation for the weight decrease solely found for the fibres. This huge fibre surface area is much more sensitive to degrading attacks than solid samples and especially when the samples are exposed for months rather than days.

6.1.2. Adjustment for mass loss

Because the sorption isotherm showing lower lying desorption curve than adsorption curve is unrealistic, it is decided to adjust for the mass loss. The question is when and where exactly the mass loss takes place. It is well known that biodegradable attacks take place above 85-90% RH (Haygreen & Bowyer 1996) and in this case it is assumed to take place during the adsorption process exclusively. Admittedly this is not the truth, but it is still the most consistent way to consider it, although it is a fact that a part of the degradation presumably takes place during the desorption region. Two small experiments could indicate whether the degradation takes place at either the adsorption or desorption or in

both. The first starting at e.g. 80% with dry fibres and ending at 96% followed by a drying and an accurate determination of changes in the weight. Likewise for an experiment starting at 96% and ending at 80% with a precise weight determination before and after the experiment.

The exact adjustments are made by correlating equilibrium weights at 3% RH adsorption and at 3% RH desorption respectively. The relative difference between the two equilibrium weights is then calculated and subsequently used as an adjustment factor to the dry weight for the adsorption measurements exclusively. Actually, the dry weight is increased by the relative difference just calculated, giving a higher absolute dry weight. For the desorption process, the dry weight found immediately after the experiment is used without adjustments. This means that the adsorption curve is given a descending offset illustrated by the red curve in Figure 6.1 due to the higher dry weight and consequent lower moisture content. An example of the calculation procedure for flax fibres in Figure 6.1 is shown below.

Equilibrium weight at 3% RH adsorption: 6.714g

Equilibrium weight at 3% RH desorption: 6.651g

Relative difference $= \frac{6.714 - 6.651}{6.651} =$ 0.0094g/g

Dry weight after experiment: 6.596g

Adjustment for dry weight: $6.596 \cdot 1.0094 =$ 6.658g

This means that the dry weight used for the calculation of the moisture content for the adsorption curve is 6.658g and the dry weight used for the desorption curve is 6.596g.

As a consequence of the adjustment of the mass loss, the adsorption and desorption curves could not be connected to each other any longer. Usually, the top point on the adsorption curve is the first point on the desorption curve but due to the descending offset, they are not connected. In the isotherms presented in the following sections, the top points are therefore not identical.

6.1.3. Determination of equilibrium moisture content in the climate chambers

In the climate chamber, the set point for the RH is given a nominal value controlled by the PID-process controller as well as the temperature. This nominal value is kept constant until equilibrium is obtained in all the samples within the chamber after which the RH increases or decreases depending on the experiment. In a parallel process, the RH and temperature are monitored and data processed in a computer to prove the real conditions inside the chamber. This procedure was introduced as a safety measure because seemingly inexplicable problems have occurred a couple of times, especially during the running-in period. This makes it crucial to be able to explain the exact humidity conditions during the experiment. When the experiment is finished, the corresponding values of the moisture

content for each weighing and the RH tells when equilibrium is reached and which values for the moisture content should be the final values.

In Figure 6.2, a typical time course curve is illustrated covering the change in RH from 15% to 25%. The moisture content for each sample is shown on the left axis and on top of that, the RH profile is illustrated on the right. As can be seen there is an increase in the moisture content identical with the jump in RH. This takes place every time the RH is changed and the final moisture content at this particular RH is determined as an average of a number of points that are at a constant level during consecutive weighings. The number of points for the average value varies from time to time and is based on a subjective opinion. The variation in the number of points (measurements) makes it necessary to match the measured RH in the chamber with a corresponding measurement of moisture content.

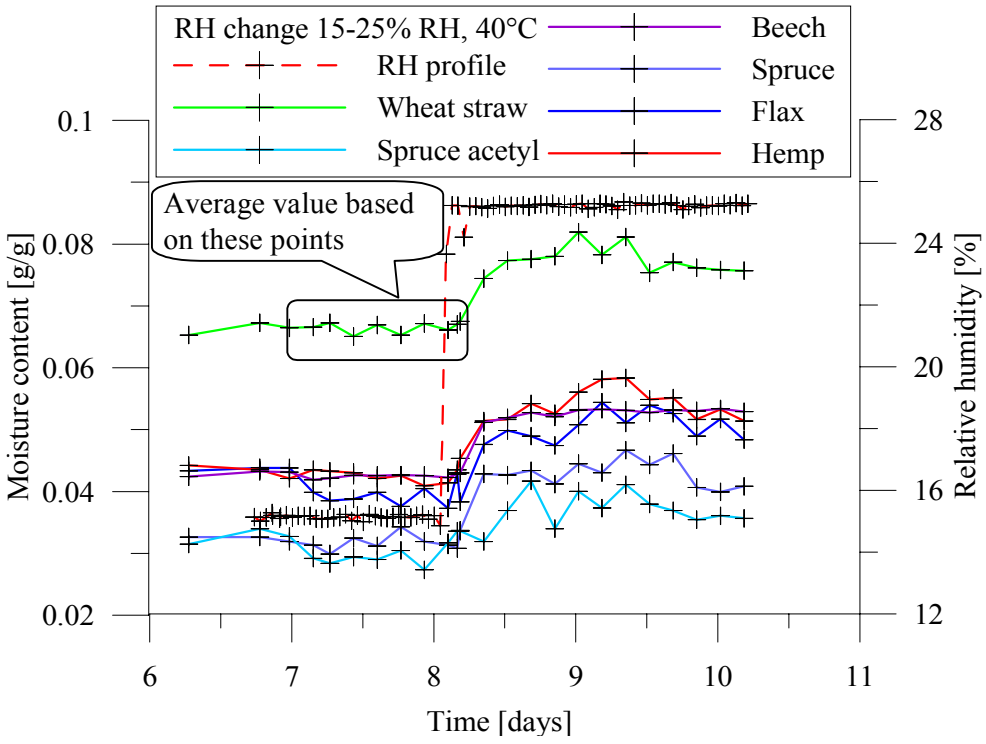

Figure 6.2. Time course curve for RH change from 15% to 25 % at 40° C.

Although it sounds easy to determine the moisture content even if somewhat tedious, the first set of experiments in the 40°C climate chamber caused big problems when increasing the RH. In addition to the general problem of controlling RH above 94%, the carrousel sometimes dropped the samples making it necessary to open the chamber and replace them thus disturbing the climate and the adsorption/desorption process. This is illustrated in Figure 6.3, showing the full course of the moisture content in the samples and the RH profile in the climate chamber. The lowest curve in Figure 6.3 is not present in Figure 6.2. On top of that, experience showed that the humidity sensor was affected by the high temperature and RH, and began to drift, showing another value for RH than the real RH. To avoid sensor drift it is calibrated regularly above well defined certified saturated salt solutions. The calibration process is a two step process. The sensor was in the first step

calibrated and then in the second step adjusted to show the values in agreement with the saturated salt solutions.

After the experiment, it is then possible to adjust the measured values to real values when the sorption isotherm is calculated. The results illustrated in Figure 6.3 are obtained from the first run with the carrousel and are all adjusted in the following way. Because the actual sensor was not calibrated correctly from the outset, the measurements from 0% to 90% RH are adjusted in accordance with a similar sensor calibrated before use. This is not the perfect way to adjust the sensor but assuming identical behaviour for similar sensors, it should be valid. From 90% to 98% and further to 90%, the measurements are adjusted knowing calibration values from a similar sensor at 90% adsorption and from comparison with a new sensor inserted instead at 90% desorption. The movement of the sensor is noticed by a decrease in the moisture content when the measured RH values are kept constant. In this case, it is very difficult to tell what the exact RH was, but comparison with the results in the neighbouring region makes it possible to establish a good estimate.

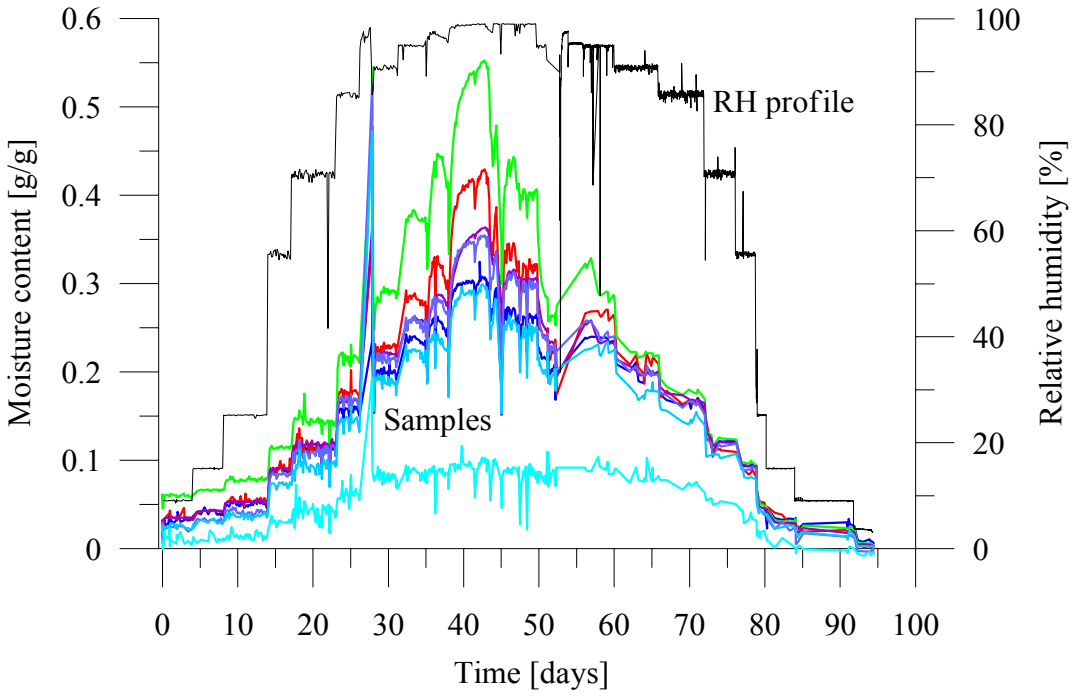

Figure 6.3. Moisture content and RH profile in the samples in the climate chamber at 40°C.

Due to the experience just mentioned, the sensor used at the end of the experiment from 90% to 0% RH was calibrated and adjusted both before and after its use in the climate chamber. This procedure made it easy to adjust the measured values. In order to avoid such problems in the future, a much more rigid calibration routine was implemented.

6.1.4. Present calibration routine

Calibrations during every experiment are done frequently whether it is at 20°C, 40°C or 60°C, and each time the humidity sensor is first calibrated and then adjusted. Software

exclusively made for the sensor makes it possible to adjust the sensor permanently after the calibration to secure agreement between measured and actual values of both temperature and relative humidity. The sensor is merely connected to the RS232 port of a computer and the sensor head placed in a small calibration cell containing a certified saturated salt solution. Typically, after 1 to 2 hours, equilibrium is reached in the cell and the computer reads the measured value. Then, the sensor is adjusted according to a predefined RH value for the particular saturated salt solution.

This process is carried out for the sensor before the experiment starts. When RH reaches 90% the sensor is exchanged with another new calibrated sensor and the first sensor is again calibrated in the meantime until the second sensor finishes the adsorption process at 98% RH. At this point, the first sensor is put back into the chamber until the desorption process is in equilibrium at 90% RH. At this point, the second sensor is again put into the chamber which is also newly calibrated. The first sensor is again calibrated and when the experiment is finished, the second sensor is finally calibrated again.

This procedure seems complicated. However, to be sure the sensor does not float in the region above 90% it is a necessity for accurate measurements. Regarding all the calibration results, it is possible to adjust the measured RH values during the experiment and then calculate the right sorption isotherm.

The temperature sensor is not as sensitive to movement or collapse as the humidity sensor and it is therefore not necessary to adjust as often as the humidity part. Nevertheless, the temperature sensor is controlled at every humidity calibration.

6.1.5. Humidity measurements

In addition to the regular calibration of the humidity sensors a chilled mirror hygrometer is used to measure the immediate humidity within the chamber. Each time the samples in the climate chambers are weighed the hygrometer is first connected and a reading made of the relative humidity and temperature. The readings are later used in comparison with the monitored values from the humidity sensors. This comparison forms the basis of the determination of the true relative humidity in the climate chamber.

6.2. Sorption isotherms – pure fibres

In this section, all the measured sorption isotherms are modelled and plotted for further analysis. All the data belonging to the curves are tabulated as well. Due to the large number of measurements, not all the data are presented in this chapter. The majority of results are tabulated in Appendix A. For each curve, the corresponding values of relative humidity and moisture content are tabulated.

6.2.1. Modelling

In the modelling approach it is first decided which of the selected models fits the investigated samples best. This is done by comparison of sorption curves fitted by the different models. The parameters for each of the sorption isotherms were determined by using either non-linear or linear regression techniques.

Sorption curves for spruce wood fibres and flax plant fibres are illustrated in Figure 6.4 and Figure 6.5, respectively. The sorption curves are modelled by BET, Hailwood–Horrobin (H–H) and BET including the effect of capillary condensation. Spruce fibres and acetylated spruce fibres are in addition modelled by H–H and the SORP model in Figure 6.6. In the region from 0-60% RH both the BET and H–H provide a good and almost identical fit to the points. From 60-95% RH the H–H model still provides a good fit while the BET does not. It is known (Skaar 1988) that the BET model is best used below 50% RH and therefore use of the model on the current data was not prudent.

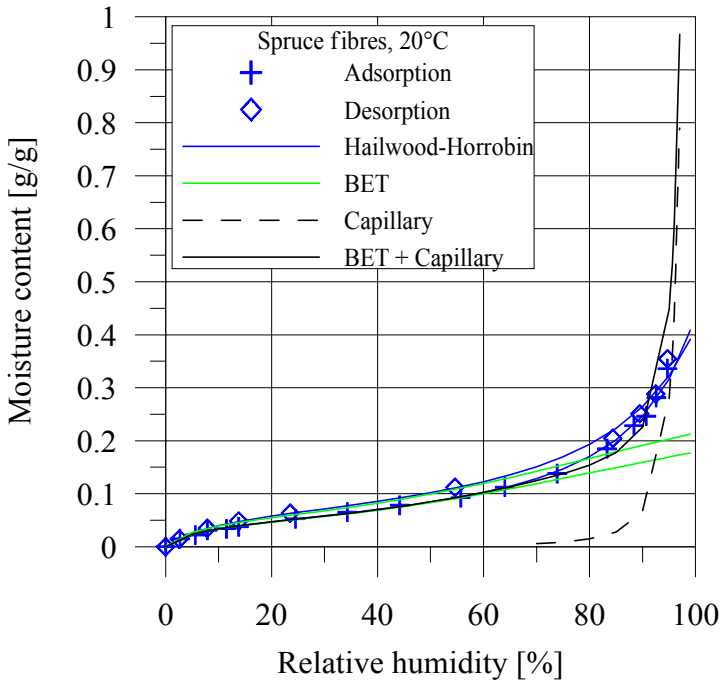

Figure 6.4. Sorption curve for spruce fibres at 20°C modelled by BET, Hailwood–Horrobin and capillary condensation.

The dashed line is the contribution due to capillary condensation in pores and cracks in the fibre wall and liquid water in the lumen. This contribution is calculated by the Kelvin equation relating the radius of a capillary to the relative humidity at which condensation occurs. Cylindrical capillaries are assumed. The equation 2.9 is almost species independent and thus contributes with the same amount of water for each sample. Only the length of the capillary per gram of dry material enters in the equation and can be discussed. This parameter is estimated to 10^{10}cm/g in the literature (Skaar 1988).

As illustrated, the capillary contribution increases rapidly when the RH exceeds 90%. Moreover, this condensation first contributes from a RH of 70%, because of the theoretical limitations in meniscus size not allowing meniscii to be formed below approximately 70% RH. Adding the capillary contribution to that of the BET, as proposed by Simpson (1973), gives the cumulative curve indicated by a black solid line in the figures. Here again the capillary contribution increases the moisture content exponentially at high relative humidities.

The humidity level at which Kelvins capillary condensation contributes to the moisture content depends on the radius of the pore. According to Kelvins equation 70% relative humidity corresponds to a radius of 0.0029µm at 27°C. The radius of the water molecule is 0.0005µm (Skaar 1988). Because the concept of surface tension assumes that large numbers of water molecules are involved it is questionable whether capillary condensation already occurs at 70% RH. It is more likely to occur beyond 90% RH.

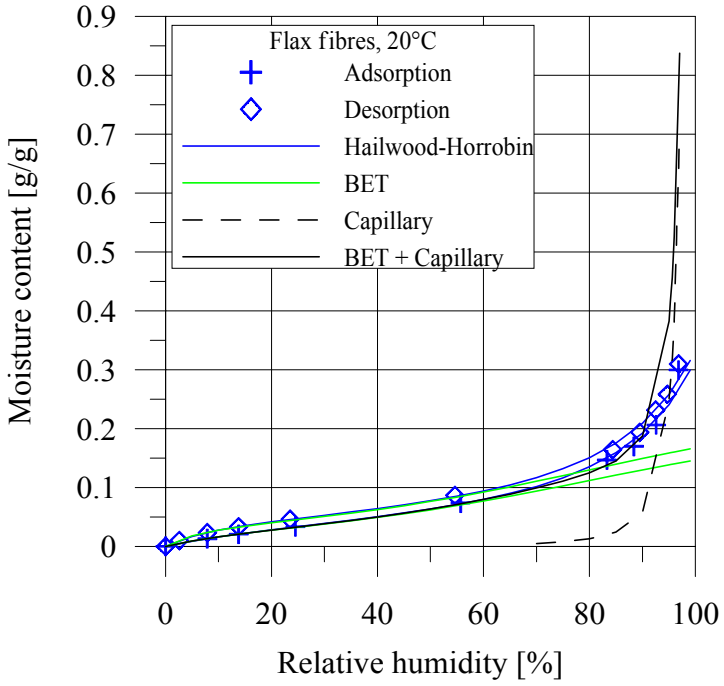

Figure 6.5. Sorption curve for flax fibres at 20°C modelled by BET, Hailwood–Horrobin and capillary condensation.

Comparing the curve for capillary condensation with that of the H–H model indicates, in general, that the capillary contribution is too steep in relation to the data points, including the curves on Figure 6.7 and Figure 6.8 at 40°C. On the other hand, the H–H model does not seem to rise enough when the RH is beyond 95%. Prolonging the curves will intersect the y-axis instead of rising infinitely, which would have been a more realistic course.

Summing up in the RH region from 50% to almost 100% shows that the model proposed by Hailwood–Horrobin and the SORP model give the best fit to the data points obtained from the sorption experiment. Although not satisfactory close to 100%, no other models proposed in the literature seem to give a more reasonable result.

In the region from 0% to about 50% RH the BET, SORP and H–H models are all appropriate. Since the BET model is based on a layering theory, the number of layers is variable and one has to decide the maximum numbers of layers in the equation. Usually the number is about 7 for wood materials; this is the value used in Figure 6.4 to Figure 6.8. In Figure 6.9, the same sorption isotherm as used in Figure 6.4 is modelled with a varying number of maximum layers of water molecules on the surface. Again, the BET model is

not valid beyond 50% RH as indicated in the figure. Whether the numbers of layers is between 5 and 9 does not seem to make any difference in the region from 0% to 30% RH.

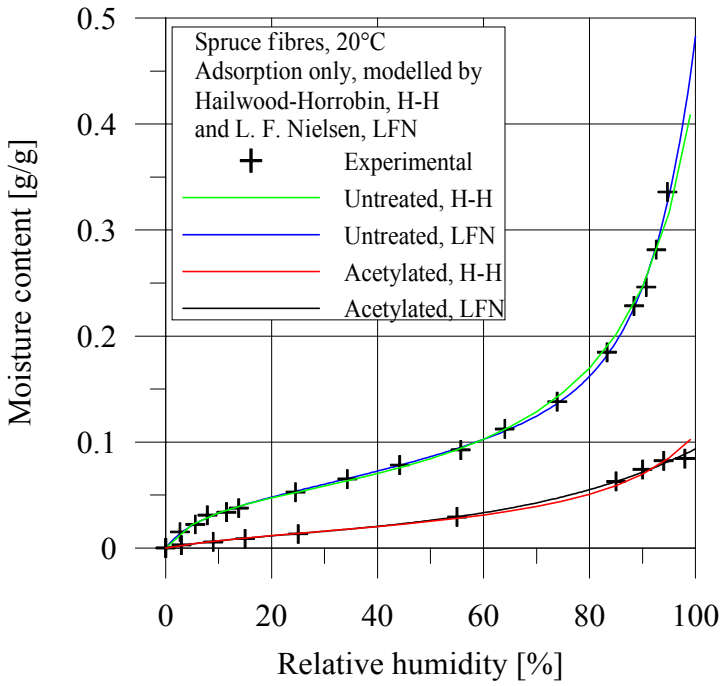

Figure 6.6. Sorption curve for spruce fibres and acetylated spruce fibres at 20°C modelled by H–H and the SORP model.

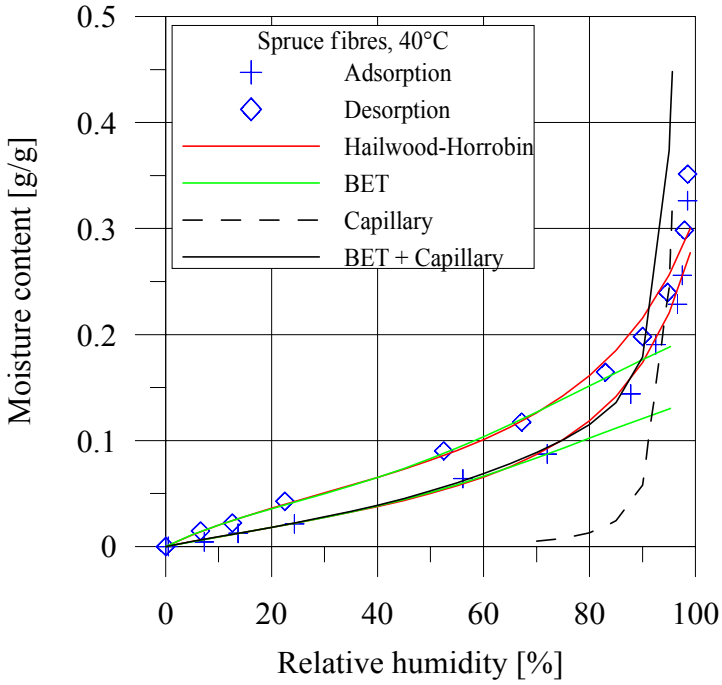

Figure 6.7. Sorption curve for spruce fibres at 40°C modelled by BET, Hailwood–Horrobin and capillary condensation.

From 30% to 50% RH, the curves for 5 and 6 layers are lower than the other curves, and lower than the actual data points and therefore not relevant for further analysis. N equals 7, 8 or 9 layers each fits the points quite well and maybe n equals 8 gives a slightly better fit than 7. 9 layers are probably too high. Generally speaking, it is impossible just to recommend a single value, but it has to be based on individual evaluations. Since the BET model does not fit the sorption isotherms better than the H–H model in the lower RH region and since the SORP and H–H models are most appropriate beyond 50% RH it is decided to use either the SORP model or the H–H model in the further analysis of other isotherms.

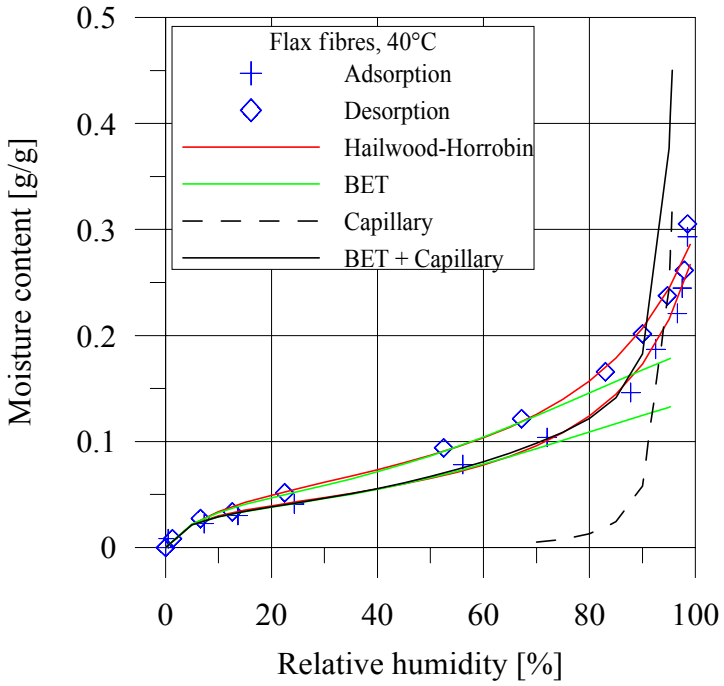

Figure 6.8. Sorption curve for flax fibres at 40°C modelled by BET, Hailwood–Horrobin and capillary condensation.

The SORP model and the H–H model are almost similar in the modelling of the two very different isotherms in Figure 6.6. Actually, it looks like the SORP model provides a slightly better fit according to the individual data points. However, the H–H model estimates the sorption isotherm from a mathematical fit including three parameters whereas the SORP model has five parameters included in the fit. Therefore it is decided to use the H–H model in the further analyses.

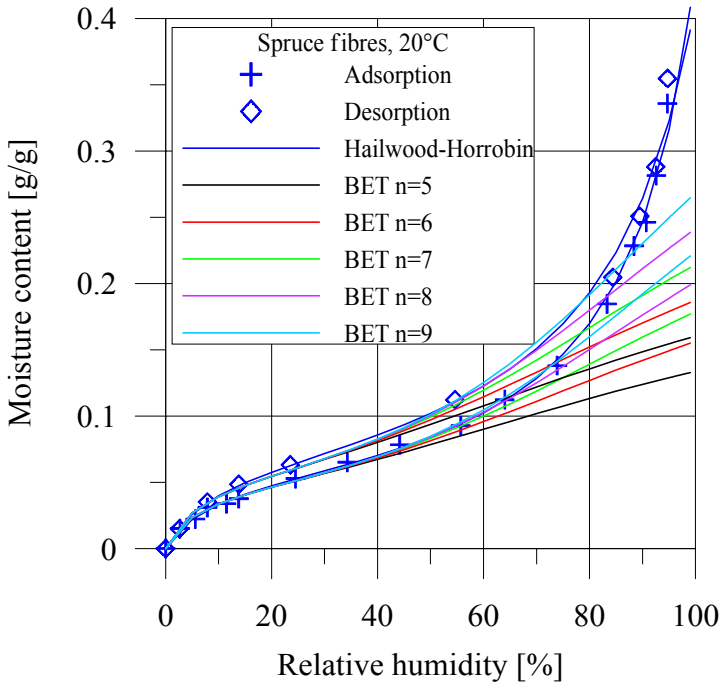

Figure 6.9. Sorption curve fitted by BET with a varying maximum number of layers of water molecules on the surface.

6.2.2. Sorption isotherms at different temperatures.

Sorption isotherms at three different temperatures 20°C, 40°C and 60°C have been determined experimentally and plotted in the following graphs. Both adsorption and desorption are measured and all the data are modelled by H–H. On Figure 6.10, spruce fibres are plotted showing the general trend of reduced equilibrium moisture content at a given relative humidity. This matches an increase in the relative humidity of the sorbed water in the samples.

The decrease in the equilibrium moisture content is due to thermodynamic considerations, as discussed in Chapter 2. The adsorption curve for spruce at 60°C is almost identical to the similar curve at 40°C in conflict with the general trend. The reason is supposed to be experimental errors like especially the last point showing a higher equilibrium moisture content than the corresponding desorption point, which from a theoretical point of view is impossible. The fit of the 60°C curve also shows an inconsistent intersection of the adsorption and desorption curves. The intersection is presumably due to the second point from the top of the adsorption curve showing a higher moisture content than the last point, which definitely is not true.

Apart from that, all three isotherms show hysteresis as expected, although of varying degree. The adsorption/desorption (A/D) ratio is higher for the 40°C curve than for the other two. This is unexpected and is probably due to the experimental error in that particular experiment, the first at elevated temperatures. The following curves for 40°C show the same tendency.

The hysteresis or A/D ratio is expected to change between the curves at varying temperatures. On the curves for spruce the hysteresis at 60°C is less than at 20°C, indicating a decreasing hysteresis with increasing temperature in agreement with Skaar (1988).

The plots in Figure 6.11 of beech fibres are again at three different temperatures. Generally, the curves tend to lie above each other in the right order of increasing temperatures. However, the desorption curves for 20°C and 40°C are very close to each other, especially below 60% RH, this shows less variation than expected. In comparison with the spruce fibres, this is unexpected because the same comparison on solid beech and solid spruce shows almost coincident curves (Figure 6.12) and it was therefore expected that the fibres would show a similar behaviour.

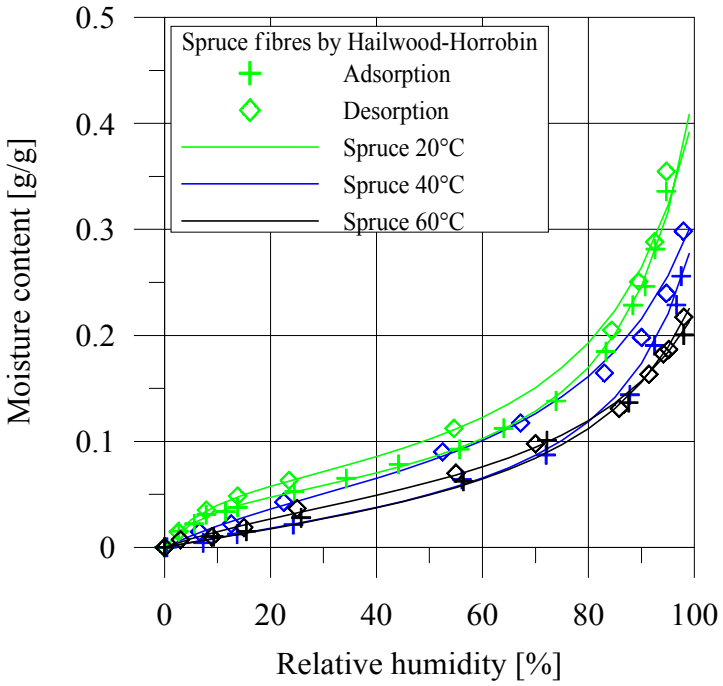

Figure 6.10. Sorption isotherms for spruce fibres measured at 20°C, 40°C and 60°C and modelled by Hailwood–Horrobin.

Curves for spruce fibres, solid spruce, beech fibres and solid beech are plotted in Figure 6.12. Though the "solid" curves are almost identical, the "fibre" curves do not. The curve for spruce fibres is clearly above the beech fibre curve. The reason is difficult to determine and in spite of small differences in the chemical constituents, such a deviation is clearly not due to the different amounts of the constituents. Rather, it could be caused by the treatment in the defibration process where the fibres amongst other things are heated up. And, the spruce- and beech fibres are not necessarily treated in exactly the same way or at least not from the same batch. The defibration process could therefore affect the sorption properties under the assumption that beech and spruce were assumed to behave almost similarly. Otherwise, these results just show the real difference existing between those species.

The beech fibre curve measured at 20°C is diverging from the corresponding spruce fibre curve showing lower moisture content and therefore almost identical with the 40°C curve in Figure 6.11. There is no obvious reason for this close position. In the vicinity of 100% RH, the 20°C modelled spruce fibre curve also tends to approach a higher saturation value than the similar modelled beech curve in Figure 6.12 contrary to the 40°C curves in Figure 6.10 and Figure 6.11. The spruce fibres approaches 0.4g/g, and the beech fibres only 0.3g/g moisture content at 20°C.

The hysteresis at 40°C is expected, again, to be due to the experimental error in this particular experiment. But for 60°C something seems to be wrong with regard to the adsorption part. This curve is below the other adsorption curves, as expected, but it seems to be too low from 40% RH to 100% RH. This may be explained by the fact that the material degrades when exposed to high humidity and elevated temperatures increasing the rate of degradation. This may be an explanation for the peculiar adsorption curve. Since the curves in the following figures do not show a similar behaviour, it may be concluded that there is no general experimental error.

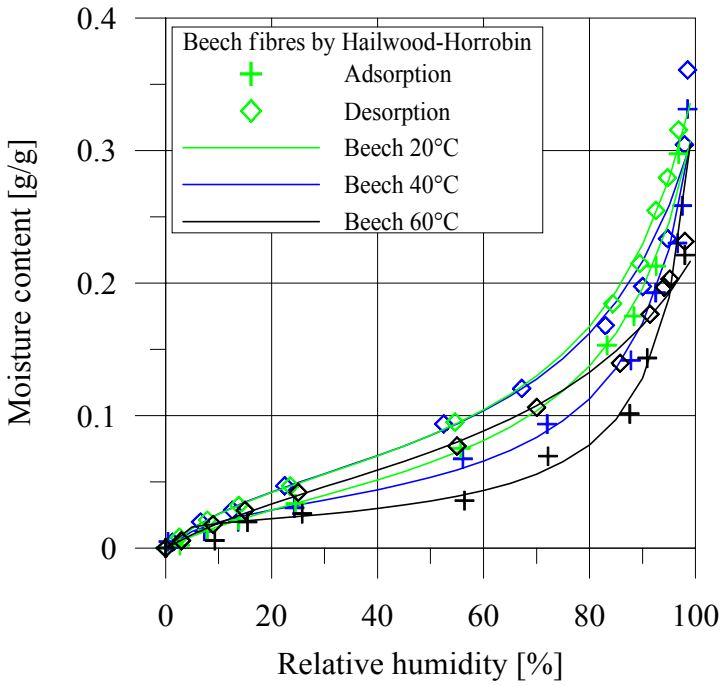

Figure 6.11. Sorption isotherms for beech fibres measured at 20°C, 40°C and 60°C and modelled by Hailwood–Horrobin.

Figure 6.13, Figure 6.14 and Figure 6.15 are sorption isotherms from different plant fibres. The sorption curves are measured at 20°C, 40°C and 60°C for flax, hemp and wheat straw fibres. There is an increasing moisture content going from flax to hemp and further to wheat straw. It is particularly true for the high humidity region above 80% RH and further more beyond 90% RH. Specifically, the moisture content at 20°C for flax, hemp and wheat straw at approximately 95% RH is about 0.30g/g, 0.35g/g and 0.50g/g. Especially the

wheat straw seems to have a remarkably higher saturation value than the other plant fibres and wood fibres in previous plots. The same pattern is valid at 40°C and 60°C.

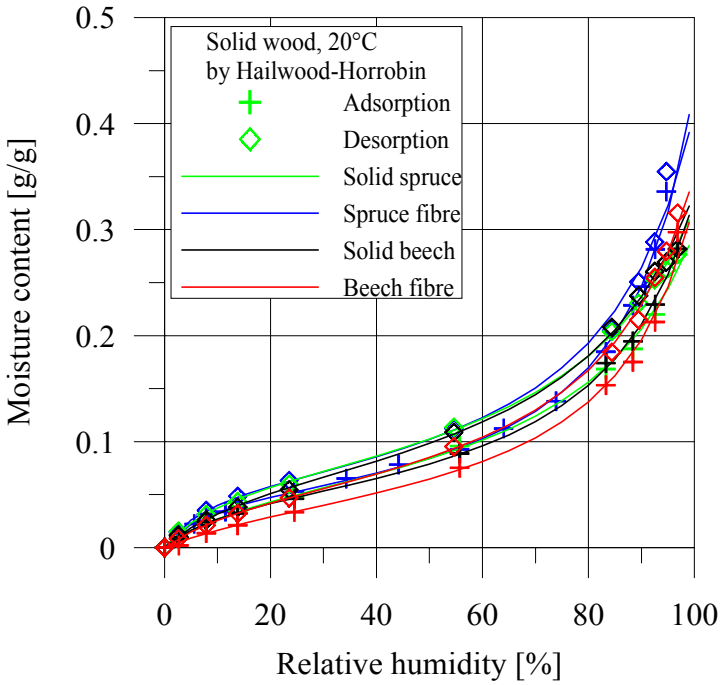

Figure 6.12. Sorption isotherms for spruce fibres, solid spruce, beech fibres and solid beech measured at 20°C and modelled by Hailwood–Horrobin.

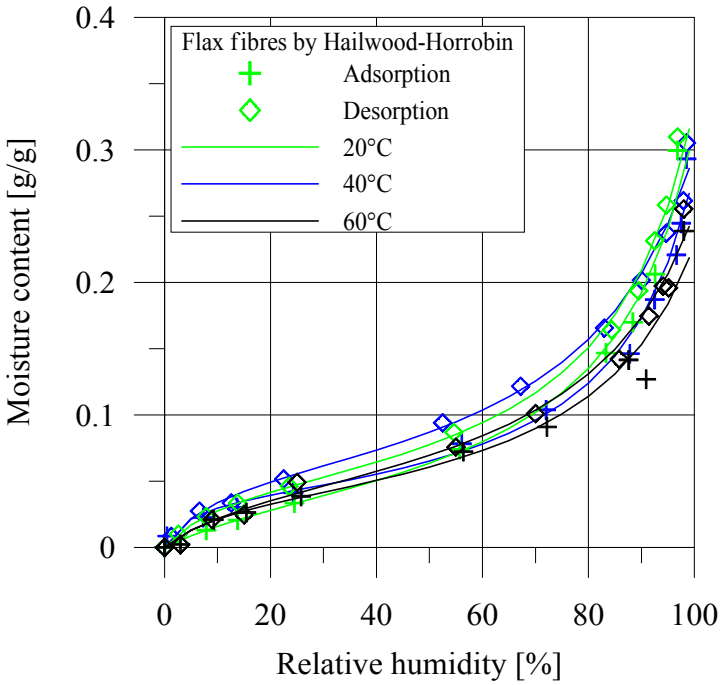

Figure 6.13. Sorption isotherms for flax fibres measured at 20°C, 40°C and 60°C and modelled by Hailwood–Horrobin.

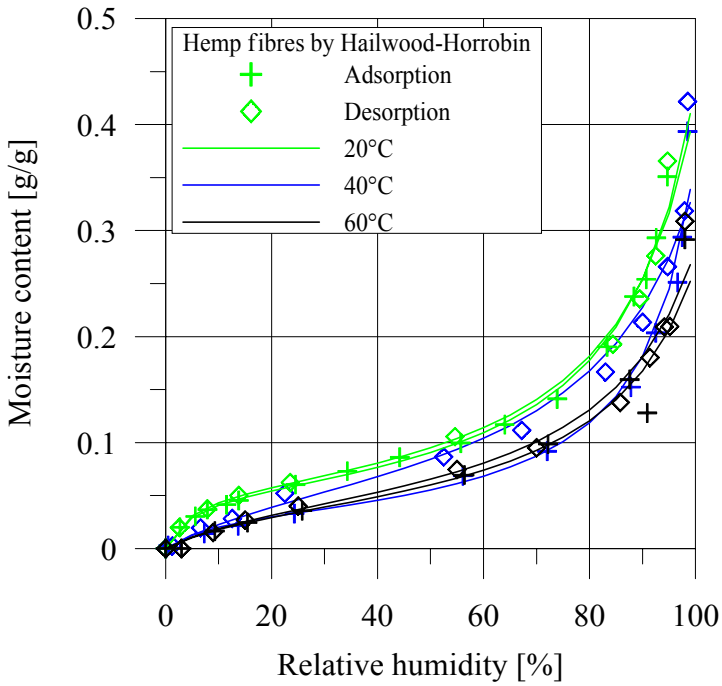

Figure 6.14. Sorption isotherms for hemp fibres measured at 20°C, 40°C and 60°C and modelled by Hailwood–Horrobin.

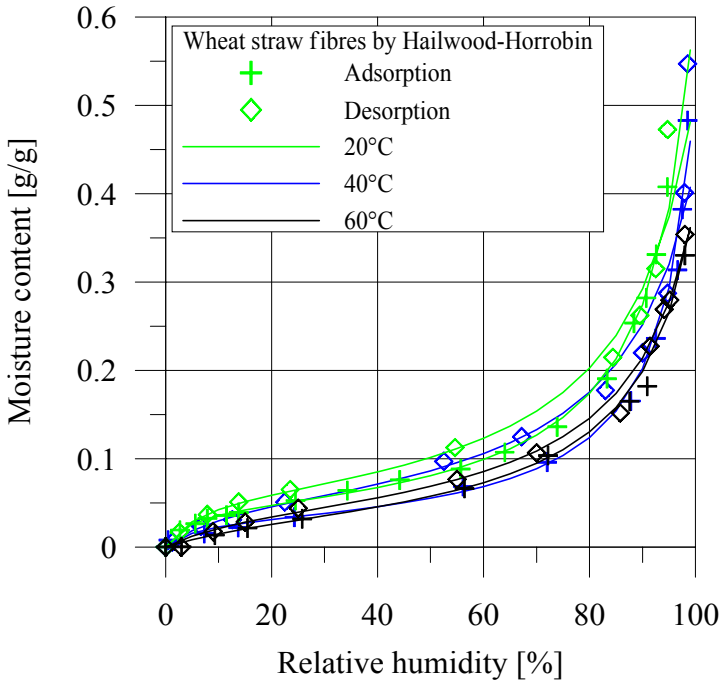

Figure 6.15. Sorption isotherms for wheat straw fibres measured at 20°C, 40°C and 60°C and modelled by Hailwood–Horrobin.

The reason for this difference may lie in a difference in the chemical composition. According to Table 6.1 the major difference is in the lignin content between wheat straw

and hemp and flax fibres. Since lignin is supposed to adsorb the least amount of water among these three constituents, the position of the sorption curves is caused by something else. The hemicellulose content could be the answer regarding the total heat of wetting and hygroscopicity. Hemicellulose generally has a higher moisture content than cellulose and lignin (Stamm 1964, Skaar 1988) and likewise for the total heat of wetting (Stamm 1964). The total heat of wetting therefore indicates that hemicellulose is more willing to adsorb water than the cellulose or lignin.

Another reason could be the degree of crystallinity of the cellulose. Although fibres have the same cellulose content, the crystallinity of the cellulose strongly influence the behaviour related to water (Salmén 1997). The degree of crystallinity is not available.

Table 6.1. Chemical composition of a selection of wood and plant fibres (McDougall et al. 1993).

Species	Cellulose (%)	Hemicellulose (%)	Lignin (%)	Extractives, ash (%)
Spruce/beech	40-45	20-30	20-30	0.3
Flax	56.5	15.4	2	-
Hemp	67	16.1	3.3	-
Wheat straw	51-54	26-30	16-18	7-8

Extrapolating the sorption curves up to 100% RH would theoretically approach complete saturation, and it is evident that the fibre saturation point M_f, thus estimated, decreases with increasing temperature. The curves shown here are not extrapolated to 100% since the H–H model estimates values too high to plot on the same graph. It is reported by Stamm that there is a decrease of approximately 1% in M_f per 10°C increase in temperature between 25°C and 100°C. The figures show clearly a higher fibre saturation point for wheat straw than for flax.

A more detailed study of the plots shows some peculiarities that need commenting. For the flax fibres, the isotherm at 20°C is subject to uncertainty. A large part of the curve is below the other two curves, which from a theoretical point of view is impossible. Since the hemp and wheat straw are measured in the same climate chamber at the same time and they look as expected, the error is anticipated to be due to the sample.

The curves at 40°C all demonstrate a wide hysteresis like the previous wood fibres and this is assumed to be due to the same reasons concerning experimental errors. At 60°C, the adsorption point at 90% RH for all three plants fibres are clearly wrong. It is simply too low and assumed to be caused by an error in the humidity control in the climate chamber.

6.2.3. Discussion

A review of all the plotted sorption isotherms, Figure 6.16 (adsorption only), indicates the weakness of the H–H model in the high humidity region. However, neither the BET nor the capillary contribution proposed by Simpson fit the curves satisfactorily. Moreover, the BET is not valid beyond 50% RH. Another approach would be an attempt to find a more plant specific model for the plant fibres as well as models for wood and wood based

products. This is because, generally, some of the plant fibres presented have very high moisture contents when close to 100% RH and the models used do not fit the curve properly. Nevertheless, none of the present models seem to explain the sorption of water for plants more accurately than the H–H model and it is therefore still the right choice.

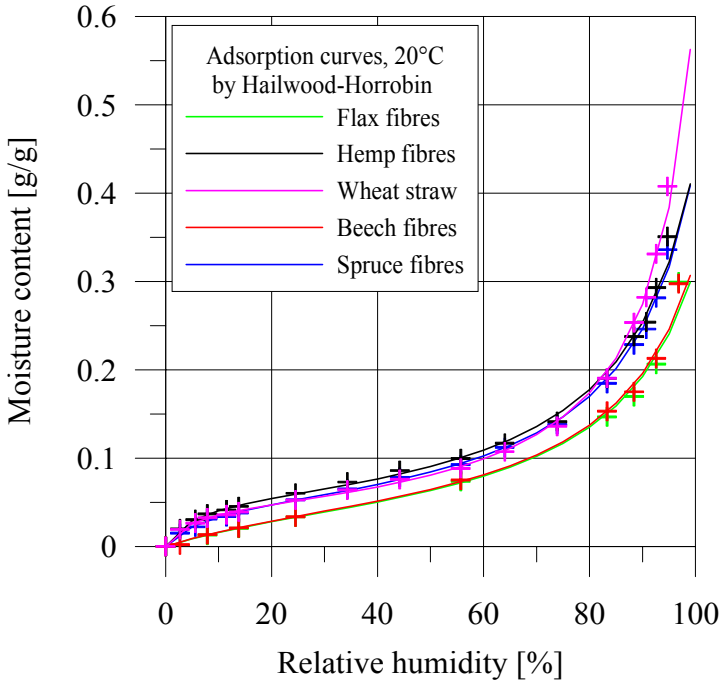

Figure 6.16. Review of sorption isotherms of flax, hemp, wheat straw, beech and spruce fibres at 20°C.

Since there is such a significant increase in the moisture content, especially in the plant fibres (e.g. in wheat straw) when reaching about 95% RH, other mechanisms are probably contributing. Extrapolation of the curves to 100 % RH, theoretically approaching complete saturation, determines the fibre saturation point (FSP). Within wood science, it is common practice to use a value for FSP in the range from 27-32% moisture content (Skaar 1988). However, great variations exist which depend on the method used for the determination.

For those of the plant fibres showing a large increase in the moisture content near 100% RH, the fibre saturation point seems to be much more than 30%. Here the fibre saturation point is rather about 40% or 50%.

The fibre saturation point is achieved when the cell wall is fully saturated with moisture. For some specific fibre types, the FSP is probably achieved before reaching 100% RH (Skaar 1988). However, the determination of the FSP is still discussed and different opinions exist between researchers. For instance, it is still discussed whether the presence or absence of liquid water in the cell wall cavities or voids are included.

With regard to the high moisture content at 95% RH in e.g. wheat straw this gives rise to several interpretations. It could be caused by capillary condensation or the formation of clusters of water molecules (Hartley & Avramidis 1993). If this is true, it reveals the FSP to be achieved before 100% RH is reached. According to an investigation by Berthold et al.

(1994), the number of water molecules adsorbed per hydroxyl group reaches one H_2O/OH group at 92% RH, corresponding to the FSP.

6.3. Sorption isotherms – chemically modified fibres

6.3.1. Acetylated fibres

This section presents experimental results for spruce and beech fibres chemically modified by acetyl. In an attempt to reduce the water uptake in the fibres, they have been acetylated. The acetylation process blocks the hydroxyl groups by acetyl thus increasing the hydrophobicity. As a result, there is a relation between the degree of acetylation and the weight gain or mass acetyl content. The longer the material has been acetylated the more acetyl is adsorbed and the weight gain increases. A more detailed description of the acetylation treatment can be found in Chapter 5.

Another, and very important, reason for the acetylation of the fibres is to test the hypothesis that micro pores do not exist in the wood and plant cell walls. Why is this hypothesis put forward? For a long time, it has been a point of discussion whether or not micro pores exist in the cell wall. If the micro pores exist, capillary condensation will occur and contribute to the moisture content. If the fibres are acetylated the hydroxyl groups are blocked with acetyl, prohibiting water adsorption. But capillary condensation is still a valid phenomenon because this mechanism is caused by the geometry of the pores and not the individual sorption sites. Therefore, if the acetylation treatment significantly decreases the moisture content all the way from 0 to about 100% RH it indicates the absence of micro pores. The acetylation treatment of the fibres does indeed substantiate the evidence for this hypothesis.

The spruce fibres were treated for 10, 60 and 240 minutes and the beech fibres for 20, 60 and 240 minutes. Table 6.2 presents the treating times and the corresponding mass acetyl contents for spruce and beech fibres.

Table 6.2. Treatment times and mass acetyl content for acetylated fibres.

Spruce fibres		Beech fibres	
Treatment time (minutes)	Mass acetyl content (%)	Treatment time (minutes)	Mass acetyl content (%)
10	7.06	20	13.19
60	17.09	60	15.57
240	20.55	240	19.16

The results of the sorption studies on the treated fibres are shown in Figure 6.17 and Figure 6.18. There is a pronounced effect of acetylation on both types of fibres. The most pronounced difference for spruce fibres is seen for fibres treated for only 10 minutes. Already after such a short treatment time, the reduced water adsorption is significant. Although the water adsorption is further reduced, when treatment time is prolonged, the

first treatment is more effective relatively speaking. Extending the treatment time from 60 to 240 minutes does reduce the sorption propensity but relatively less than an extension from 10 to 60 minutes. Looking at the curves, it is evident that the acetylation treatment at RH below 50% has a fairly large impact on the material. It is an indication that all of the hydroxyl groups on the surface are easily accessible. At RH above 60%, it is more difficult, indicating the need for more time to penetrate into the cell wall and cell wall cavities to find hydroxyl groups.

For the beech fibres in Figure 6.18, it is generally the same pattern, but the curve for 20 minutes acetylation is slightly lower than the 10 minute curve for spruce. For the 60 and 240 minutes acetylation, it is reversed, that is, a lower curve for spruce than for beech. However, it is not possible just to compare the curves this way. The reduction in water adsorption has to be related to the untreated curve.

6.3.2. Discussion

For untreated spruce, the highest moisture content is about 0.34g/g and is reduced to about 0.20g/g after 10 minutes acetylation, a 40% reduction in total. After 60 minutes acetylation, it is reduced to about 0.10g/g corresponding to a 70% reduction, and after 240 minutes treatment it is reduced to about 0.08g/g corresponding to a 75% reduction in water adsorption.

For untreated beech, the highest moisture content is about 0.32g/g and is reduced to about 0.15g/g after 20 minutes treatment. This is a reduction of 53%. After 60 minutes treatment it is reduced to 0.13g/g equal to 59% reduction. After further treatment to 240 minutes, the moisture content is reduced to about 0.11g/g equal to 66% reduction.

By comparing the treatment of the two types of wood fibres, it is seen that there is a more effective reduction in moisture content for spruce than for beech fibres. 10 and 20 minutes treatments are not straightforward to compare because of the different treatment times and different species. Still, 20 minutes treatment time further reduces the moisture content than 10 minutes does. For 60 minutes, it is 71% versus 59% and for 240 minutes, it is 75% versus 66%. Comparing the acetyl content gives for 60 minutes 17.09% versus 15.57% and for 240 minutes 20.55% versus 19.16%.

This proves that there is a relation between the reduction in moisture uptake and acetyl content in the acetylation treatment. Why then is there a difference between spruce and beech fibres? However, with the same treatment, spruce fibres are more susceptible than beech fibres. The surface area per gram of material is supposed to be the same for both spruce and beech (Stamm 1964). When the fibres are immersed into the acetyl solution the penetration takes place by conduction and diffusion. In the beech fibre vessel elements, the conduction process prevails whereas in the libriform fibres and in the spruce fibres the adsorption of acetyl primarily takes place by a zig-zag diffusion through the pits.

Another reason for the difference in the acetylation could be the sizes of the fibres in general. The technique used in this case for the acetylation caused some problems and indeed some fibre loss occurred as part of the process due to the small fibre size. Moreover, beech fibres are smaller than spruce fibres.

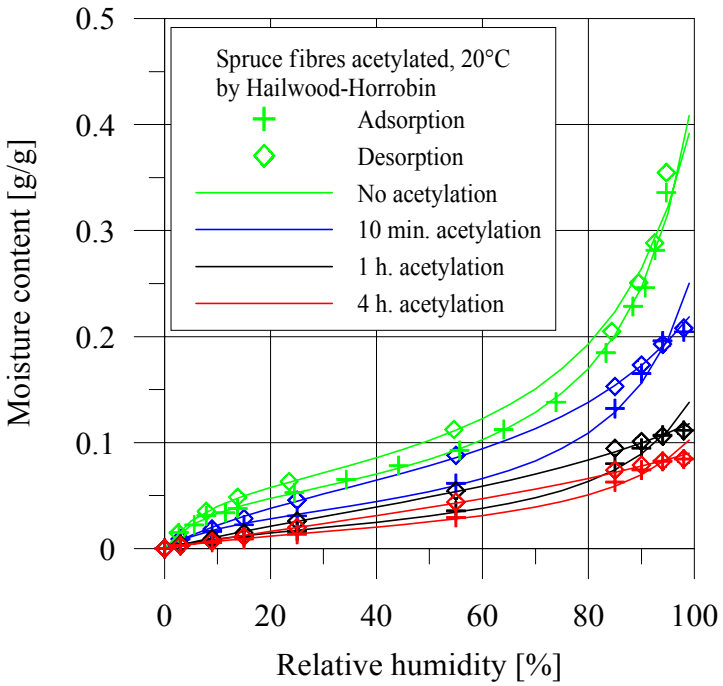

Figure 6.17. Sorption isotherms for untreated spruce fibres and spruce fibres treated with acetyl for 10, 60 and 240 minutes.

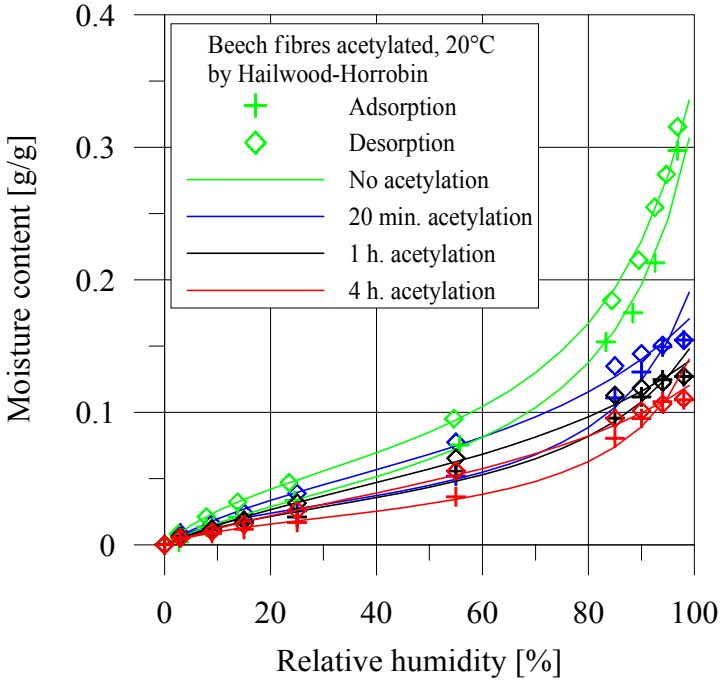

Figure 6.18. Sorption isotherms for untreated beech fibres and beech fibres treated with acetyl for 20, 60 and 240 minutes.

6.3.3. Acetylated fibres at different temperatures

Sorption isotherms for acetylated spruce fibres have also been measured at elevated temperatures. The results (Figure 6.19 and Figure 6.20) show the expected behaviour at 40°C. Even though the position of the curves is in right order, the curve for 10 minutes acetylation has a large hysteresis. Although not as large, the curve for untreated spruce fibres also has a large hysteresis. In comparison to the similar curves at 20°C the curve for untreated spruce fibres at 40°C is slightly below the 20°C curve, and the 10 minutes acetylation curve at 20°C is, contrary to expectation, higher than the 40°C curve. That is, higher moisture content at a higher temperature, which is definitely wrong. This must be due to the problems, mentioned earlier, with the difficulty in controlling RH in this first experiment at elevated temperatures. The curves for 240 minutes treatment are almost identical for both 20°C and 40°C and actually also for 60°C.

In Figure 6.20, there is plotted almost only desorption curves for 10 and 240 minutes treatment. The few points measured for adsorption are plotted with a dashed line in between. The desorption curve for 10 minutes acetylation at 60°C crosses the curve for untreated spruce about 75% RH which is unexpected.

6.3.4. Discussion

The curves for 240 minutes treatment at 40°C and 60°C are almost similar as mentioned above. Often, the most distinct difference is above 90% RH and since data in this high humidity region are generally not very reliable it is difficult to measure any difference. In addition, it is at elevated temperature thus increasing the difficulty in accurate measurements.

The mistake in the crossing of the 10 minutes desorption curves seems primarily to be caused by the curve for untreated spruce fibres, since this curve is very low. However, the curve for 10 minutes acetylation also seems to be too high in the region from 0% to 50% RH and therefore the curves cross each other. One reason could be the combination of high temperature and humidity initiating a biodegradation starting in the high humidity region, but not succeeding until 0% RH.

If biodegradation occurs then it should also influence the 240 minutes curve and maybe does, but it is difficult to quantify. However, acetylated fibres are usually very resistant to degradation and the reason for the position of the curves is more likely to be found elsewhere. Since there is a general offset from 70% to 0% RH for 10 minutes acetylation above that of untreated spruce and since the offset starts where the adsorption measurement starts, there is probably a relation. The fibres acetylated for 10 minutes have been exposed to the high temperature for less time than the untreated fibres because this particular experiment was delayed. The crossing curves are perhaps induced by this mechanism.

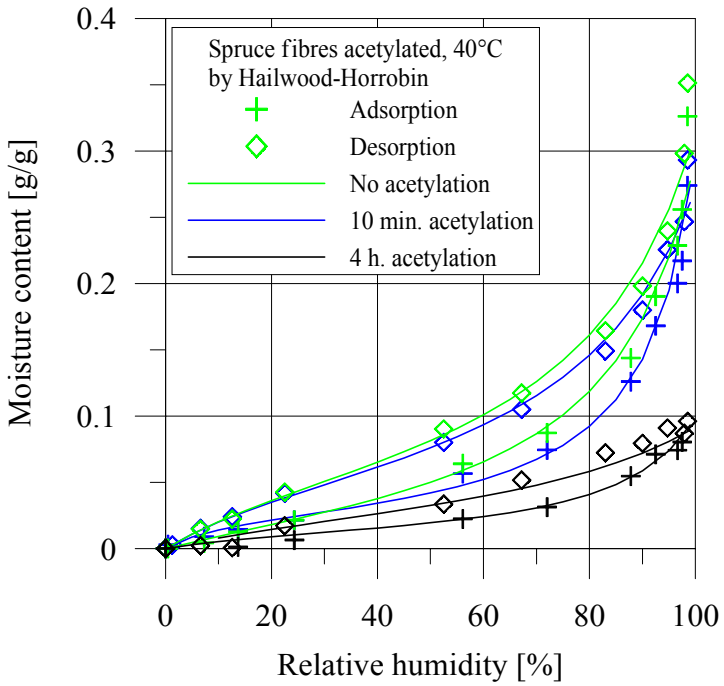

Figure 6.19. Sorption isotherms for untreated spruce fibres and spruce fibres treated with acetyl for 10 and 240 minutes at 40°C.

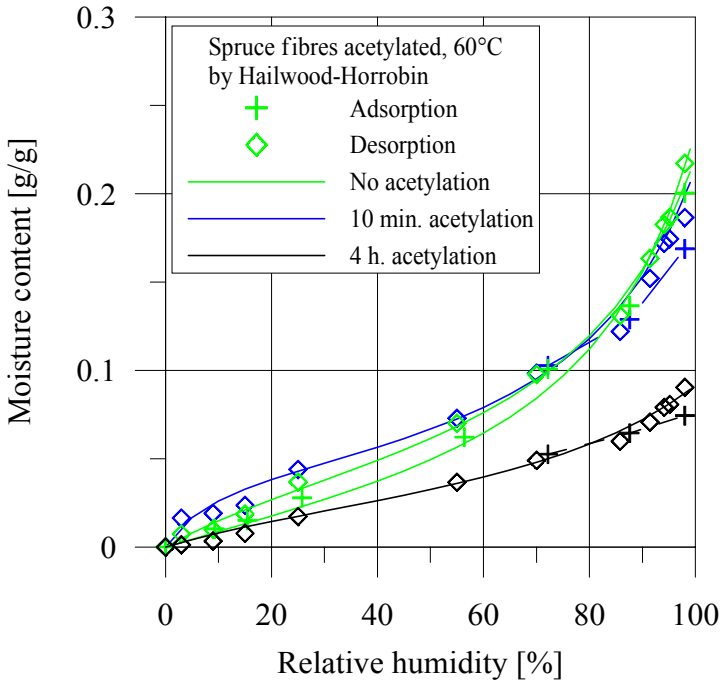

Figure 6.20. Sorption isotherms for untreated spruce fibres and spruce fibres treated with acetyl for 10 and 240 minutes at 60°C. There is only a few measurements available for 10 and 240 minutes.

6.3.5. Hypothesis on micro pores

In this section, it is attempted to prove the hypothesis on the presence of micro pores in the cell wall. It is already a fact that the acetylation treatment decreases the moisture content significantly. At 20°C, 40°C and 60°C the reduced moisture content is obvious, and in addition, it is reduced relatively equal all the way from 0 to almost 100% RH. To emphasize the relative reduction, the difference in moisture content for untreated fibres and acetylated fibres is calculated and shown in Figure 6.21.

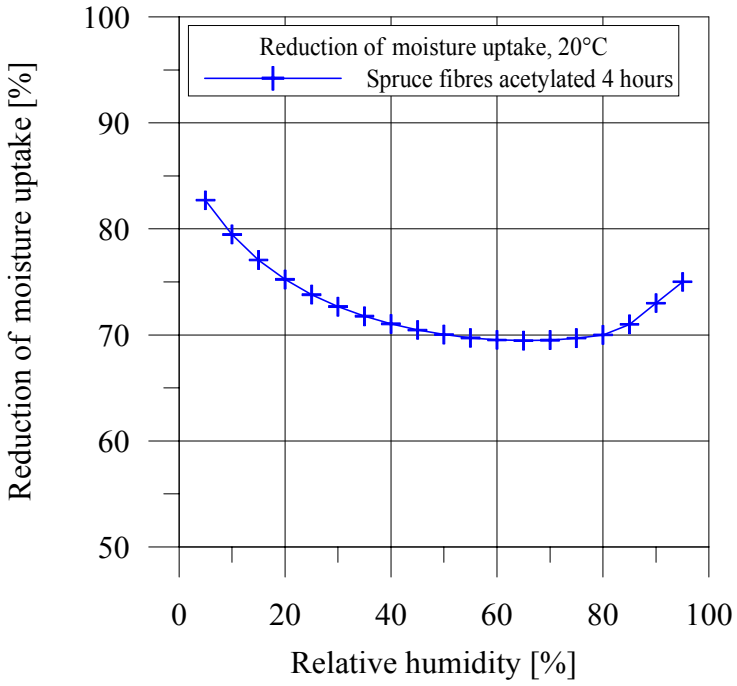

Figure 6.21. Reduction in moisture uptake for acetylated spruce fibres at 20°C.

Generally, in Figure 6.21, there is a pronounced reduction in the moisture uptake. From 0% RH until 70% RH there is a decreasing tendency too indicating the strong influence on the hygroscopicity of the material. From 70% RH until about 100% RH there is a slight increasing tendency. The question whether the micro pores are existing or not is discussed based on this curve.

If the decreasing tendency was continued all the way to 100% RH it seemed that the micro pores would have been absent, but one could argue that the slight increase beyond 70% indicates their existence. Beyond that, the general reduction in moisture uptake above approximately 75% strongly demonstrate the lack of micro pores. Otherwise, the moisture content in the sample would not have been reduced so drastically. Furthermore, if the micro pores do not exist, there is still the possibility that the slight increase beyond 70% in Figure 6.21 is due to capillary condensation of a fraction of the cell lumen. However, capillary condensation does not usually act before 99.5% RH (pore diameter 0,1-1µm) and may therefore not initiate the slight increase of the curve already at 70%. However, sometimes fibres are damaged during the defibration whereby small cracks are created in the cell wall thus allowing water to condense. Again, it is questionable whether capillary condensation can act at relative humidities as low as 70% considering the corresponding

pore radius where a capillary meniscus is formed. According to a previous section pores corresponding to a RH of 70% are assumed to be too small for capillary condensation.

6.3.6. Discussion

In the attempt to prove the hypothesis of the presence of micro pores a comparison of the pore size distribution for the untreated and acetylated fibres is made. The calculation of the pore size distribution is based on the sorption isotherms for the materials. First, the pore radius corresponding to the relative humidity is calculated by the Kelvin equation 2.2. Thereafter it was attempted to calculate the pore volume for both the untreated and the acetylated spruce fibres. Since the density and the swelling of the fibres are not alike the volume would be difficult to determine. Therefore, it is decided to plot the pore size distribution as the pore radius versus the water content per gram of dry material. It seems to be the most reasonable way to compare the fibres. The plot presented is in Figure 6.22.

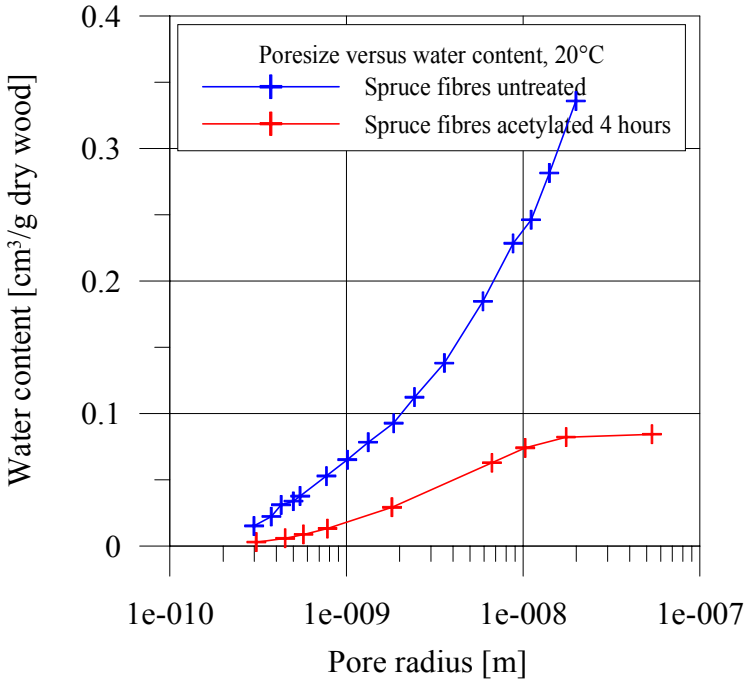

Figure 6.22. Cumulated pore size distribution of untreated and acetylated spruce fibres at 20°C.

The cumulated pore size distribution in Figure 6.22 shows a significant difference in the treated and untreated material. This also indicates the absence of micro pores in the cell wall due to the limited amount of pores available in the acetylated sample. Actually, the acetylated fibres show a declining tendency in the pore volume despite the curve for untreated fibres continuously increasing. In this respect it is worth noting that the pore size distribution is not surprising since it is based on calculations from the sorption isotherms in Figure 6.17 showing the same tendency. Still, it contributes to prove the hypothesis on the presence of micro pores. The combination of the reduced moisture uptake in all the region from 0% to almost 100%, and the cumulated pore size distribution demonstrating the absence of micro pores, indicates that the hypothesis is reliable. That is, the micro pores do no exist.

6.3.7. Enzyme treated fibres

The purpose of the enzyme treatment is to enhance composites made of wood and plant fibres. The enzyme oxidizes the lignin to create free radicals improving the cross linking of fibres in a composite board. A further description of the enzyme treatment is found in Chapter 5. Sorption isotherms for spruce and beech fibres treated with enzymes are shown in Figure 6.23. It is very clear, that the enzyme treated fibres and control fibres behave in a significantly different manner compared to all other types of fibres presented.

The adsorption curve in particular has been subject to a significant increase in moisture content in the region from 5% to 80% RH. Where all other sorption curves presented are of type II with the sigmoid shape this adsorption curve tends to increase at a constant slope until 100% RH. At this point, when the desorption starts, there is a significant drop off in the moisture content and the desorption curve goes below the corresponding curve for untreated fibres. Generally, the curves for both enzyme treated spruce and beech fibres show a remarkably wide and reversed hysteresis.

The moisture content beyond 80% RH is lower than that for the untreated fibres. Extrapolating the curves for untreated spruce to 100% RH demonstrates a higher fibre saturation point than the enzyme treated fibres.

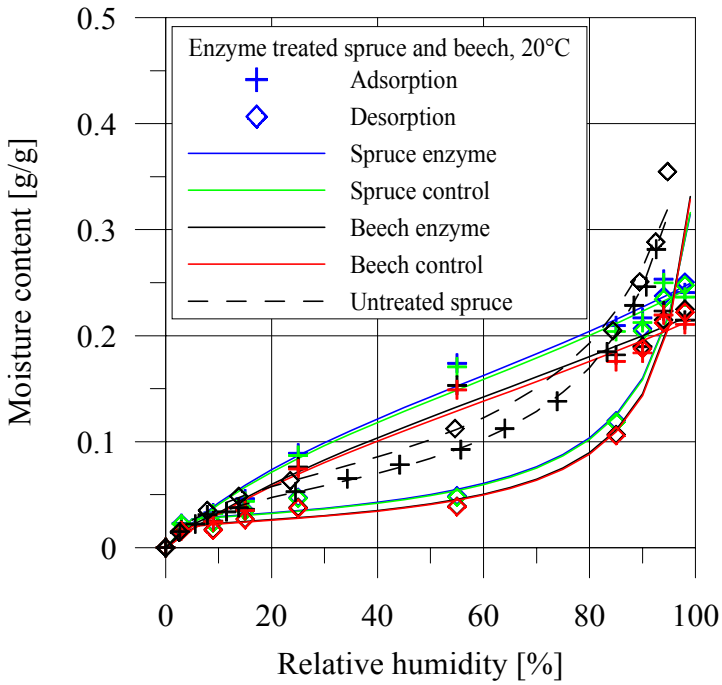

Figure 6.23. Sorption isotherms for enzyme treated spruce and beech fibres. The control fibres are treated like the enzyme treated fibres but without enzyme (laccase) added. All the isotherms are modelled by H–H.

6.3.8. Discussion

The reason why the adsorption curve for enzyme treated fibres is above the curve for untreated fibres may be due to the chemical influence on the surface of the material. Because the enzyme treatment is made in an attempt to oxidize the lignin more water is

attracted by the laccase enzyme which is used as the catalyst. It seems that the material behaves as a polymolecular sorption site indicating an increasing number of layers concurrent with the increase in humidity.

It is known that the enzyme treatment decays when the humidity increases and this may be one of the reasons why the curve levels off in the vicinity of 100% RH instead of increasing exponentially like the ordinary curve. This decay of the enzyme treatment is also part of the reason for the sharp decreasing desorption curve.

Surprisingly, the control fibres show an almost identical sorption behaviour in adsorption and desorption, respectively, as does the enzyme treated fibres. The control fibres were not expected to deviate from the curve for untreated spruce as shown. This indicates that the enzyme treatment is to be without importance. The control fibres have been washed in water for 30 minutes at 40°C and this relatively mild treatment was not expected to make significant changes in the sorption properties.

The experiment was only carried out once, but with the two different species, spruce and beech, each from its own batch. This should reduce the risk for mistakes during the measurement.

After the washing process, the fibres are dried at 60°C for 24 hours. When the water is poured off after the washing, there is a possibility that small particles from the fibre suspension are drained and not any longer found in the fibre sample. The small particles left between the fibres from the defibration process are exactly the parts of the lignin from the middle lamella where the fibres are supposed to be separated. During the defibration the middle lamella is broken down and is likely to be smaller than the individual fibres. Therefore, parts of the lignin are lost during the draining if it is not carried out with caution. A reduced lignin content in the fibre sample leads to an increased moisture content as indicated in the figure.

Another possible mechanism is a sort of restructuring of the fibre cell wall. Is it possible that the fibre wall restructures when soaked into water to a more energetically favourable position and thereby allows more water to be sorbed than usual. The restructuring only lasts until the fibre is again almost saturated, as is the case when RH is near 100%. At this point, the restructuring goes back to the point where the fibres were before the washing process and the moisture content decreases along with desorption. However, it does not completely explain the very wide and reversed hysteresis.

Generally, it is impossible to explain the exact reason why the curves for both enzyme treated fibres and control fibres show this behaviour. The enzyme treatment seems to be without action in comparison with the control fibres. The sorption behaviour for the control fibres are most probably caused by various elements difficult to extract one by one. To be certain of the measured sorption properties the experiment has to be repeated but with a new batch for each fibre type.

6.4. Sorption isotherms – hygrothermally treated fibres

In this section sorption studies on hygrothermally treated fibres will be presented. The fibres are all spruce and they have been treated in an autoclave at four different

temperatures and two different time spans. The temperatures are 160°C, 170°C, 180°C and 190°C and the treatment times were 20 and 40 minutes. 20 minutes is termed /5 and 40 minutes is termed /3. Fibres termed 160/3 have been treated at 160°C for 40 minutes and fibres termed e.g. 180/5 have been treated at 180°C for 20 minutes.

Figure 6.24 shows sorption curves for 40 minutes treatment time at 160°C, 170°C, 180°C and 190°C. The corresponding curve for untreated spruce is included for comparison. Generally there is a descending offset of all four sorption curves already taking place from about 5% RH and ending about 90-95% RH. In the high humidity region the offset seems to disappear. There is no general trend at which temperature treatment will decrease the moisture content most effectively. The highest temperature 190°C retains most moisture at the beginning but least at the end and the second highest temperature 180°C keeps the least amount of moisture at the beginning and most at the end. The lowest temperatures 160°C and 170°C are in between. The hysteresis is more pronounced for the 190°C curve than the others are as it also crosses the other curves from being the top curve to the lowest curve.

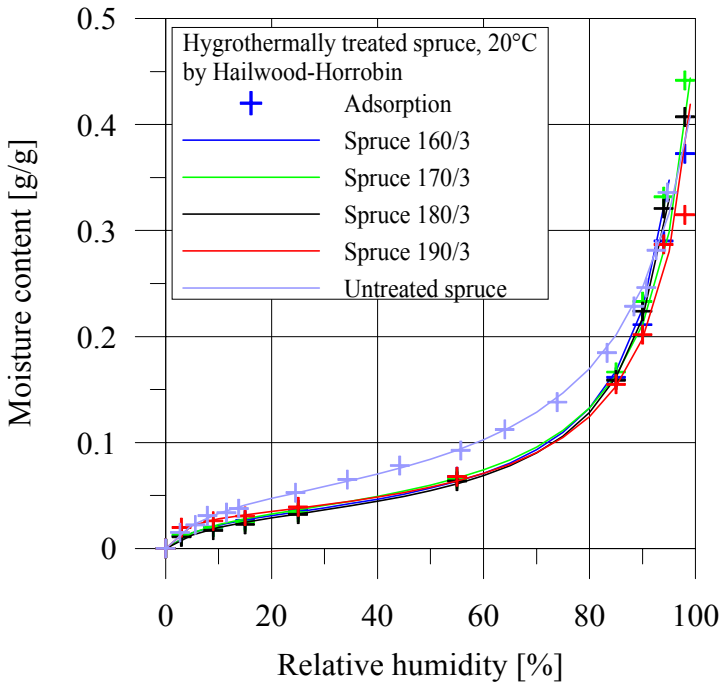

Figure 6.24. Sorption isotherms measured at 20°C for hygrothermally treated and untreated spruce fibres. Only curves for adsorption are shown. Treatment time was 40 minutes at 160°C, 170°C, 180°C and 190°C.

Figure 6.25 shows similar curves to those in Figure 6.24 but only treated for 20 minutes. The general pattern is not the same as before. Although the curves are again shifted downward the curves this time cross each other at about 85-90% RH so the lowest curves become the top curves. The curves are in a more “logical” order on top of each other with the 190°C curve lowest at the beginning and the 180°C above and further the 170°C and 160°C curves. This is until the curves shift to reverse order in the high humidity region.

The hysteresis for the treated curves is less than the untreated but seems to be of the same size no matter what.

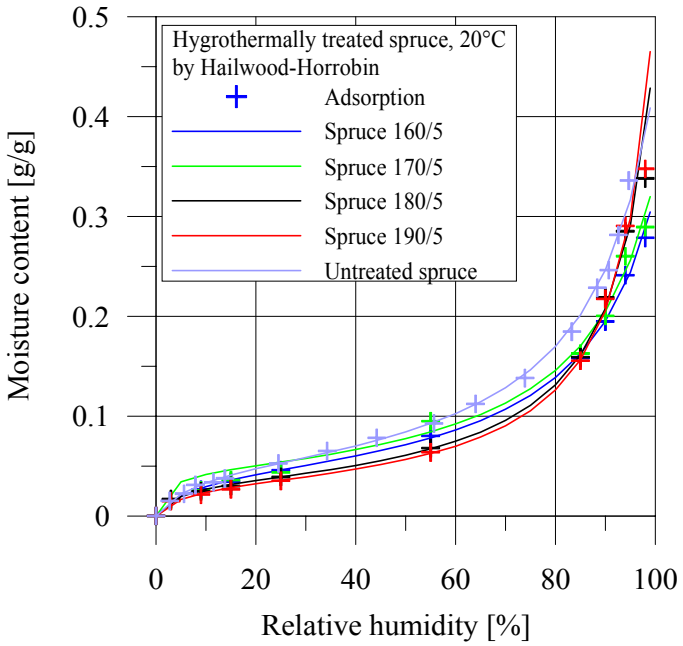

Figure 6.25. Sorption isotherms measured at 20°C for hygrothermally treated and untreated spruce fibres. Only curves for adsorption are shown. Treatment time was 20 minutes at 160°C, 170°C, 180°C and 190°C.

6.4.1. Discussion

Which processes are comprised in the hygrothermally treatments and by that the primary reason for the sorption behaviour? There are two possible reactions occurring in the material. The first is the breakdown of the hemicellulose and the second is the breakdown of the lignin structure. These reactions do not take place at the same time and the first to go is supposed to be the hemicellulose. This is caused by the fact that the glass transition temperatures for hemicellulose vary over a span of 150°C to 220°C depending on the chemical composition and configuration, especially in the side groups (Back & Salmén 1982). For native lignin the glass transition temperature is reported as high as 205°C. Though, adsorbed water can lower the glass transition temperature, hemicellulose is more sensitive to water than lignin and therefore still keeps the lowest glass transition temperature (Back & Salmén 1982).

Another argument is the result of extraction analysis carried out to determine the sugar content in the fibres. In the analysis no xylan (hemicellulose) was left indicating this particular constituent to be broken down.

The shift in the position of the curves in Figure 6.25 is illustrated more clearly in Figure 6.26 where only two plots are drawn. Figure 6.27 shows again two plots but this time with a more uniform shape presumably due to the higher temperature. The shift in Figure 6.26 could be an indication of the breakdown of the hemicellulose and further the breakdown of the lignin when the treatment time is extended. Since the difference between the curves

in Figure 6.27 is less evident the temperature is assumed to be the reason. At elevated temperature, the breaking-down process of the lignin is getting closer and thereby already seems to be initiated.

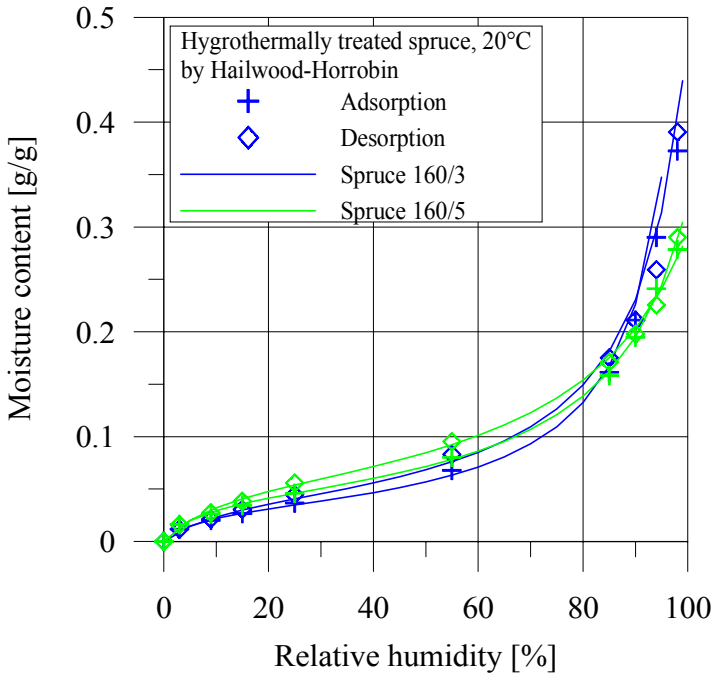

Figure 6.26. Comparison of sorption isotherms measured at 20°C for hygrothermally treated spruce fibres when treated at 160°C for 40 and 20 minutes respectively.

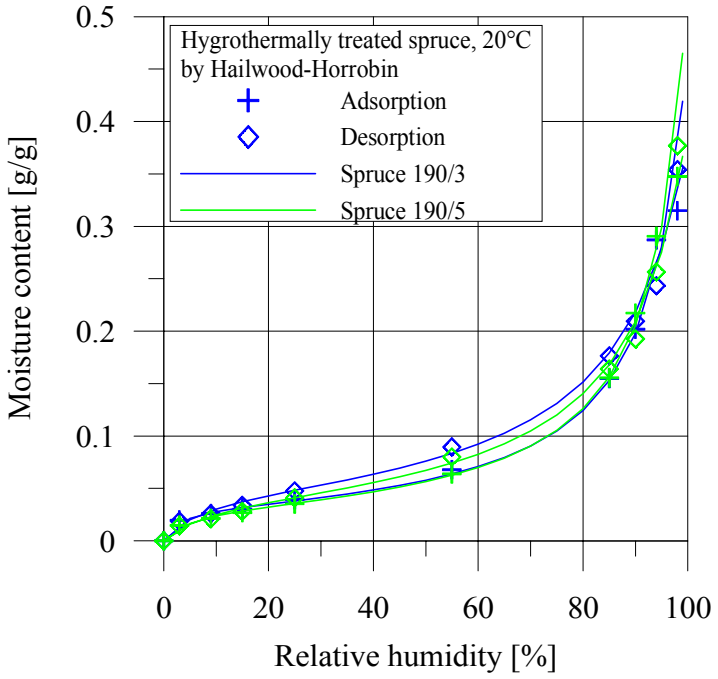

Figure 6.27. Comparison of sorption isotherms measured at 20°C for hygrothermally treated spruce fibres when treated at 190°C for 40 and 20 minutes respectively.

6.5. Discussion on sorption isotherms

6.5.1. Sorption modelling

Throughout this study, the results are presented in such a manner as to consider the sorption process. Models based on multilayering (BET) and solution (H–H) concepts have been used in an attempt to fit the measurements into a smooth curve. The model made by Hartley & Avramidis in the water cluster theory based on different physical considerations, are a third approach but are not applied on the current data.

Still, it is difficult to decide which model is the most appropriate one and of course none of them are completely perfect. Often combinations have to be applied. The following discussion is based on the presented sorption isotherms.

In this study, the BET model, the model by Simpson, the H–H model and to a limited degree the SORP model have been used. The Dent model is also a mutilayering solution but from a previous investigation it is concluded that the model of H–H and Dent are the same (Hartley & Avramidis 1994). It is obvious that the BET model does not fit the results satisfactory because of the 50% RH limit and since the capillary contribution from the model of Simpson was too significant, this model was also discarded. The advantage of less constants in the H–H model in comparison to the SORP model is the reason for the choice of the H–H model.

The third approach concerning the water cluster theory is argued to be a valid model according to Hartley & Avramidis (1993). Though evaluated and used on wood samples it is difficult to denote the water cluster theory as the true answer when the clusters are beginning to form. It is remarkable to observe that the cluster first starts about 20% moisture content. This is almost identical to the contribution from capillary condensation and it would therefore be interesting to test the hypothesis to prove or disprove this relation.

What forms the clusters? The theory describes the cluster formation as being initiated near 20% moisture content where newly adsorbed molecules have the tendency to randomly attach to existing bridges of water molecules. Above 25% moisture content, the clusters become larger and larger and have, near the fibre saturation point, an average size of 10 water molecules. Larger clusters indicate average values of 98 molecules, which is too high according to cluster size in bulk water (Hartley & Avramidis 1993). These indications are questionable and still leave room for the capillary theory.

However, the capillary theory is old and developed for stiff porous materials and the fact that wood swells when wet, restrains its use for gel-like materials like wood and plant fibres. Anyway, it is not discarded. Individual fibres are hollow, cylindrical, and thereby feasible for capillary condensation when exposed to high humidity conditions.

The isotherm can be divided or discussed in three regions corresponding to relative humidity (Hartley & Avramidis 1994). Region I: 0-30%, Region II: 30-55% and Region III: 55-100%. In the first region, the dominant sorption mechanism is chemical attraction between the available sorption sites and water molecules. Region II is considered as an

organizational region and region III is described by the physio-sorption dominant mechanism process.

In the first region the monolayer begins to form and continues in region II and probably also in region III. According to Berthold et al. only one water molecule is adsorbed to each of the amorphous hydroxyl groups at 92% RH. This result involves a specific binding and thus does not favour the cluster theory or the classic multiplayer adsorption theory. However, so that we do not forget it, the cluster formation does not occur before about 90% RH (Hartley & Avramidis 1993) and is therefore not completely identical to that of Berthold et al. Until the fibre saturation point, it is rather an extension.

The sorption of water by wood and plant fibres is influenced by ionic groups and different charged groups. The important binding sites are the hydroxyl groups and carboxylic acid groups (mainly present in the xylan). In addition, it is demonstrated that the amount of water adsorbed is dependent upon the crystallinity of the material. According to Salmén (1997) only the hydrophilic sites are responsible for the water adsorption and each of these have on average one water molecule attached at 92% RH as he and Berthold et al. were in agreement on. It is thus evident that changes in the sorptive behaviour of lignocellulosic materials cannot be affected in other way than by chemically altering the sorption sites.

This is exactly what happens during the acetylation process. Acetyl groups are sorbed onto the hydrophilic sorption sites thus restraining the water adsorption. In the isotherms for acetylated fibres, there is a significant decrease in the moisture content. Not only in region I and II but in all the RH region. This proves the hypothesis about restrained sorption when chemical changes are made in accordance to Salmén. In particular, it is interesting to notice the difference between the hygrothermal and acetylation treatment. Still the great difference in the high humidity region can surprise. The ability to adsorb water is sustained for the hygrothermally treated fibres contrary to the acetylated.

Ionic groups can affect the moisture content and is probably one reason for the difference. If ionic groups have being created during the hygrothermal treatment and are present, the cluster formation could appear in this situation. Alternatively, it is the capillary condensation.

It is likely to be expected that water adsorb to hydroxyl groups until one molecule is attached to every group. Apparently, more water has the ability to be adsorbed to the structure but seems to be attached to cavities or micro pores and capillaries. The micro pores are, however, questionable according to the hypothesis about their presence. Despite the fact that more water is adsorbed to the cell wall than just a single molecule to each hydroxyl group it is difficult to prove the existence of micro pores. The reduction of moisture uptake due to acetylation indicates the absence of cavities or micro pores.

6.5.2. Acetylation versus hygrothermal treatment

The purpose of the acetylation and hygrothermal treatment is among other things to reduce the water adsorption. By comparison of the results carried out is it possible to decide which method is most beneficial. Still there could be other advantages beyond the reduced water adsorption e.g. decreased shrinkage/swelling or dimensional stability but

this is not taken into account here. Therefore, this comparison only considers the treatment from a water sorption point of view.

Figure 6.28 shows the sorption isotherms with the acetylated and hygrothermally treated fibres plotted, and it is obvious that acetylation for 60 and 240 minutes are more efficient regarding reduced water sorption. But the 10 minutes acetylation is more or less comparable to that of the 160/5 hygrothermal treatment. The largest difference between these two treatments is in the high humidity region. The reduction in moisture content for the acetylated fibres is greater than the other fibres and with that more effective in this region.

If fibres were acetylated for more than 240 minutes it is probable that the moisture uptake will be even further reduced. It would be an interesting experiment to see where the maximum in acetylation and reduction of moisture uptake is. The current experiment already shows a relative diminishing effect when acetylation is increased. The effect from 60 to 240 minutes acetylation is less than from 10 to 60 minutes indicating that acetylation is declining with time.

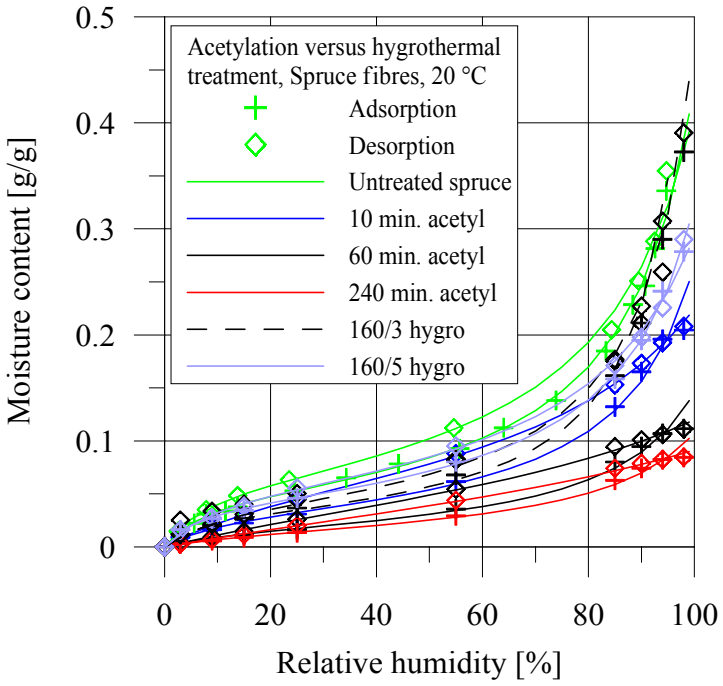

Figure 6.28. Comparison of acetylation versus hygrothermally treatment of spruce fibres. 160/3 and 160/5 are hygrothermally treated fibres at 160°C for 40 and 20 minutes respectively.

Why is there this difference between the treatments? The hygrothermal treatment causes a breakdown of the xylan and lignin structure but still leaves many available sorption sites in the amorphous part of the cellulose structure. The acetylation acts inversely. This process does not break down the chemical constituents but instead blocks the hydroxyl sorption sites by acetyl and thereby increases the acetyl content whereby the materials gain weight.

What actually happens in the high humidity region is still not yet completely understood. Regarding the fibre saturation point it is suggested it is obtained at the time when every

sorption site is attached to one water molecule occurring at 92% RH (Berthold et al. 1994). It indicates a capillary contribution in the high humidity region as proposed in one the previous mentioned sorption models (Simpson 1973), and appears to be most probable here. But along with the hygrothermal treatment when the hemicellulose is broken down, new pores and cracks are created as the material of hemicellulose disappears. These newly created pores then actually may contribute to the increase in moisture content in the high humidity region.

The hygrothermal treatment does not block the hydroxyl groups and in particularly not the lumen and cavities in the cell wall thus allowing water to be condensed in capillaries. When acetyl is present most of the hydroxyl groups are blocked diminishing the possibility for water molecules to adsorb to the cell wall and perhaps even to penetrate into the cell wall to condense in the cavities. The influence from acetyl somehow decreases or completely excludes the capillary contribution, which is even more evident for the longest acetylation time in Figure 6.28.

Whether the acetyl blocks the hydroxyls and even hinders water from penetrating into the possible micro pores is uncertain. Most likely, the acetyl will not be able to hinder the penetration of water into the micro pores if they exist, only hinder the adsorption to the sorption sites. The acetylation does not change the porosity of the wood or plant cell wall, only reduces the number of sorption sites. The circumstance, that the reduction of moisture adsorption is significant after the acetylation, points in the direction of few or none micro pores.

Summing up the considerations about the hypothesis: Both the hygrothermal treatment and the acetylation reduces the moisture uptake significant. In the high humidity region, only the acetylated fibres show reduced moisture content proving the hypothesis. That is, no micro pores exist. Since the hygrothermally treated fibres still adsorb moisture in the high humidity region, this is caused by the pores and cracks created during the hygrothermal treatment due to the material loss.

6.6. Suction measurements

In this study, the technique has been applied to a variety of wood and plant fibres including spruce, beech, flax and hemp. The results are tabulated in Table 6.3 and presented in Figure 6.29, Figure 6.30, Figure 6.31 and Figure 6.32. The results marked with an * were carried out as part of a M.Sc. study by Henning Berggren Jørgensen (HBJ 1999) under my supervision. The table contains the corresponding values of the applied pressure and moisture content. In addition, the standard deviation, the number of samples and the corresponding relative humidity are summarised. The results for Scots pine shown in Figure 6.31 and Figure 6.32 are presented in Appendix B.

Table 6.3. Summary of the results of the moisture content and suction pressure relationship. *Experiments from HBJ 1999.

Species	P_{suc} (bar)	Moisture content (g/g)	Standard deviation. (g/g)	Relative humidity (%)	No. of samples (-)
Flax fibres	100.0	0.762	0.1327	92.86	5
	31.6	0.864	0.0979	97.69	6
	10.0	0.896	0.0698	99.26	5
	1.3	1.299	0.0937	99.91	2
	1.0	1.522	0.2625	99.93	4
	0.4	1.511	0.1871	99.97	2
	0.1	1.444	0.1186	99.99	3
Beech fibres	100.0	0.787	0.0230	99.26	3
	10.0	1.309	0.0352	99.93	4
	0.1	1.388	0.0665	99.99	2
Flax fibres *	100.0	0.5454	0.0149	92.86	3
	31.6	0.6028	0.0505	97.69	2
	10.0	0.7096	0.0096	99.26	3
	4.0	0.7293	0.0451	99.71	3
Spruce fibres*	100.0	0.2907	0.0097	92.86	3
	80.0	0.3520	0.0164	94.25	3
	33.0	0.6600	0.0443	97.59	3
	10.0	0.6082	0.0457	99.26	3
	9.0	0.5767	0.0137	99.34	3
	3.1	1.1088	0.4984	99.77	3
Hemp fibres*	100.0	0.0452	0.0024	92.86	2
	31.6	0.5741	0.0291	97.69	3
	10.0	0.7467	0.0301	99.26	3
	4.0	0.6706	0.0849	99.71	3

6.6.1. Results

Figure 6.29 shows first of all the sorption measurements plotted for beech and spruce fibres as already shown in a previous section. On top of that are the suction measurements demonstrating the huge increase in moisture content in the vicinity of 100% RH. Plotting the suction curves as a contribution to the sorption isotherms in the same diagram gives a poor picture of the results. The suction measurements especially for beech fibres do not seem to agree very well with those from the sorption measurements since there is a jump from the sorption to the suction curve.

Figure 6.30 shows again the suction measurements presented as an extension of the sorption isotherm. This time again there is a huge increase in the moisture content and a similar jump for the flax fibres from the sorption curve to the suction curve.

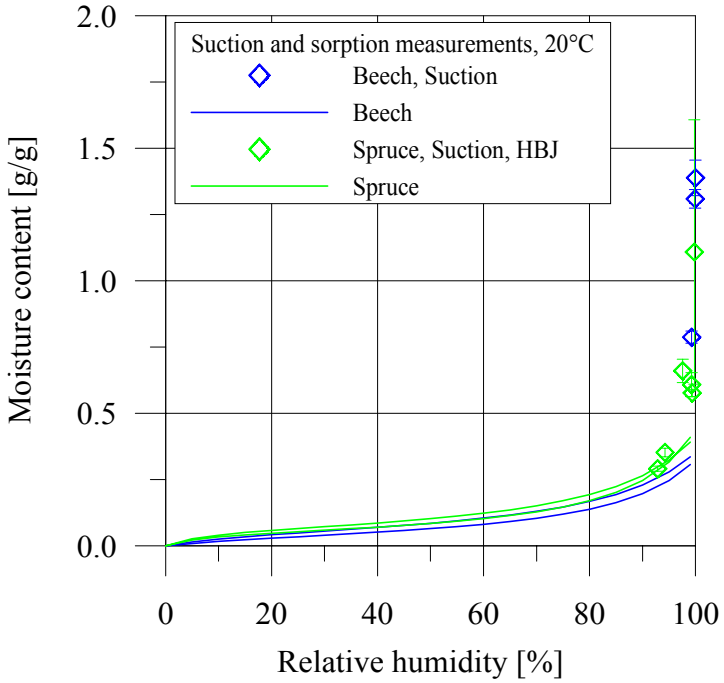

Figure 6.29. Sorption isotherm for beech and spruce extended with suction measurements.

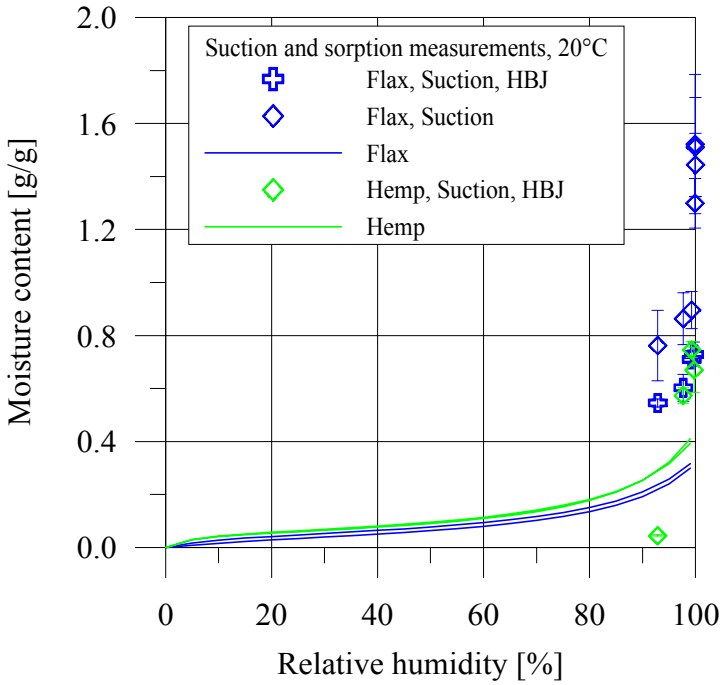

Figure 6.30. Sorption isotherm for flax and hemp extended with suction measurements.

In order to avoid congestion of the data points from the suction measurements a semi-log scale is used in Figure 6.31 and Figure 6.32. Instead of the relative humidity, the suction pressure is used as unit. In Figure 6.31 several different measurements are shown. The green and blue curve illustrates the sorption and suction curves for beech and spruce fibres respectively. In this figure, the jump from the sorption curve to the suction curve is clearly demonstrated. It indicates an inferior agreement between the methods. For each point the standard deviation is shown and indicates small variations for the beech fibres.

For the spruce fibres, the results from the suction measurements are in agreement with the values from the sorption measurements. This is expected although the deviation is large in the point at 3.1 bar. For comparison, data for solid Western hemlock (Tremblay et al. 1996) is plotted to confirm the validity of the pressure plate and pressure membrane method. The data from Tremblay et al. are both adsorption and desorption whereas all other measurements are only desorption. The moisture content for these samples exceeds all the other samples and some of the data points have been measured at a lower pressure too.

The three black curves are solid Scots pine measured in the three directions tangential, radial and longitudinal. There is a discrepancy between the tangential curve and the other two directions.

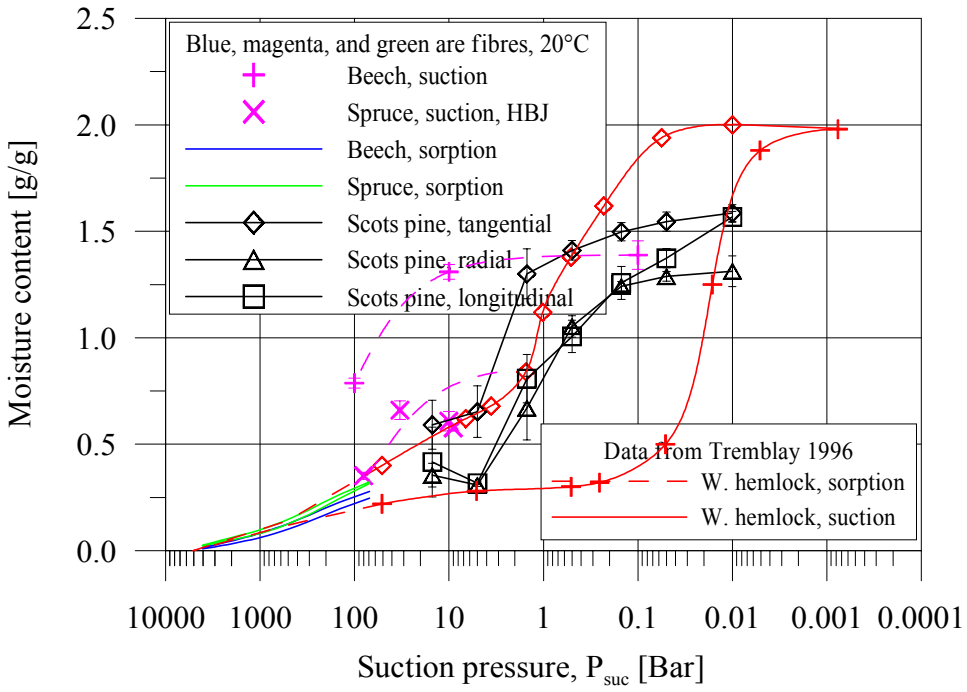

Figure 6.31. Suction curve for beech and spruce fibres. Comparisons are made to solid Scots pine and Western hemlock.

In Figure 6.32 flax and hemp fibres are illustrated in a semi-log scale like beech and spruce. There is a significant offset for both flax and hemp in the region where the sorption and suction curves are overlapping. The flax and hemp measurements from HBJ are almost coincident and with small deviations, when the other and similar flax curve has a

higher moisture content. The latter also contains measurements at lower pressures. The moisture content at pressures in the region from 1 to approximately 0.1 bar increases significantly and ends at 1.6g/g, more than four times the end point in the sorption isotherm. There is a slight tendency for the two last points to decline in spite of expected higher moisture content. It is worth noting that the deviation for each point on the flax curve is larger than the former two curves.

For comparison, the curve for solid Scots pine in radial direction is plotted. It reaches almost the same high moisture content as the flax fibres but also levels off at 1.6g/g moisture content.

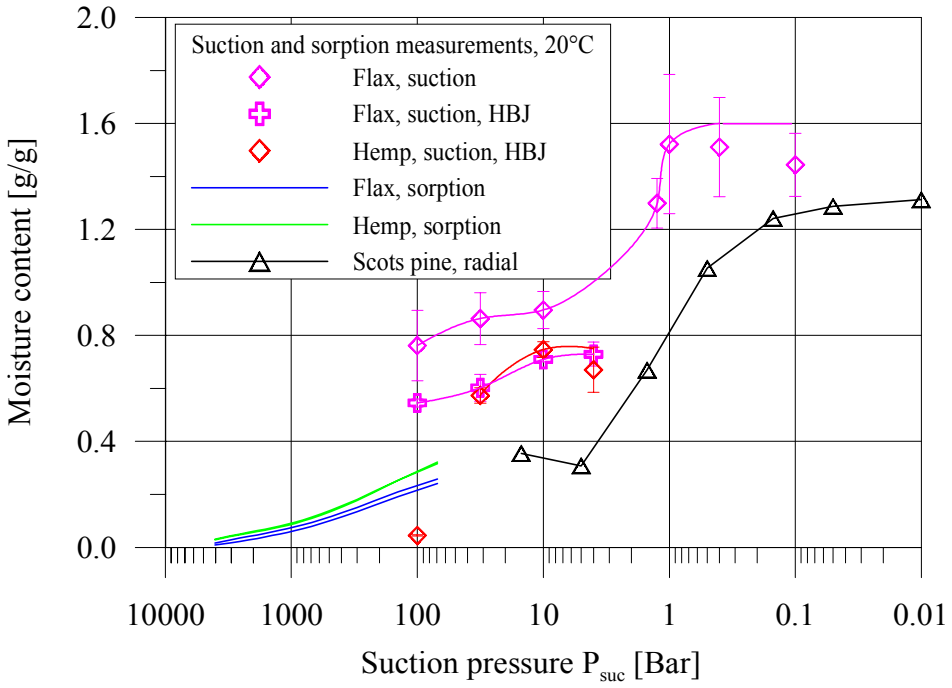

Figure 6.32. Suction curve for flax and hemp fibres. Comparison is made to solid Scots pine.

6.6.2. Discussion

The determination of the suction curve for a material is somehow related to the fibre saturation point. The fibre saturation point can be estimated from the sorption isotherm by extrapolating the sorption curve at a relative humidity up to about 98-100%. However, the fibre saturation point is not necessarily first reached at 100%. This may lead to some confusion. When a sharp upward break occurs on the sorption curve it indicates capillary condensation and thereby the fibre saturation is already exceeded. Usually this break occurs at about 98-100% RH, but sometimes before. According to Berthold et al. (1994) values as low as 92% have been suggested as the moisture content level where all hydroxyl groups each have one water molecule attached corresponding to the fibre saturation point.

In Figure 6.31, the moisture content for the suction curves generally is much higher than that suggested from the sorption curves. This is due to capillary condensation but still there should be an agreement between the sorption and suction curve. For the beech fibres, the point on the suction curve at 100 bars is about 0.5 g/g moisture content above that of the

sorption curve though they ought to be identical. This offset could be due to a lack of equilibrium, but since the same equilibrium criteria have been applied in all experiments this is of little importance, unless the criteria of 48 hours without any water dripping in the burette is not enough. The corresponding criterion for the Western hemlock curve was 72 hours (Tremblay et al. 1996), and therefore 48 hours seems appropriate. The general trend for the beech fibres is higher moisture contents than that of the spruce fibres. In the region from 100 to 1 bar, it is also above the Scots pine and Western hemlock. This could be explained by a general error in the experiment since the moisture content for beech is supposed to be about the same as for spruce and pine because the fibre saturation point is about 27% - 30% for all species. More water could probably have been trapped between the individual beech fibres than for spruce thus increasing the moisture content.

Looking at the curves for flax and hemp in Figure 6.32 the same phenomenon is present and an obvious reason could be the pressure plate method itself, when used on fibres. The problem with fibres is the water between the fibres and not the water in the fibres. Because it is impossible to separate the fibres in individual fibres there will be bridges of water between some of the fibres. How much water there will appear between the fibres is impossible to estimate, but it has to be taken into consideration when analysing the results.

For the flax fibres in Figure 6.32 there is a plateau at about 50-10 bars before increasing to moisture content about 1.6g/g. The plateau is supposed to be due to the capillary structure of the flax fibres. The difference in diameter between fibres (flax, 20-23µm), vessels (beech, 5-100µm) and other components such as longitudinal parenchyma could explain the difference between the curves.

In addition to the fibre curves, curves for the three different structural directions for solid Scots pine are plotted as well. In comparison to the curve for beech fibres, especially the curve for the tangential direction of Scots pine is above that of the beech fibres from 1 to 0.1 bar. Moreover, this particular curve seems generally to be at a higher moisture content level than the other two directions. However, it is apparent from the figure that the three curves almost share the same slope but the tangential is not identical to the other two, as was expected. In accordance to Cloutier et al. (1995), a similar discrepancy has been observed in a previous study of the structural direction. In this study, it was due to lack of equilibrium.

The moisture content for radial and longitudinal direction at about 15 bars is either too high or it is too low at about 5 bars; the moisture content is not decreasing from 15 to 5 bars. This behaviour is assumed to be caused by an experimental error.

In comparison to the flax fibres, the moisture content for Scots pine is generally lower. Both curves level off at about 1.2-1.6g/g moisture content and due to the large deviations in the flax measurements, the tendency is the same. Like the beech fibres, flax and hemp are also characterised by a starting offset at the point where sorption and suction measurements were supposed to agree. Again, the same considerations as for beech have to be kept in mind.

The suction curves for Western hemlock presented in Figure 6.31 show measurements for both adsorption and desorption. The relationship presents a strong hysteresis, a behaviour that can be attributed mainly to the “ink-bottle” effect. This effect in wood is due to the

capillary system consisting of large cavities interconnected by narrow channels (Tremblay et al. 1996). Since the apparatus used in this investigation is exclusively for desorption measurements no adsorption curves are presented for the current data. The curve for hemlock indicate a much more pronounced hysteresis than ever seen in the hygroscopic region from 0 - 98% RH. In an attempt to fully quantify the moisture content and water vapour relationship, such measurements for wood and plant fibres would have been of great value.

The general perspective of the presented suction measurements indicates a doubtful certainty for some of the data points. As already mentioned there is a problem related to water bridges occurring between the individual fibres. Furthermore, the excess pressure established in the pressure plate apparatus is hard to maintain very accurately for a long time. With this in mind future experiments have to be carried out very carefully. Since there is a satisfactory agreement between the sorption and suction curves for spruce fibres and the two species of solid wood presented the suction method seems reliable. There is no doubt that experience in the experimental technique is required in order to obtain reliable results. Still, more experiments have to be carried out on fibrous material to obtain results providing a safe proof of the agreement between the sorption and suction curve.

6.7. Thermodynamics of sorption

Measurements have been carried out in the calorimeter in an attempt to quantify the structure of the material. Moreover, sorption isotherms at two or more temperatures also provide information about differential heat of sorption. First, the sorption isotherms at two different temperatures are used in connection with the Clausius-Clapeyron equation and thereafter compared with calorimetric measurements.

6.7.1. Differential heat of sorption

Since sorption measurements have been carried out at 20°C, 40°C and 60°C and only two temperatures are required, three different combinations exist. 20°C and 40°C or 40°C and 60°C or 20°C and 60°C are the possibilities. However, because of the inaccuracy in the 40°C experiment it is decided to use the combination 20°C and 60°C.

Calculations are made on four different fibres. For each fibre, readings are made on the sorption isotherms at specific moisture contents. The corresponding relative humidity at both 20°C and 60°C are then noted as indicated in Figure 2.21 and substituted into equation 2.19 for further calculations.

$$\Delta H_S \approx R T_1 T_2 [\ln(h_2 / h_1)/(T_2 - T_1)]_m \qquad (2.19)$$

The readings are made on the figures where sorption curves for 20°C, 40°C and 60°C are plotted (Figure 6.10, Figure 6.11, Figure 6.14, Figure 6.17 and Figure 6.20 depending on species). On each curve between three and four readings are made and the readings from all four species are tabulated in Table 6.4. For e.g. hemp fibres the relative humidity is 0.02 at 20°C and 0.07 at 60°C for a moisture content of 0.015g/g. In equation 2.19 R = 8.314 J/mol·K, giving $\Delta H_S \approx 8.314(293.15 \cdot 333.15) \cdot [\ln(0.07/0.02)/40] = 25.4$ kJ/mol for hemp

fibres at 0.015g/g moisture content. Since ΔH_s is the differential molar heat of sorption, Q_s is defined as $\Delta H_s/18.02$, where 18.02 is the molar mass of water. Thus $\Delta H_s = 25.4 \cdot 10^3/18.02 = 1410$ J/g.

Table 6.4. Corresponding readings for moisture content and relative humidity at 20°C and 60°C. Further, the differential heat of sorption is calculated by equation 2.19.

Species	Moisture content (g/g)	Relative humidity at 20°C (-)	Relative humidity at 60°C (-)	Differential heat of sorption Q_s (J/g of water)
Spruce fibres	0.05	0.22	0.50	925
	0.075	0.45	0.65	414
	0.20	0.84	0.98	174
Beech fibres	0.05	0.39	0.66	593
	0.10	0.68	0.86	265
	0.20	0.90	0.95	60.9
Spruce fibres	0.03	0.40	0.48	205
acetylated 240 min.	0.05	0.65	0.75	161
	0.08	0.92	0.95	36.2
Hemp fibres	0.015	0.02	0.07	1412
	0.10	0.56	0.72	283
	0.20	0.83	0.95	152
	0.29	0.92	0.97	59.6

This process is repeated for each set of readings from the figures and finally the curve for differential heat of sorption is plotted. The plot for hemp fibres is in Figure 6.33.

Assuming the total area under the curve is equal to the total heat of wetting, W an exponential fit for the curve is made. The fit is shown in the figure. Integration of this equation from zero percent moisture content until the fibre saturation point provides the total heat of wetting. Before integration the fibre saturation point has to be determined and is assumed to 30% according to the Skaar.

However, the fibre saturation point can be estimated from heat of wetting measurements in the calorimeter. This is based on the assumption that heat is only generated when the moisture content is below FSP. Close to FSP the heat of wetting approaches zero. An attempt was made to determine the FSP this way but the calorimeter broke down after the initial measurements on dry samples were made. Therefore, the FSP is not estimated from own measurements.

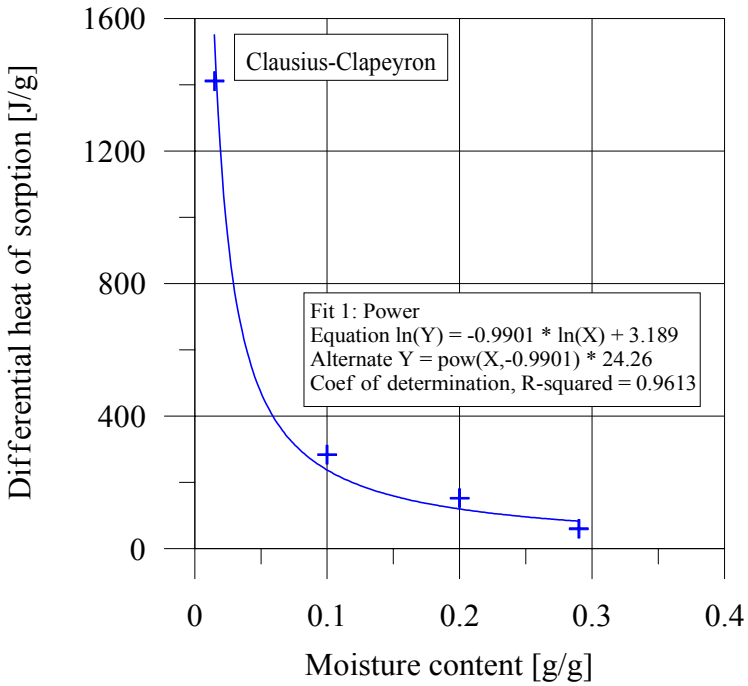

Figure 6.33. Differential heat of sorption in relation to moisture content for hemp fibres. Calculations based on the Clausius-Clapeyron equation. A power fit is made to the curve thus allowing the area under the curve to be calculated. The total area under the curve is equal to the total heat of wetting.

The equation applied in Figure 6.33 is of the power type and when integrated for the spruce fibres the result is

$$W_0 = \int_0^{FSP} Q_s dm = \int_0^{FSP} a m^b dm = \left[a \frac{1}{b+1} m^{b+1} \right]_{\to 0}^{FSP}$$

$$W_0 = \int_0^{0,3} Q_s dm = \int_0^{0,3} 24,26 m^{-0,9901} dm = \left[24,26 \frac{1}{-0,9901+1} m^{-0,9901+1} \right]_{\to 0}^{0,3} = 131,9 \, [J/g \, dry \, material]$$

This result and similar results from the others fibres are in Table 6.5 and also the coefficient of regression R^2 is tabulated. This is from the curve fit based on the corresponding points in Table 6.4. In addition, the measured values of the total heat of wetting from the calorimentry is also quoted.

Table 6.5. Total heat of wetting from calculation based on the Clausius-Clapeyron equation.

Species	Calculated total heat of wetting (J/g of dry material)	R^2 coefficient
Spruce fibres	113	0.863
Beech fibres	80.9	0.999
Spruce fibres acetylated 240 min.	20.1	0.924
Hemp fibres	132	0.961

6.7.2. Heat of wetting

The differential heat of sorption Q_s and the heat of wetting W are interrelated, and furthermore Q_s is calculated from sorption isotherms, while W is measured directly by calorimetry. For comparison, experiments have been carried out in the calorimeter to validate if values obtained by classic techniques are more reliable than those based on sorption isotherms.

Experiments were carried out on completely dry samples from the same species as used in the sorption studies. Corresponding values of the heat generation versus time are logged and plotted as in Figure 6.34. Then the total heat of wetting W is calculated according to Schaumann & Jacobsen (1996) and the results for the same species as obtained from the sorption isotherms are tabulated in Table 6.6.

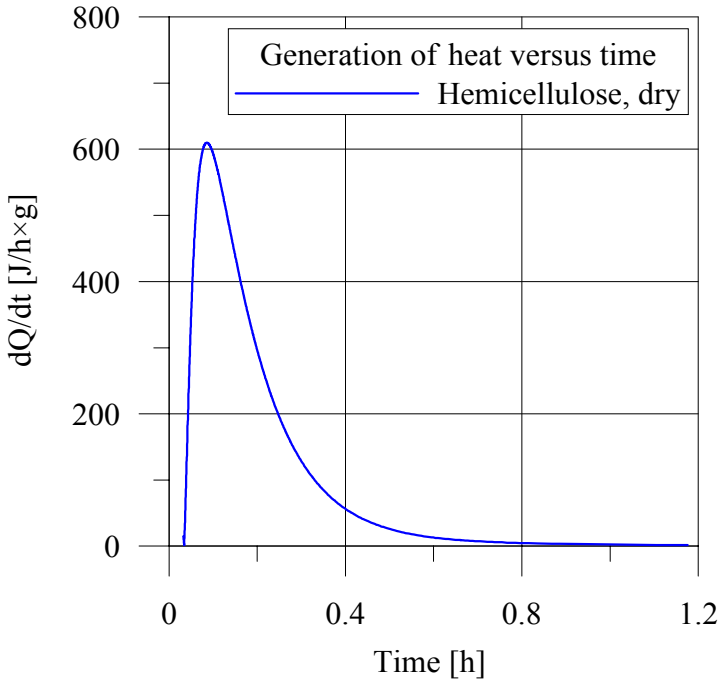

Figure 6.34. Generation of heat versus time for hemicellulose when soaked in an excess of water. The amount of water is sufficient to wet the sample well above the fibre saturation point.

Table 6.6. Total heat of wetting from experimental measurements by calorimetry.

Species	Measured total heat of wetting (J/g of dry material)
Spruce fibres	28.7
Beech fibres	47.4
Spruce fibres acetylated 240 min.	11.8
Hemp fibres	28.5

In addition, measurements on the primary constituents of the wood- and plant fibres are presented in Table 6.7. Since no sorption isotherms at two or more temperatures have been measured for those constituents, no comparison is being made to differential heat of sorption obtained from isotherms.

Not surprisingly, the heat of wetting for the hemicellulose is very high, and the expected increasing trend starting with cellulose then holocellulose and finally hemicellulose proves the reliability.

Table 6.7. Heat of wetting for wood and plant fibre constituents measured by calorimetry.

Species	Measured total heat of wetting (J/g of dry material)
Cellulose	51
Hemicellulose	112
Holocellulose	74

Analysing the results in Table 6.5 and Table 6.6 indicate very large deviations between values obtained from sorption isotherms and those obtained from calorimetric measurements. The general trend is lower values obtained by calorimetry, but especially spruce and hemp are pronounced. They are almost four times less the value obtained from the sorption isotherms and beech and acetylated spruce approximately two times less.

6.7.3. Discussion

In comparison to the values obtained from the sorption isotherms and by calorimetry there is a discrepancy between some of them. To determine whether the incorrect values are those based on the sorption isotherms or calorimetry, values from the literature have been used for comparison. Table 6.8 shows values for some of the materials used in this investigation and corresponding values from Stamm. Since the values from the literature only seldom are carried out on exactly the same species comparisons has to be exercised with caution.

For spruce and beech fibres the values from Stamm seems to be halfway between the calculated and measured values perhaps indicating none of them to be sufficiently accurate. Apart from the holocellulose all the values from the literature are higher than

those obtained in this investigation. This general trend somehow indicates the measured values to be too low or otherwise the values from the literature too high.

The fact that total heat of wetting for hemicellulose is above that of the other constituents proves the theory about the branched structure with tightly bound water molecules, followed by holocellulose and cellulose. However, the holocellulose was expected to show an increased energy release in proportion to the cellulose according to the ratio of hemicellulose in the holocellulose. This indicates that the measurement of 67.9 J/g for holocellulose used for comparison from Stamm is unreliable.

Like spruce, the hemp fibres show a high value for the calculated heat of wetting. Since the constituents according to Table 6.1 are substantially different, e.g. cellulose and lignin content in hemp is 67% and 3% when in spruce it is 40-45% and 20-30%, there is supposed to be a difference. Due to the high cellulose and low lignin content it is more likely the hemp fibres releases more heat than spruce. Though the heat contribution from lignin is limited it is assumed to play a role here.

With this in consideration, results that are more reliable should be able to be obtained. In order to achieve this more experiments have to be carried out, especially in the calorimeter.

Table 6.8. Comparison between values of heat of wetting from experiments and literature.

Species	Sorption isotherms, Calculated total heat of wetting (J/g of dry material)	Calorimetry, Measured total heat of wetting (J/g of dry material)	Calorimetry, Total heat of wetting from Stamm (J/g of dry material)
Spruce fibres	113	28.7	76.0
Beech fibres	80.9	47.4	69.5
Cellulose	-	51	68.0 – 85.0
Hemicellulose	-	112	151
Holocellulose	-	74	67.9

The difference between the differential heat of wetting and the heat of sorption has been discussed by many researchers for years. From that point of view, it is not surprising there is a difference in the values just presented. According to Skaar some of the inaccuracies in the values obtained from the sorption isotherms are due to the fact that the Clausius-Clapeyron equation assumes reversibility in the sorption isotherms. This is not true due to hysteresis as is demonstrated in the sorption curves earlier presented.

Since the theoretical approach, using Clausius-Clapeyron's equation, may not be the most reliable method to obtain the differential heat of wetting, more efforts should be put into the classic calorimetric technique unless accurate climate chamber facilities are available.

6.8. Crystallinity

To characterise the different water sorption properties for those wood and plant fibres used in this investigation crystallinity measurements is one more method. The crystallinity is related to the structure of the cellulose chains and therefore provides information about how they are arranged. Crystalline is synonymous with a structure of regions of ordered cellulose chains while less crystalline or amorphous means a less ordered or branched structure thus allowing more water to be sorbed onto the surface.

Experiments were carried out by x-ray diffractometry on a variety of the fibres. Since the results of the measurements are relative to each other, a sort of reference is needed as a basis. Microcrystalline powder was used as a first reference because it was recommended by colleagues and it was assumed that the crystalline material was within reach. Unfortunately, it was impossible to get any precise information about the degree of crystallinity from the producer. A value about 80% is found in the literature and is therefore used (Chen et al. 1996). Later it appeared that a reference for an amorphous material was needed as well in the characterisation of the wood and plant fibres.

Since no standard material was available from the chemical suppliers, it was decided to use glucose. Then glucose was used both as a crystalline reference and as an amorphous reference. Measurements were made on the raw glucose under the assumption that it is almost 100% crystalline and afterward an amount of glucose was melted in an oven whereby it caramelises. The caramelised form was then supposed to be almost 100% amorphous.

In addition to these references, a measurement was carried out on a polyethylene (pe) fibre provided by a colleague. This polyethylene fibre was assumed to be highly crystalline. By comparison, these references show a surprisingly dissimilarity thus making it difficult to analyse the results from the wood and plant fibres. In Figure 6.35 three diffractograms of polyethylene fibres, microcrystalline cellulose and glucose are presented. From the plots, it is evident how difficult the interpretation of the measurements is. Not only the angle at which the peaks appears are deviating from each other but also the intensity. The difference in intensity is presumably due to the different number of reflections from the individual samples. This again is due to the varying thickness of the samples investigated.

A fourth plot of a crystalline material is in Appendix C. Here a piece of standard Whatmann filter paper is plotted against the microcrystalline cellulose and the caramel. The filter paper is also supposed to crystalline since it consists of almost pure cellulose, and indeed, it is in agreement with the microcrystalline cellulose in general. The peak values are lower for the filter paper and the peaks marked with Si are peaks from the silicon plate where the filter paper was sticked. The Si peaks are therefore not of interest.

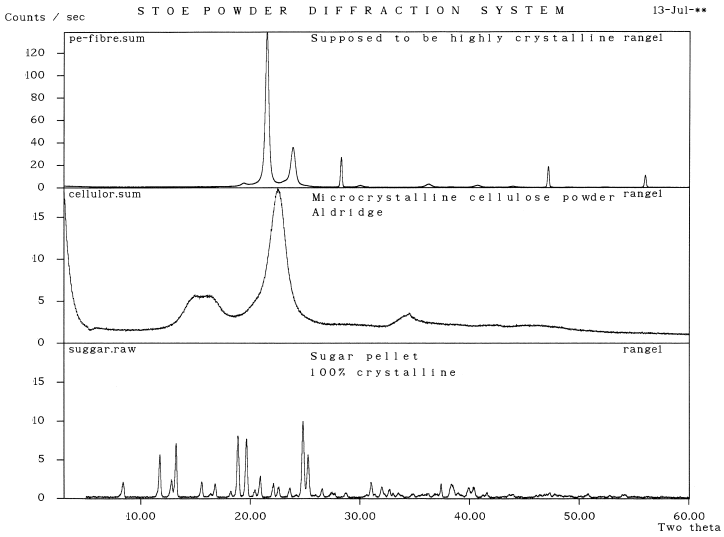

Figure 6.35. Diffractograms of three crystalline reference materials. Polyethylene fibres, microcrystalline cellulose and glucose.

The amorphous reference is plotted together with the crystalline glucose in Figure 6.36. From the figure, it is clear there is a distinct difference between the two different states in the material as was of course expected.

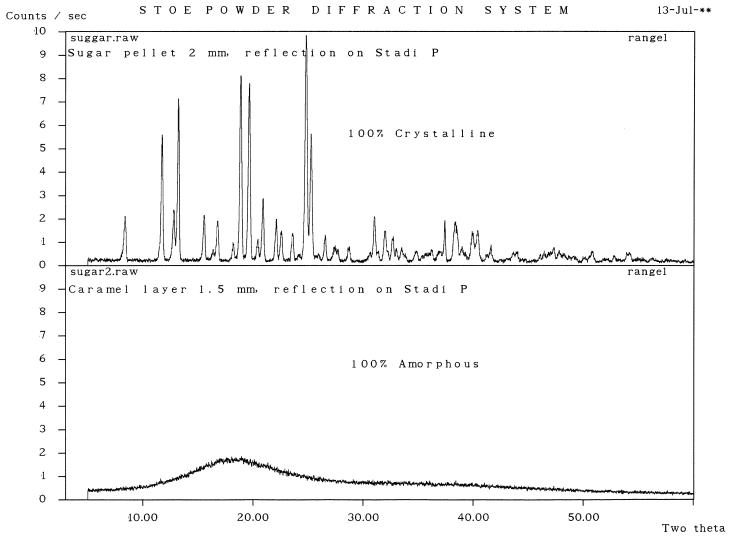

Figure 6.36. Diffractograms for the crystalline and amorphous glucose used as reference materials.

To begin with, the fibres were measured in transmission but because of weak results, it was decided to press pellets of the fibres for use in reflection measurements instead. Examples of the results are presented in Figure 6.37 and Figure 6.38. These figures show the plots of the investigated wood and plant fibres together with cotton and viscose. In Appendix C, an individual plot of the spruce fibres is presented. This plot is the result of the more detailed size and just illustrates what all the other plots look like before stacked on top of each other in the same plot.

Generally, all the diffractograms are blurred in comparison with the measurements on the crystalline samples in Figure 6.35. One of the reasons for the blur is supposed to be due to the more or less random packing of the fibres when formed into a pellet and moreover the heterogeneous morphology. The difference between the measurements was expected to be more distinct and thereby enabling one to quantify the degree of crystallinity for the individual species. For comparison, all the plots presented have the unit counts per second on the y-axis. The total counts would have been another way to plot the diffractograms but more complex to evaluate since there is such a variation between the fibres.

For comparison purposes, a calculation of the ratio between the peak value and the background value is made for the polyethylene fibres and the glucose. Both materials are supposed to be highly crystalline. In the raw data used for the diffractometry analysis the total counts are available. Unfortunately, the raw data are not included in this thesis because the software, exclusively made for the x-ray diffractometer, is required to get access to them.

For polyethylene fibres the major peak is about an angle at 22° (two theta) in Figure 6.35 and the corresponding total counts is 140000. The background value is read from a point where no peaks are visible and in this case an angle of 50° (two theta) is chosen. Here the total counts are 320. The polyethylene ratio therefore becomes:

Polyethylene fibres 140000/320=438

For glucose the corresponding readings for the major peak and background are 1140 and 24 respectively. The ratio then becomes:

Glucose 1140/24=48

It is tempting to compare these values but it is more complicated than that. From the values it apparently seems like the polyethylene fibres are (much) more crystalline than the glucose. Here it is worth remembering that the polyethylene fibres consist of almost endless chains of CH_2 molecules contrary to the glucose units. The glucose units are individual crystallites almost randomly mixed and thereby not the same crystalline structure as the polyethylene fibres. Because of these varieties between the species and their individual disposition, it is not obvious to compare the results directly.

Analogous calculations are however also the case for all the other species applied to diffractometry. Therefore it is also difficult to make comparisons among the different wood and plant fibres. Since the crystalline cellulose chains are assumed to be aligned differently from specie to specie the diffractogram will always diverge from each other.

The diffractograms for spruce, beech, wheat straw, hemp and flax fibres have generally the same shape. They are characterised by two peaks although the first peak consists of two smaller peaks itself. The intensity is higher for hemp and flax than for spruce, beech and wheat straw.

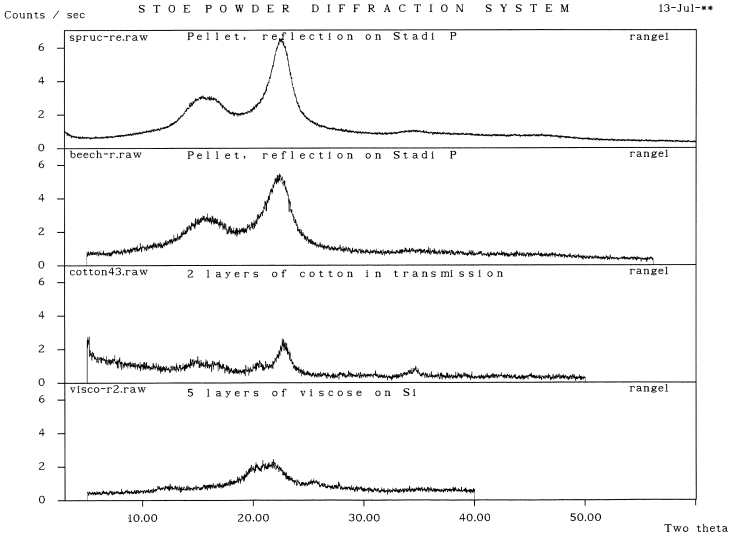

Figure 6.37. Diffractograms of spruce fibres, beech fibres, cotton and viscose.

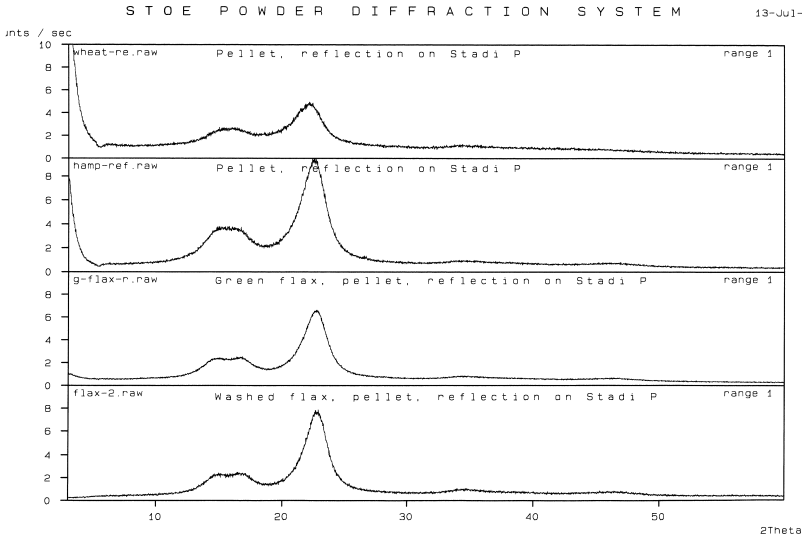

Figure 6.38. Diffractograms of wheat straw, hemp fibres, flax fibres and washed flax fibres.

6.8.1. Discussion

Figure 6.39 shows a presentation of diffractograms from the literature. For viscose fibres the diffractogram is in agreement with that in Figure 6.37 because of the very small peak beyond 10° and the two peaks about 22°. This indicates the measurements to be valid, though the cotton linters seem to differ from the cotton in Figure 6.37. Especially the major peak at 23° is less distinct in Figure 6.37 than in Figure 6.39. Apart from that, the minor peaks at 15-16° and 35-36° agree. The numbers marked at the peaks in Figure 6.39 indicates the different lattice planes of the space unit for cotton. However, this is not used in this investigation.

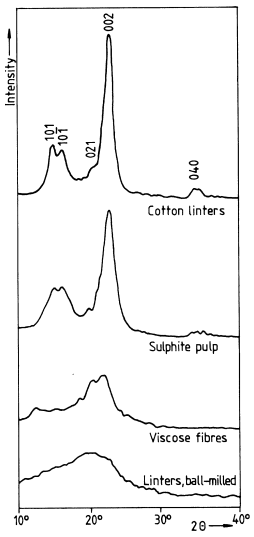

Figure 6.39. Diffractograms of various celluloses (Fengel & Wegener 1984).

A quantitative comparison with the microcrystalline cellulose in Figure 6.35 indicate a higher degree of crystallinity for the former fibres hemp and flax than spruce, beech and wheat straw. In accordance with the calculation made above, it is indeed complicated to interpret the results in a more absolute or precise manner. Surprisingly all the investigated samples appeared to be more similar than expected. Even a tendency is difficult to state because of the apparent uniformity of the diffractograms for the species. Therefore, no conclusions can be made on the crystallinity of the investigated species, only the fact that all the wood and plant fibres are amazingly identical.

Conclusion

The present investigation has contributed to the establishment of an accurate experimental method for the assessment of the sorption properties of wood and plant fibres. From the measurements in the newly designed climate chambers at ambient temperature, it is concluded that:

The accuracy of the humidity control in the region from 3% RH to 94% RH is ±1% RH and the temperature is controlled at 20°C at an accuracy of ±0.5°C.

The closed process where the samples are maintained and weighed within the chamber during the experiment reduces the time to equilibrium significantly. In comparison to the desiccator method, the time is reduced from 1 week to 2 or 3 days.

In particular, for wood and plant fibres it is of outmost importance that the samples are kept within the chamber when the samples are weighed to avoid disturbance from the surroundings.

The fully automated climate chamber for elevated temperature measurements has proven its capacity at 40°C and 60°C, and from the experimental experience it is concluded that:

The automatic weighing of samples allows the samples to be weighed more frequent and is thereby a faster and more precise way to determine the time when equilibrium is reached. This is due to the increased number of data, thus making a more reliable time course curve.

The accuracy of the relative humidity at 40°C and 60°C is ±1% RH from 3% RH to 85% RH, and from 85% RH to 94% RH it is ±2% RH. The temperature accuracy is ±1°C.

The fact that humidity control beyond 94% RH is very difficult to establish has been proven. Furthermore, reliable humidity measurements require a dew-point sensor instead of a hygrometer based on either capacitive or resistive measurements.

A regular calibration of the temperature and humidity sensor is of great importance.

The mathematical modelling of the sorption isotherms has shown serious shortcomings of all available models in the high humidity region. Different models have been verified in an attempt to find the most appropriate one. It is found that:

The model by Hailwood–Horrobin is the most appropriate to fit all the results

obtained through the experiments in the humidity range from 3% RH to close to 100% RH.

The models by BET and Simpson were found to be insufficient for the characterisation in the complete humidity region from 3% to close to 100% RH.

The SORP model gave a satisfactory fit of the results but was rejected due to the number of fitting parameters in comparison to the H–H model.

It was attempted to establish an almost complete sorption isotherm including measurements at 99.99% RH by the pressure plate apparatus. Additional measurements from 93% RH to 99.99% RH was carried out by applying this method. The results show that:

There is an abrupt increase in the moisture content in the transition to overlapping measurements from the desorption curves measured in the climate chambers.

The increase in moisture content is supposed to be due to water molecules trapped between the individual fibres when placed in the sample container.

The estimation of the moisture content on individual fibres is very difficult although results on solid wood samples have proved the method adequate. The expected extension of the sorption isotherm was not proved satisfactorily.

The hygrothermal treatment and acetylation of fibres have shown a significant reduction in the hygroscopicity, and for the acetylation there is an evident relation between the reduction in moisture uptake and treatment time. Moreover, it is strongly indicated that the hypothesis on the absence of micro pores is true. From the measurements, it is concluded that:

The moisture content for hygrothermally treated fibres is reduced from 0% RH to 93% RH, due to the breakdown of hemicellulose reducing the number of available sorption sites.

The significant uptake of water beyond 93% RH is assumed to be caused by capillary condensation in pores and cracks created by the degraded and lost hemicellulose during the hygrothermal treatment.

A reduction in moisture uptake from 0% RH to close to 100% RH of approximately 75% for 4 hours acetylation in combination with the reduced moisture content for hygrothermally treated fibres verifies the absence of micro pores.

The degree of crystallinity was attempted to use as a measure for the prediction of the sorption properties of the fibres. X-ray diffractometry measurements were carried out, but the limited variation between the different species made it difficult to put unambiguous numbers on the degree of crystallinity for the investigated samples and the conclusion was that:

X-ray diffractometry measurements were not satisfactory and did thereby not provide accurate information about the crystalline structure for the prediction of the sorption properties.

Future research

Future research in the establishment of sorption properties for wood and plant fibres has to be concentrated on the following issues: Improved climate control in the high humidity region from 94% RH to close to 100% RH in the climate chambers. This is to establish as accurate measurements as possible but also to establish a smooth transition to the results obtained through the pressure plate technique.

For the pressure plate technique the measuring procedure on individual fibres is not satisfactory and has to be improved to obtain more reliable results. Results on solid wood samples have shown the capacity of the methods to be adequate.

The current discussion on the absence of micro pores in the fibre cell wall can be verified by further experiments. The acetylation experiments provided useful information in the quantification of micro pores. An important source of information may be obtained by pressure plate experiments carried out on solid wood samples of both untreated and acetylated wood. Such measurements will provide additional information about the absence of micro pores.

Symbols and abbreviations

m	Fractional moisture content	kg/kg
m_0	Dry weight of sample	kg
m_1	Weight of sample at equilibrium	kg
σ	Surface tension	N/m
θ	Contact angle	°
ρ	Density of water	kg/m^3
R	Gas constant	J/K·mole
T	Absolute temperature	K
M_w	Molecular weight of water	kg/mole
r	Radius of cylindrical pore	m
L	Length of pore	m
p	Partial vapour pressure	Pa
p_0	Saturated vapour pressure	Pa
ΔH_V	Heat of vaporization of sorbed water	J/g
ΔH_O	Heat of vaporization of liquid water	J/g
ΔH_S	Differential molar heat of sorption	J/g
ΔH_W	Enthalpy of free water	J/g
Q_S	Differential heat of sorption	J/g
W	Heat of wetting	J/g
W_O	Total heat of wetting	J/g
W	Molecular weight of the wood per mole of sorption sites	kg/mole
C	Constant that depends upon the heat of adsorption	-
n	Number of molecular layers	-
m_m	Moisture content, complete monolayer coverage	kg/kg
A_O	Total area available for sorption	m^2
A_1	Area covered with 1 layer of water molecules (monolayer)	m^2
A_i	Area covered with i layers of water molecules	m^2
b_1	Equilibrium constant relating the primary water to liquid water	-
b_2	Equilibrium constant relating the secondary water to liquid water	-
m_h	Fractional moisture content corresponding to the hydrated water	kg/kg
m_d	Fractional moisture content corresponding the dissolved water	kg/kg
K_h	Equilibrium constant similar to b_1	-
K_d	Equilibrium constant similar to b_2	-
Q	Fitting parameter	-
P	Fitting parameter	-
M	Fitting parameter	-
H	Relative humidity	-
MC	Moisture content	-
EMC	Equilibrium moisture content	-

Bibliography

Atkins, P. W. (1994) “Physical Chemistry.” Fifth edition. Oxford University Press. 1031 pp.

Back, E. L., Salmén, L. (1982) “Glass transition of wood components hold implications for molding and pulping processes.” Tappi, Vol. 65, No. 7.

Barkas. W. W. (1949) “The Swelling of Wood under Stress.” Dep. Sci. Ind. For. Prod. Res. GB, 99 pp.

Berthold, J., Desbrières, J., Rinaudo, M., Salmén, L. (1994) “Types of Adsorbed Water in Relation to the Ionic Groups and their Counter-ions for some Cellulose Derivatives.” Polymer 35 (26), 5729-5736 pp.

Bodig, J., Jayne, B. A. (1993) “Mechanics of Wood and Wood Composites.” Krieger Publishing Company, Florida. 712 pp.

Bradley, R. S. (1936) “Polymer Adsorbed Films II. The General Theory of Condensation of Vapours on Finely Divided Solids.” J. Chem. Soc. 1799-1804 pp.

Brunauer, S., Emmet, P. H., Teller, E. (1938) “Adsorption of Gases in Multimolecular Layers.” Journal of American Chemical Society, 60, 309.

Caulfield, D. F., Weatherwax, R. C. “Tensile modulus of paper wet-stiffened by crosslinking.” Forest Products Laboratory, Forest Service, U.S. Department of Agriculture, Madison, Wisconsin, USA.

Chen, J. N., Yan, S. Q., Ruan, J. Y. (1996) ”A study on the preparation, structure, and properties of microcrystalline cellulose.” Journal of Macromolecular Science – Pure and Applied Chemistry. Vol. A33, No. 12, 1851-1862 pp. ISSN 1060-1325.

Cloutier, A., Tremblay, C., Fortin, Y. (1995) “Effect of specimen structural orientation on the moisture content – water potential relationship of wood.” Wood Science and Technology 29, pp 235-242. Springer Verlag.

Delmer, D. P., Stone, B. A. (1988) “Biosynthesis of Plant Cell Walls.” The Biochemistry of Plants, Vol. 14. Academic Press, Inc.

Dent, R. W. (1977) “A Multilayer Theory for Gas Sorption I. Sorption of a Single Gas.” Text Res. J., 47, 145-152 pp.

Emons, A. M. C., Mulder, B. M. (1998) “The making of the architecture of the plant cell wall: How cells exploit geometry.” Proc. Natl. Acad. Sci. USA Vol. 95, pp 7215-7219, June 1998, Plant Biology.

Fengel, D., Wegener, G. (1984) “Wood – Chemistry, Ultrastruture, Reactions.” Walter de Gruyter, Berlin. 613 pp.

Fujita, M., Harada, H. (1991) "Ultrastructure and Formation of Wood Cell Wall." Wood And Cellulosic Chemistry. Ed. by Hon, D. N.-S., Shiraishi, N. Marcel Dekker, Inc. New York. 3-57 pp.

Giddings, T. H., Brower, D. L., Staehelin, L. A. (1980) "Visualization of Particle Complexes in the Plasma Membrane of Micrasterias Denticulata Associated with the Formation of Cellulose Fibrils in Primary and Secondary Cell Walls." J. Cell Biol. 84, 327-339 pp.

Goring, D. A. I. (1977) "A Speculative Picture of the Delignification Process." Cellulose Chemistry and Technology. ACS Symposium Series 48, 273-277 pp.

Hartley, I. D., Avramidis, S. (1993) "Analysis of the Wood Sorption Isotherm Using Clustering Theory." Holzforschung, Vol. 47 No. 2, 163-167 pp.

Hartley, I. D., Avramidis, S. (1994) "Water Clustering Phenomenon in Two Softwoods During Adsorption and Desorption Processes." J. Inst. Wood Science, 13(4), 467-474 pp.

Haygreen, J. G., Bowyer, J. L. (1996) "Forest Products and Wood Science–An Introduction." Iowa State University Press/Ames, Third Edition, 484 pp.

Hearle, J. W. S. (1960) "The Structure of Fibres." Moisture in textiles, The Textile Institute, Butterworths Scientific Publications.

Herth, W. (1985) "Plasma-membrane rosettes involved in localized wall thickening during xylem vessel formation of Lepidium sativum L." Planta 164, 12-21 pp.

Jørgensen, H. B. (1999) "Bestemmelse af vandoptagelse i træ- og plantefibre." Master Thesis (in danish), Department of Structural Engineering and Materials, Technical University of Denmark.

Kadita, S. (1960) "Studies on the Water Sorption of Wood." Wood Res., 23, 1-61 pp.

King, G. (1960) "Theories on Multilayer Adsorption." In. Hearle, J. W., Peters, R. H. (eds) Moisture in Textiles. Wiley Interscience, New York. 59-82 pp.

Langmuir, I. (1918) "The Adsorption of Gases on Plain Surfaces of Glass, Mica and Platinum." Journal of American Chemical Society, 40, 1361-1403 pp.

Malmquist, L. (1958) "Sorption as Deformation in Space." Kyltekn. Tidskr. 4, 1-11 pp.

Malmquist, L. (1995) "Sorption Equilibrium in Relation to the Spatial Distribution of Molecules." Holzforschung, 49(6), 555-564 pp.

McDougall, G. J., Morrison, I. M., Stewart, D., Weyers, J. D. B., Hillman, J. R. (1993) "Plants Fibres: Botany, Chemistry and Processing for Industrial Use." J. Sci. Food Agric. 1993, 62, 1-20 pp.

Mueller, S. C., Brown, Jr., R. M. (1980) J. Cell Biol. 84, 315-326 pp.

Mühlethaler, K. (1965) "The Fine Structure of the Cellulose Microfibril." Proc. Cellular Ultrastructure of Woody Plants. Ed. by W. A. Côté, Syracuse University Press, USA 1965.

Nielsen, L. F. (1993) "Moisture in Porous Material–A Modified BET-description." Proc. 3th Symposium on Building Physics in the Nordic Countries: Building Physics '93. Thermal Insulation Laboratory, Technical University of Denmark.

Pierce, F. T. (1929) “A Two-Phase Theory of the Adsorption of Water Vapour by Cotton Cellulose.” J. Text. Inst. 20, T 133-150 pp.

Ruben, G. C., Bokelman, G. H., Krakow, W. (1989) “Triple-Stranded Left-Hand Helical Cellulose Microfibril in Acetobacter Xylinum and in Tobacco Primary Cell Wall. Plant Cell Wall.” Polymers-Biogenesis and Biodegradation. ACS Symposium Series 399, 278-298 pp.

Salmén, L (1997) “The Sorption Behaviour of Wood.” Proc. Mechanical Performance of Wood and Wood Products: Wood-Water Relations. COST Action E8, ED. by P. Hoffmeyer, Copenhagen, Denmark 1997.

Schaumann, J., Jacobsen, U. G. (1996) “Lignocellulosematerialers befugtningsvarme bestemt ved isotermkalorimetri.“ (in danish) Department of Structural Engineering and Materials, Technical University of Denmark. Report Series I no. 2.

Simpson, W. T. (1973) “Predicting Equilibrium Moisture Content of Wood by Mathematical Models.” Wood Fiber, 5, 41-49 pp.

Simpson, W (1979) “Sorption Theories Applied to Wood.” Proc. Symposium on Wood Moisture Content – Temperature and Humidity Relationships. Virginia Polytechnic Institute and University, Blacksbrug, Virginia, USA 1979.

Sisko, M., Pfäffli, I (1994) “Fiber Atlas–Identification of Papermaking Fibres” Springer Series in Wood Science, Springer Verlag.

Sjöström, E. (1981) “Wood Chemistry, Fundamentals and Applications.” Academic Press, Inc. 223 pp.

Skaar, C. (1988) “Wood–Water Relations.” Springer-Verlag. 283 pp.

Stamm, A. J. (1964) “Wood and Cellulose Science.” The Ronald Press Company, New York. 549 pp.

Strømdahl, K. (1997) “Fugt i byggematerialer – med fokus på vandbinding i det overhygroskopiske område.” (in Danish; Moisture in building materials – with focus on the water retention in the superhygroscopic region”, MSc. Thesis, Department of Structural Engineering and Materials, Technical University of Denmark, Vol. 1 and 2.

Terashima, N., Fukushima, K., He, L.-F., Takabe, K. (1993) “Comprehensive Model of the Lignified Plant Cell Wall.” Forage Cell Wall Structure and Digestibility 1993, ASA-CSSA. SSSA, WI, USA.

Tremblay, C., Cloutier, A., Fortin, Y. (1996) “Moisture content–water potential relationship of red pine sapwood above the fiber saturation point and determination of the effective pore size distribution.” Wood Science and Technology 30, pp 361-371. Springer Verlag.

U.S. Forest Products Laboartory (USFPL) (1999) Wood Handbook. USDA Forest Service. Madison, Wisconsin. USA.

Van den Berg, C., Bruin, S. (1981) “Water Activity and Estimation in Food Systems. Theoretical Aspects.” In: Rockland LB, Ed. by Stewart, G. F., Water Activity. Influence on Food Quality. Academic Press, New York. 1-61 pp.

Wadsö, L. (1997) “Sorption på lignocelluloser.“ (in swedish) Department of Structural Engineering and Materials, Technical University of Denmark. Report Series R no. 20.

Wiederhold, P. R. (1997) “Water Vapour Measurement–Methods and Instrumentation.” Marcel Dekker, Inc. 357 pp.

Zimm, B. H., Lundberg, J. L. (1956) “ Sorption of Vapours by High Polymers.” J. Phys. Chem. 60, 425-428 pp.

Östberg, G., Salmén, L. (1991) “Effect of Fibrillation of Wood Fibres on their Interaction with Water. Nord. Pulp Pap. Res. J. 6 (1), 23-26 pp.

APPENDIX A

Sorption measurements

Spruce fibres

Temperature	20°C		40°C		60°C	
	Relative humidity (%)	Moisture content (g/g)	Relative humidity (%)	Moisture content (g/g)	Relative humidity (%)	Moisture content (g/g)
Adsorption and Desorption	0.0	0.000	0.0	0.000	0.0	0.000
	2.7	0.015	0.5	-	3.0	-
	5.6	0.022	7.3	0.004	9.3	0.010
	7.9	0.031	13.7	0.012	15.5	0.015
	11.5	0.034	24.3	0.021	25.8	0.028
	13.8	0.038	56.1	0.064	56.4	0.062
	24.5	0.053	72.0	0.087	72.2	0.101
	34.3	0.065	87.8	0.144	87.6	0.137
	44.2	0.078	92.5	0.190	90.9	0.100
	55.7	0.093	96.6	0.229	98.0	0.200
	64.0	0.112	97.5	0.256	95.2	0.170
	73.9	0.138	98.5	0.326	94.1	0.166
	83.3	0.185	97.9	0.298	91.4	0.163
	88.4	0.228	94.7	0.240	85.8	0.131
	90.7	0.246	90.0	0.198	70.0	0.098
	92.6	0.281	83.0	0.164	55.0	0.070
	94.7	0.336	67.2	0.117	25.0	0.037
	92.5	0.288	52.5	0.090	15.0	0.019
	89.5	0.251	22.5	0.043	9.0	0.010
	84.4	0.205	12.6	0.022	3.0	0.007
	54.6	0.112	6.6	0.015	0.0	0.000
	23.5	0.063	1.3	-		
	13.8	0.048	0.0	0.000		
	7.9	0.035				
	2.6	0.015				
	0.0	0.000				

Beech fibres

Temperature	20°C		40°C		60°C	
	Relative humidity (%)	Moisture content (g/g)	Relative humidity (%)	Moisture content (g/g)	Relative humidity (%)	Moisture content (g/g)
Adsorption and Desorption	0.0	0.000	0.0	0.000	0.0	0.000
	2.7	0.002	0.5	0.005	3.0	0.014
	7.9	0.014	7.3	0.013	9.3	0.006
	13.8	0.021	13.7	0.020	15.5	0.020
	24.5	0.033	24.3	0.030	25.8	0.026
	55.7	0.075	56.1	0.067	56.4	0.036
	83.3	0.153	72.0	0.094	72.2	0.069
	88.4	0.175	87.8	0.142	87.6	0.101
	92.6	0.213	92.5	0.193	90.9	0.143
	96.8	0.298	96.6	0.230	98.0	0.221
	94.7	0.280	97.5	0.258	95.2	0.203
	92.5	0.255	98.5	0.331	94.1	0.197
	89.5	0.215	97.9	0.305	91.4	0.177
	84.4	0.184	94.7	0.234	85.8	0.140
	54.6	0.095	90.0	0.197	70.0	0.106
	23.5	0.047	83.0	0.168	55.0	0.077
	13.8	0.032	67.2	0.121	25.0	0.042
	7.9	0.021	52.5	0.094	15.0	0.029
	2.6	0.008	22.5	0.047	9.0	0.018
	0.0	0.000	12.6	0.029	3.0	0.006
			6.6	0.020	0.0	0.000
			1.3	0.004		
			0.0	0.000		

Hemp fibres

Temperature	20°C		40°C		60°C	
	Relative humidity (%)	Moisture content (g/g)	Relative humidity (%)	Moisture content (g/g)	Relative humidity (%)	Moisture content (g/g)
Adsorption and Desorption	0.0	0.000	0.0	0.000	0.0	0.000
	2.7	0.020	0.5	0.003	3.0	-
	5.6	0.030	7.3	0.014	9.3	0.017
	7.9	0.037	13.7	0.022	15.5	0.024
	11.5	0.041	24.3	0.033	25.8	0.036
	13.8	0.045	56.1	0.069	56.4	0.069
	24.5	0.060	72.0	0.092	72.2	0.098
	34.3	0.073	87.8	0.152	87.6	0.159
	44.2	0.086	92.5	0.204	90.9	0.128
	55.7	0.100	96.6	0.251	98.0	0.292
	64.0	0.117	97.5	0.294	95.2	0.210
	73.9	0.141	98.5	0.393	94.1	0.209
	83.3	0.190	97.9	0.319	91.4	0.180
	88.4	0.238	94.7	0.266	85.8	0.138
	90.7	0.254	90.0	0.214	70.0	0.095
	92.6	0.293	83.0	0.167	55.0	0.075
	94.7	0.351	67.2	0.112	25.0	0.040
	92.5	0.276	52.5	0.087	15.0	0.027
	89.5	0.236	22.5	0.052	9.0	0.015
	84.4	0.193	12.6	0.028	3.0	-
	54.6	0.106	6.6	0.020	0.0	0.000
	23.5	0.062	1.3	0.003		
	13.8	0.050	0.0	0.000		
	7.9	0.038				
	2.6	0.020				
	0.0	0.000				

Flax fibres

Temperature	20°C		40°C		60°C	
	Relative humidity (%)	Moisture content (g/g)	Relative humidity (%)	Moisture content (g/g)	Relative humidity (%)	Moisture content (g/g)
Adsorption and Desorption	0.0	0.000	0.0	0.000	0.0	0.000
	2.7	-	0.5	0.008	3.0	0.002
	7.9	0.013	7.3	0.023	9.3	0.021
	13.8	0.021	13.7	0.030	15.5	0.026
	24.5	0.033	24.3	0.041	25.8	0.039
	55.7	0.074	56.1	0.078	56.4	0.072
	83.3	0.147	72.0	0.104	72.2	0.091
	88.4	0.170	87.8	0.146	87.6	0.141
	92.6	0.206	92.5	0.187	90.9	0.127
	96.8	0.300	96.6	0.221	98.0	0.239
	94.7	0.258	97.5	0.245	95.2	0.196
	92.5	0.232	98.5	0.293	94.1	0.197
	89.5	0.194	97.9	0.262	91.4	0.175
	84.4	0.164	94.7	0.237	85.8	0.142
	54.6	0.087	90.0	0.202	70.0	0.101
	23.5	0.046	83.0	0.166	55.0	0.076
	13.8	0.033	67.2	0.122	25.0	0.049
	7.9	0.023	52.5	0.094	15.0	0.025
	2.6	0.010	22.5	0.052	9.0	0.021
	0.0	0.000	12.6	0.034	3.0	0.002
			6.6	0.027	0.0	0.000
			1.3	0.008		
			0.0	0.000		

Wheat straw fibres

Temperature	20°C		40°C		60°C	
	Relative humidity (%)	Moisture content (g/g)	Relative humidity (%)	Moisture content (g/g)	Relative humidity (%)	Moisture content (g/g)
Adsorption and Desorption	0.0	0.000	0.0	0.000	0.0	0.000
	2.7	0.019	0.5	0.008	3.0	-
	5.6	0.026	7.3	0.015	9.3	0.013
	7.9	0.032	13.7	0.022	15.5	0.021
	11.5	0.036	24.3	0.034	25.8	0.032
	13.8	0.039	56.1	0.069	56.4	0.066
	24.5	0.053	72.0	0.096	72.2	0.104
	34.3	0.064	87.8	0.165	87.6	0.165
	44.2	0.076	92.5	0.236	90.9	0.182
	55.7	0.088	96.6	0.314	98.0	0.330
	64	0.107	97.5	0.382	95.2	0.280
	73.9	0.136	98.5	0.483	94.1	0.269
	83.3	0.191	97.9	0.401	91.4	0.227
	88.4	0.253	94.7	0.287	85.8	0.152
	90.7	0.282	90.0	0.220	70.0	0.107
	92.6	0.331	83.0	0.177	55.0	0.077
	94.7	0.408	67.2	0.125	25.0	0.044
	92.5	0.315	52.5	0.097	15.0	0.028
	89.5	0.262	22.5	0.051	9.0	0.018
	84.4	0.215	12.6	0.031	3.0	-
	54.6	0.113	6.6	0.023	0.0	0.000
	23.5	0.065	1.3	0.006		
	13.8	0.051	0.0	0.000		
	7.9	0.037				
	2.6	0.017				
	0.0	0.000				

Solid spruce

Temperature	20°C	
	Relative humidity (%)	Moisture content (g/g)
Adsorption and Desorption	0.0	0.000
	2.7	0.009
	7.9	0.024
	13.8	0.033
	24.5	0.048
	55.7	0.096
	83.3	0.168
	88.4	0.187
	92.6	0.220
	96.8	0.277
	94.7	0.262
	92.5	0.253
	89.5	0.231
	84.4	0.204
	54.6	0.114
	23.5	0.060
	13.8	0.044
	7.9	0.031
	2.6	0.015
	0.0	0.000

Solid beech

Temperature	20°C	
	Relative humidity (%)	Moisture content (g/g)
Adsorption and Desorption	0.0	0.000
	2.7	0.010
	7.9	0.024
	13.8	0.032
	24.5	0.046
	55.7	0.089
	83.3	0.174
	88.4	0.194
	92.6	0.229
	96.8	0.282
	94.7	0.269
	92.5	0.261
	89.5	0.237
	84.4	0.208
	54.6	0.109
	23.5	0.055
	13.8	0.038
	7.9	0.026
	2.6	0.012
	0.0	0.000

Acetylated spruce fibres, acetylation time 10 minutes

Temperature	20°C		40°C		60°C	
	Relative humidity (%)	Moisture content (g/g)	Relative humidity (%)	Moisture content (g/g)	Relative humidity (%)	Moisture content (g/g)
Adsorption and Desorption	0.0	0.000	0.0	0.000	0.0	0.000
	3.0	0.009	0.5	0.003	3.0	-
	9.0	0.016	7.3	0.009	9.3	-
	15.0	0.022	13.7	0.014	15.5	-
	25.0	0.031	24.3	0.021	25.8	-
	55.0	0.061	56.1	0.057	56.4	-
	85.0	0.132	72.0	0.074	72.2	0.103
	90.0	0.165	87.8	0.126	87.6	0.129
	94.0	0.196	92.5	0.168	90.9	-
	98.0	0.205	96.6	0.200	98.0	0.169
	94.0	0.193	97.5	0.217	95.2	0.174
	90.0	0.173	98.5	0.274	94.1	0.172
	85.0	0.153	97.9	0.247	91.4	0.152
	55.0	0.088	94.7	0.226	85.8	0.122
	25.0	0.046	90.0	0.180	70.0	0.098
	15.0	0.029	83.0	0.149	55.0	0.073
	9.0	0.019	67.2	0.105	25.0	0.044
	3.0	0.009	52.5	0.080	15.0	0.024
	0.0	0.000	22.5	0.042	9.0	0.019
			12.6	0.024	3.0	0.016
			6.6	0.015	0.0	0.000
			1.3	0.003		
			0.0	0.000		

Acetylated spruce fibres, acetylation time 1 hour

Temperature	20°C	
	Relative humidity (%)	Moisture content (g/g)
Adsorption and Desorption	0.0	0.000
	3.0	0.004
	9.0	0.008
	15.0	0.011
	25.0	0.016
	55.0	0.036
	85.0	0.080
	90.0	0.095
	94.0	0.107
	98.0	0.111
	94.0	0.106
	90.0	0.101
	85.0	0.095
	55.0	0.055
	25.0	0.026
	15.0	0.015
	9.0	0.010
	3.0	0.004
	0.0	0.000

Acetylated spruce fibres, acetylation time 4 hours

Temperature	20°C		40°C		60°C	
	Relative humidity (%)	Moisture content (g/g)	Relative humidity (%)	Moisture content (g/g)	Relative humidity (%)	Moisture content (g/g)
Adsorption and Desorption	0.0	0.000	0.0	0.000	0.0	0.000
	3.0	0.003	0.5	-	3.0	-
	9.0	0.006	7.3	-	9.3	-
	15.0	0.009	13.7	0.001	15.5	-
	25.0	0.013	24.3	0.006	25.8	-
	55.0	0.029	56.1	0.022	56.4	-
	85.0	0.063	72.0	0.031	72.2	0.053
	90.0	0.074	87.8	0.055	87.6	0.065
	94.0	0.082	92.5	0.071	90.9	-
	98.0	0.084	96.6	0.074	98.0	0.074
	94.0	0.083	97.5	0.080	95.2	0.081
	90.0	0.079	98.5	0.088	94.1	0.079
	85.0	0.074	97.9	0.087	91.4	0.071
	55.0	0.044	94.7	0.091	85.8	0.060
	25.0	0.020	90.0	0.079	70.0	0.049
	15.0	0.011	83.0	0.072	55.0	0.037
	9.0	0.007	67.2	0.052	25.0	0.017
	3.0	0.003	52.5	0.034	15.0	0.008
	0.0	0.000	22.5	0.017	9.0	0.004
			12.6	0.001	3.0	0.001
			6.6	0.002	0.0	0.000
			1.3	-		
			0.0	0.000		

Acetylated beech fibres, acetylation time 10 minutes

Temperature	20°C	
	Relative humidity (%)	Moisture content (g/g)
Adsorption and Desorption	0.0	0.00
	3.0	0.01
	9.0	0.01
	15.0	0.02
	25.0	0.03
	55.0	0.05
	85.0	0.11
	90.0	0.13
	94.0	0.15
	98.0	0.15
	94.0	0.15
	90.0	0.14
	85.0	0.14
	55.0	0.08
	25.0	0.04
	15.0	0.02
	9.0	0.02
	3.0	0.01
	0.0	0.00

Acetylated beech fibres, acetylation time 1 hour

Temperature	20°C	
	Relative humidity (%)	Moisture content (g/g)
Adsorption and Desorption	0.0	0.00
	3.0	0.01
	9.0	0.01
	15.0	0.02
	25.0	0.02
	55.0	0.06
	85.0	0.10
	90.0	0.11
	94.0	0.12
	98.0	0.13
	94.0	0.12
	90.0	0.12
	85.0	0.11
	55.0	0.07
	25.0	0.03
	15.0	0.02
	9.0	0.01
	3.0	0.01
	0.0	0.00

Acetylated beech fibres, acetylation time 4 hours

Temperature	20°C	
	Relative humidity (%)	Moisture content (g/g)
Adsorption and Desorption	0.0	0.00
	3.0	0.01
	9.0	0.01
	15.0	0.01
	25.0	0.02
	55.0	0.04
	85.0	0.08
	90.0	0.10
	94.0	0.11
	98.0	0.11
	94.0	0.11
	90.0	0.10
	85.0	0.10
	55.0	0.06
	25.0	0.03
	15.0	0.02
	9.0	0.01
	3.0	0.01
	0.0	0.00

Enzyme treated spruce fibres

Temperature	20°C			
	Enzyme treated fibres		Control fibres	
	Relative humidity (%)	Moisture content (g/g)	Relative humidity (%)	Moisture content (g/g)
Adsorption and Desorption	0.0	0.000	0.0	0.000
	3.0	0.023	3.0	0.022
	9.0	0.033	9.0	0.032
	15.0	0.046	15.0	0.044
	25.0	0.089	25.0	0.087
	55.0	0.174	55.0	0.171
	85.0	0.209	85.0	0.204
	90.0	0.217	90.0	0.212
	94.0	0.253	94.0	0.250
	98.0	0.241	98.0	0.236
	94.0	0.237	94.0	0.234
	90.0	0.207	90.0	0.205
	85.0	0.120	85.0	0.118
	55.0	0.049	55.0	0.048
	25.0	0.047	25.0	0.047
	15.0	0.035	15.0	0.035
	9.0	0.024	9.0	0.023
	3.0	0.023	3.0	0.022
	0.0	0.000	0.0	0.000

Enzyme treated beech fibres

Temperature	20°C			
	Enzyme treated fibres		Control fibres	
	Relative humidity (%)	Moisture content (g/g)	Relative humidity (%)	Moisture content (g/g)
Adsorption and Desorption	0.0	0.000	0.0	0.000
	3.0	0.017	3.0	0.016
	9.0	0.025	9.0	0.024
	15.0	0.036	15.0	0.035
	25.0	0.076	25.0	0.074
	55.0	0.153	55.0	0.149
	85.0	0.182	85.0	0.176
	90.0	0.190	90.0	0.184
	94.0	0.223	94.0	0.220
	98.0	0.215	98.0	0.211
	94.0	0.215	94.0	0.212
	90.0	0.190	90.0	0.188
	85.0	0.107	85.0	0.106
	55.0	0.039	55.0	0.039
	25.0	0.038	25.0	0.037
	15.0	0.027	15.0	0.026
	9.0	0.017	9.0	0.017
	3.0	0.016	3.0	0.016
	0.0	0.000	0.0	0.000

Hygrothermally treated spruce fibres

Temperature		20°C			
Treatment		160/3	170/3	180/3	190/3
	Relative humidity (%)	Moisture content (g/g)	Moisture content (g/g)	Moisture content (g/g)	Moisture content (g/g)
Adsorption and Desorption	0.0	0.000	0.000	0.000	0.000
	3.0	0.012	0.013	0.011	0.020
	9.0	0.020	0.020	0.017	0.026
	15.0	0.027	0.025	0.023	0.031
	25.0	0.037	0.034	0.032	0.039
	55.0	0.068	0.066	0.064	0.068
	85.0	0.162	0.166	0.159	0.155
	90.0	0.211	0.233	0.224	0.202
	94.0	0.290	0.332	0.321	0.287
	98.0	0.373	0.442	0.407	0.315
	94.0	0.259	0.284	0.267	0.243
	90.0	0.211	0.212	0.205	0.210
	85.0	0.175	0.175	0.172	0.177
	55.0	0.083	0.082	0.080	0.090
	25.0	0.045	0.041	0.038	0.048
	15.0	0.031	0.027	0.025	0.034
	9.0	0.022	0.020	0.017	0.026
	3.0	0.012	0.013	0.010	0.019
	0.0	0.000	0.000	0.000	0.000

Hygrothermally treated spruce fibres

Temperature		20°C			
Treatment		160/5	170/5	180/5	190/5
	Relative humidity (%)	Moisture content (g/g)	Moisture content (g/g)	Moisture content (g/g)	Moisture content (g/g)
Adsorption and Desorption	0.0	0.000	0.000	0.000	0.000
	3.0	0.016	0.015	0.017	0.015
	9.0	0.027	0.026	0.025	0.021
	15.0	0.034	0.036	0.030	0.027
	25.0	0.046	0.044	0.039	0.035
	55.0	0.080	0.095	0.068	0.064
	85.0	0.158	0.163	0.159	0.156
	90.0	0.195	0.200	0.219	0.217
	94.0	0.241	0.260	0.285	0.290
	98.0	0.279	0.289	0.338	0.348
	94.0	0.226	0.216	0.258	0.230
	90.0	0.198	0.190	0.194	0.193
	85.0	0.171	0.168	0.164	0.164
	55.0	0.095	0.087	0.082	0.080
	25.0	0.056	0.051	0.044	0.041
	15.0	0.038	0.035	0.031	0.028
	9.0	0.027	0.026	0.024	0.021
	3.0	0.016	0.015	0.017	0.014
	0.0	0.000	0.000	0.000	0.000

APPENDIX B

Suction measurements

Table 1. Summary of the results of the moisture content and suction pressure relationship for Scots Pine in the three main directions.

Species Direction	P_{suc} (bar)	Moisture content (g/g)	Standard deviation. (g/g)	Relative humidity (%)
Scots Pine	15	0.4168	0.1636	0.99
Longitudinal	5	0.3173	0.0062	0.995
	1.5	0.8079	0.1137	0.999
	0.5	1.0062	0.0760	0.9995
	0.15	1.2575	0.0775	0.9999
	0.05	1.3736	0.0451	0.99995
	0.01	1.5675	0.0257	0.99999
Scots Pine	15	0.3547	0.0559	0.99
Radial	5	0.3082	0.0059	0.995
	1.5	0.6698	0.1500	0.999
	0.5	1.0533	0.0503	0.9995
	0.15	1.2417	0.0225	0.9999
	0.05	1.2876	0.0227	0.99995
	0.01	1.3127	0.0721	0.99999
Scots Pine	15	0.5912	0.1148	0.99
Tangential	5	0.6532	0.1213	0.995
	1.5	1.3004	0.1169	0.999
	0.5	1.4107	0.0460	0.9995
	0.15	1.4977	0.0425	0.9999
	0.05	1.5454	0.0444	0.99995
	0.01	1.5850	0.0402	0.99999

APPENDIX C

X-ray diffractometry measurements

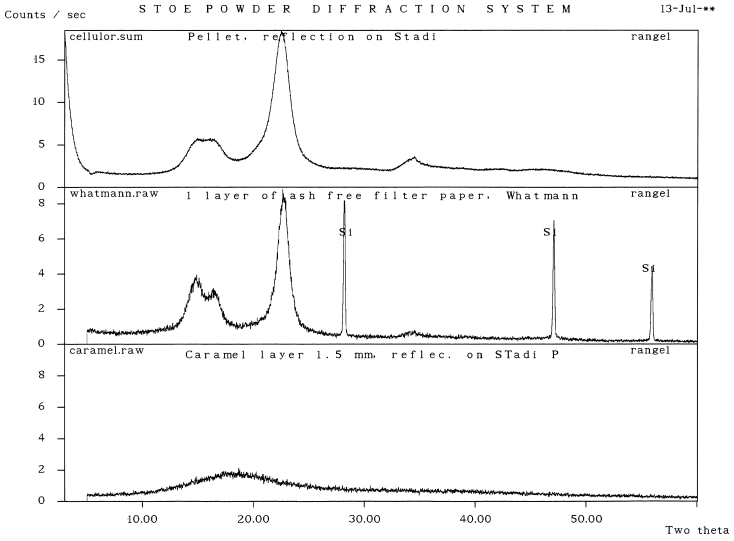

Figure 1. Diffractograms for microcrystalline cellulose powder, Whatmann filter paper, and caramel.

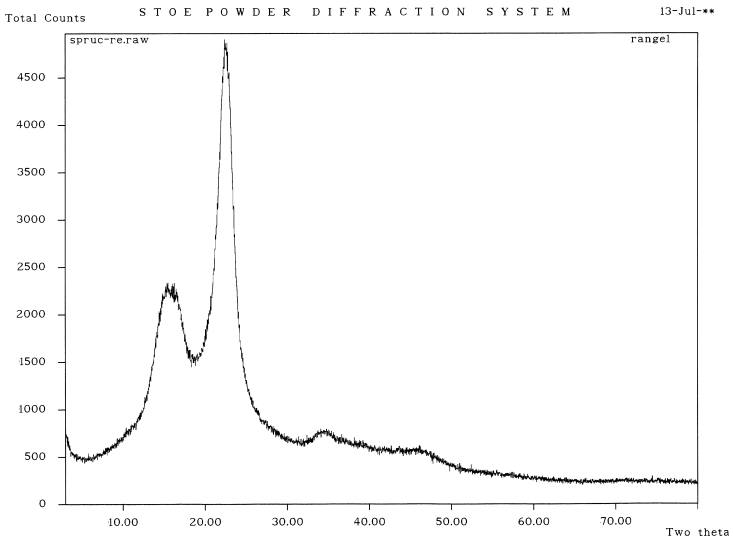

Figure 2. Diffractogram for spruce fibres.